DEFINING THE INTERPLAY BETWEEN COPPER TRANSFER AND DISULFIDE OXIDATION IN COPPER ZINC SUPEROXIDE DISMUTASE

by

Morgan Minoru Fetherolf

A dissertation submitted to the faculty of
The University of Utah
in partial fulfillment of the requirements for the degree of

Doctor of Philosophy

Department of Biochemistry

The University of Utah

May 2017

The University of Utah Graduate School

STATEMENT OF DISSERTATION APPROVAL

The dissertation of **Morgan Minoru Fetherolf**

has been approved by the following supervisory committee members:

Dennis R. Winge	, Chair	**11/17/16** Date Approved
Markus Babst	, Member	**11/17/16** Date Approved
Janet E. Lindsley	, Member	**11/17/16** Date Approved
Jared P. Rutter	, Member	**11/22/16** Date Approved
Carl S. Thummel	, Member	**11/17/16** Date Approved

and by **Wesley I. Sundquist & Christopher P. Hill** , Chair/Dean of

the Department/College/School of **Biochemistry**

and by David B. Kieda, Dean of The Graduate School.

ABSTRACT

Copper zinc superoxide dismutase (Sod1) is a critical enzyme in limiting reactive oxygen species in both the cytosol and the mitochondrial inner membrane space. Sod1 dismutes superoxide anions to hydrogen peroxide and oxygen. The catalytic reaction is dependent on an active site copper ion and a disulfide-bonded conformation. The copper chaperone for superoxide dismutase (Ccs1) mediates the activation of Sod1 either through facilitated copper ion loading, disulfide bond formation or both. In the past several decades, Sod1 has been studied extensively due to frequent mutations found in the familial form of amyotrophic lateral sclerosis (ALS). To date, over 150 mutations have been characterized in Sod1; however, the basic maturation process of the enzyme is poorly understood.

In this study, we explore the basic mechanism by which Sod1 matures. To define the activation process, we have performed extensive mutagenesis on the Cys residues in Ccs1. These mutations show a strict dependence on the CXC motif in domain 3, and the spacing of the two Cys residues. Mutations that alter the spacing or remove one of the cysteinyl residues from the CXC motif result in defects in copper metallation and disulfide oxidation. Mutations of the second Cys in the Ccs1 domain 3 or Cys146 of Sod1, which participates in the intramolecular disulfide, results in enhanced stalling of the heterdimeric complex between Ccs1 and Sod1 when affinity purification of Sod1 was performed. The two Sod1 cysteinyl residues exhibit differential phenotypes in copper

loading. A C57S Sod1 mutant is catalytically dead and devoid of bound copper when purified from yeast. In contrast, a C146S mutant is partially copper loaded and exhibits weak Sod1 activity. C57S is proposed to serve as an entry site ligand during Cu(I) loading. In an attempt to observe an entry site Cu(I) site, X-ray absorption spectroscopy was performed on Sod1 and Ccs1 mutants that stall the heterodimer. The Cu(I) coordination site with thiolate ligands was observed. We believe that this entry site is functional, and that a single redox turnover of Cu(I) to Cu(II) is necessary to generate hydrogen peroxide. We characterize that through a reaction of hydrogen peroxide with a free thiol, cysteine146 of Sod1, a sulfenic acid intermediate is fomed. We propose that the sulfenic acid intermediate is able to undergo a nucleophilic attack, potential from a thiolate from the CXC motif in Ccs1, to promote a disulfide exchange reaction.

TABLE OF CONTENTS

LIST OF TABLES

LIST OF FIGURES

CHAPTER 1

ROLE OF CCS1 IN THE OXYGEN-DEPENDENT ACTIVATION OF CU, ZN –SUPEROXIDE DISMUTASE-1

1.1 Introduction

Cu,Zn Superoxide dismutase (Sod1) is an antioxidant enzyme that is highly conserved throughout eukaryotes. Sod1 is responsible for the dismutation of two superoxide anions, a normal product of cellular respiration, to form hydrogen peroxide and oxygen [$2O_2^- + 2H^+ \rightarrow H_2O_2 + O_2$] (1). Human Sod1 is a 15.9 kDa polypeptide that forms a homodimer, with each monomer binding one copper and zinc ions within a disulfide-bonded conformer. The activation of Sod1 is dependent on the copper chaperone for superoxide dismutase (Ccs1) (2-5); however, the exact role of Ccs1 remains under debate. Sod1 shows a high degree of sequence and structural conservation between eukaryotic species. Sod1 is highly abundant in the cytoplasm, yet limiting levels are also found in the mitochondria intermembrane space (IMS) (6,7). Sod1 has also been shown to relocate to the nucleus and peroxisomes (8-10).

Superoxide anions have the ability to act as oxidants or reductants. The major adverse effects of the accumulation of superoxide anions are lipid peroxidation, deoxyribonucleic acid (DNA) damage, and Fe-S cluster oxidation (11-14). Superoxide anions are natural byproducts of several enzymes both in the mitochondria and the cytosol. In particular, Complexes I and III of the mitochondrial respiratory chain are two major sites of superoxide generation in the mitochondria along with 2-oxoacid dehydrogenases (15). The cytosolic NADPH oxidases are major contributors to cytosolic superoxide levels (16). The toxic buildup of superoxide anions is controlled by the presence of Sod1 in the mitochondrial IMS and cytosol along with the manganese superoxide dismutase Sod2, in the mitochondrial matrix (6,17,18).

Sod1 has been studied extensively since its initial discovery, and over 150

mutations in the gene that codes for Sod1 have been implicated in the familial form of the neurodegenerative disease amyotrophic lateral sclerosis (ALS) (19). The vast majority of the documented ALS cases are sporadic by nature. The familial form of ALS (fALS) makes up roughly 5-10% of all cases, with mutations in Sod1 occurring in roughly 12% of familial cases (19). The role of Sod1 in ALS has been reviewed extensively in the literature and is not a primary focus of this review (20-22).

A strong association between a toxic gain-of-function of mutant Sod1 and the motor neuron disease exists (23,24), yet the mechanism of pathogenesis remains unclear. One prominent model is the association of mutant Sod1 with mitochondria and resulting mitochondrial dysfunction (25-28). This model is supported by studies in tissues and cells obtained from ALS animal models and patients (25-28). Many ALS patient mutations in Sod1 destabilize the native fold, suggesting that the deleterious form of ALS Sod1 is a misfolded conformer (29,30).

Cells lacking Sod1 exhibit a myriad of phenotypes. The mutant cells exhibit increased sensitivity to oxidative and metal stress, decreased life span, and deficiency of respiration, among various other problems (31-35). Sod1 null mice are viable and have been used to study the role of Sod1 in ALS; however, the mice do not develop with any obvious motor neuron abnormalities (36). The mice do exhibit a variety of phenotypes including increased motor neurons, increased vulnerability to stress, mitochondrial defects, and progressive muscle loss, etc. (34,36,37).

Mammalian species also have an extracellular Cu,ZnSOD (SOD3) that catalyzes the same reaction as the intracellular Cu,Zn-Sod1 (38). Structurally, the extracellular enzyme is a tetramer with an additional disulfide bond stabilizing the structure.

1.2 Sod1 structure

Mature Sod1 is a stable homodimer, with each monomer folded into an eight-stranded Greek-key β-barrel conformer (38). The enzyme contains a solvent exposed active site copper ion located at the bottom of a deep channel outside the β-barrel (39). The active site channel comprises roughly 660 $Å^2$ and makes up ~10% of the total surface area of the enzyme (39). The channel is comprised of 18 solvent exposed residues, and the catalytic copper ion sits at the base of the channel. The copper coordination environment varies depending on the oxidation state of the copper in the active site. His46, His48, His120, and His63 coordinate the copper ion in its oxidized cupric state, resulting in a distorted square planar geometry (40,41). One of the axial directions of the copper ion is accessible to solvent (40). In its reduced cuprous state, His46, His48, and His120 coordinate Cu(I) in a trigonal planar geometry. His63 bridges the Cu(II) to a Zn(II) ion 6.3 Å removed (41-44). The Zn(II) site is buried and is tetrahedrally coordinated via three histidine ligands (His63, His71, His80) and one aspartate residue (Asp83), which is part of the β-barrel. The zinc ion has a structural role in stabilizing a polypeptide, loop thereby increasing the enzyme stability (45). In addition, the Zn(II) ion increases the redox potential of the catalytic Cu(II) ion (39). A disulfide bond between Cys57 and Cys146, both of which are invariant in eukaryotes, further stabilizes Sod1. **Figure 1.1** shows the native Sod1 structure and highlights the two metal ions and their ligands, the two important loop segments, one of which is the electrostatic segment (colored in orange). The disulfide loop (colored in purple) extends to the Zn ligand loop (colored in cyan).

Fully metallated, disulfide oxidized Sod1 is an unusually stable enzyme with a

melting temperature >90°C (46). Human apo-Sod1 with the disulfide intact has a diminished melting temperature of ~52°C, and upon reduction of the disulfide bond the apo-protein has a melting temp of ~42°C (29). The disulfide bond reduction potential of Sod1 varies in different species. The yeast, human, and *C. elegans* proteins exhibit potential of -234 mV, -248 mV, and -270 mV, respectively (47). However, due to the overall intracellular GSH:GSSG redox state of -290 mV to -310 mV (48), yeast and mammalian Sod1 molecules are expected to be reduced in the cytoplasm and disulfide oxidation must be facilitated. The unusual stability of the Sod1 disulfide in the cytoplasm suggests that other structural influences such as solvent accessibility contribute to the stability of the disulfide bond.

The metallation state and disulfide status of Sod1 affect protein homo-dimerization. The reduced apo-protein is predominantly in the monomeric state, where the addition of Zn(II) or formation of the disulfide bond favors the formation of the homodimer (49). The reduced disulfide conformer results in a rearrangement of loop IV that enhances flexibility from residues 50-61. This flexibility attenuates the dimer interaction (50,51). Binding of Zn(II), or both Zn(II) and Cu(I) limits the flexibility of this loop region and favors dimerization, even in the absence of disulfide oxidation. The bridging His63 located near the end of this loop contributes to loop stabilization.

1.3 Sod1 enzymatic activity

The function of Sod1 as a reactive oxygen-scavenging enzyme is linked to the redox properties of Cu ion in the active site. The process of superoxide anion dismutation proceeds in a two-step mechanism (38). First, the initial superoxide anion binding to

Cu(II)-Sod1 reduces the cupric ion to produce molecular oxygen and Cu(I)-Sod1. Reaction of Cu(I)-Sod1 with a second equivalent of superoxide anion results in Cu(I) oxidation and hydrogen peroxide generation. The redox cycling of the copper is accompanied by a change in its ligand environment, in which Cu(I) exists in a trigonal $(His)_3$ environment whereas the oxidized Cu(II) ion is distorted square planar with four His ligands. The enzymatic reaction of Sod1 proceeds with a rate constants of ~2 x 10^9 $M^{-1}s^{-1}$ which is approaching the rate of diffusion and is largely unaffected by pH changes from ~5-9.5 (52).

A key attribute that contributes to the phenomenal catalytic rate is the formation of a superoxide guidance channel in the enzyme (38). Long-range and short-range superoxide guidance occurs primarily by electrostatic guidance by positive charges in the active site channel. Arg143 (yeast Sod1 residue numbering) is especially critical for this guidance. Mutation of Arg143 or modification of the residue caused a dramatic loss of Sod1 activity (53,54). Arg143 forms a transient hydrogen bond with the superoxide substrate (39,53,55). The guanidinium group of Arg143, in combination with Thr137, is able to sterically block any large non-native substrates from reacting with the copper ion (43). Arg143 is located within a loop designated the electrostatic loop (**Figure 1.1**), which contains other positively charged residues contributing to electrostatic guidance of superoxide ions (55). The electrostatic loop is stabilized by the C57:C146 intra-subunit disulfide bond (40).

1.4 Additional roles of Sod1 in the cell

Sod1 has been traditionally characterized a reactive oxygen scavenging protein, yet only a small fraction of cellular Sod1 is necessary for this role and the enzyme is one of the most abundant in the cell (56). This leaves the possibility of alternative functions of Sod1 in the cell. Recently, Sod1 was shown to function in the glucose repression of cellular respiration in yeast (57). Sod1 interacts and stabilizes the membrane-bound casein kinase homologs, Yck1 and Yck2, which are involved in several nutrient-sensing pathways in the cell including glucose and amino acid sensing (58,59). Sod1 binds a C-terminal degron in Yck1 consisting of residues 367-412 (57). Both the Yck1:Sod1 interaction and the H_2O_2 product of Sod1 catalysis are necessary for Yck1/2 stabilization; an inactive Sod1 or expression of Sod2 in the cytoplasm are unable to stabilize Yck1, resulting in its degradation. In addition, human Sod1 stabilized the bovine casein kinase CK1g, demonstrating the conserved nature of this stabilization. Stabilization of the casein kinases by Sod1 links the abundance of reactive oxygen species with regulation of several signaling pathways through Sod1 (57).

Sod1 has additional regulatory roles during times of high oxidative stress. Sod1 is rapidly translocated to the nucleus in yeast and mammalian cells in response to oxidative stress (60). The hydrogen peroxide activated Mec1 mediates this oxidant-mediated translocation of Sod1 through the Dun1 kinase. Activation of Mec1 by H_2O_2 triggers the Dun1-mediated phosphorylation of yeast Sod1 at Ser60 and Ser99. The phosphorylation of these residues in Sod1 results in its translocation to the nucleus. The presence of Sod1 within the nucleus correlates with a transcriptional response of a number of genes broadly involved in oxidative stress response. The mechanism of Sod1 stimulation of gene

transcription appears to be through specific DNA binding (60).

In addition to physical interactions, hydrogen peroxide derived from Sod1 has been shown to be an important signaling molecule. Peroxide produced from enzymatically active Sod1 has been shown to inhibit the protein tyrosine phosphatase, PTP1B, by oxidizing the active site cysteine residue (61). Inhibition of Sod1 results in a decrease in phosphorylation of ERK1/2 in A431 tumor cells (61). General intracellular peroxide generation is also suggested to be a vital signaling molecule in the cell, not only for PTP1B, but also for PTEN, and MAPK (62-66). Peroxide in general has been shown to be involved in cell proliferation, apoptosis, and cell differentiation (16,67). A direct link of peroxide generated through the enzymatic reaction of Sod1 has not been demonstrated for many of these intracellular processes, however, it is reasonable to believe that at least some fraction of the peroxide produced that act as a signaling molecule could originate from Sod1.

1.5 Maturation of Sod1

The maturation of Sod1 is dependent on a series of post-translational modifications. These include Zn(II) and Cu(I) binding, disulfide bond formation and dimerization. Disruption of any of these modification steps results in an inactive protein. Sod1 maturation is mediated by the Ccs1 metallochaperone, which has been suggested to mediate Cu(I) ion insertion and disulfide bond formation, although its exact role has been debated (2-4).

In addition to its cytosolic maturation process, Sod1 is present in the mitochondrial IMS and peroxisomes (8-10). Its presence in the mitochondrial IMS is

dependent on Ccs1, which is imported into the IMS through the Mia40/Erv1 disulfide relay pathway (7,68-70). Elevated IMS levels of Ccs1 lead to increased accumulation of Sod1 in that compartment (6,7). The steps in Sod1 maturation within the IMS are less clear since all proteins entering in the mitochondria are unfolded prior to extrusion through the outer membrane TOM complex. The import of Sod1 into peroxisomes is also mediated by Ccs1 through a C-terminal peroxisomal targeting motif on Ccs1 (10). Whether Sod1 is imported in a complex with Ccs1 has not been substantiated. The following sections will discuss various steps in the maturation process in the context of cytosolic Sod1.

1.6 Insertion of zinc

The mechanism of zinc incorporation into Sod1 is unknown but is Ccs1-independent. Zinc is the second most abundant trace metal and it is not redox active. Due to the inert redox nature of zinc, it is not considered as deleterious to the cell as Fe or Cu, which can both catalyze Fenton chemistry. Total intracellular zinc concentrations for optimum growth are on the order of 10^5-10^8 molecules per cell, yet due to the high abundance of zinc metalloproteins, the "free" zinc pool may be quite low (71-73). From these experiments, many have suggested that zinc may be shuttled via metallochaperones to target proteins as a result of the low "free" pool. A more common thought is that zinc distribution is not limited by metallochaperone delivery, especially since it is so widely used as a cofactor and that no Zn metallochaperones have been discovered. In the latter scenario, labile Zn pools would be responsible to metallating the various proteins, presumably through a diffusion process. Regardless of how zinc is acquired by Sod1, it

appears that Zn binding is the first maturation event. Two observations support this conclusion. First, purification of Sod1 from yeast lacking Ccs1 was Zn-loaded, but deficient in copper and largely disulfide reduced (74). In the absence of Ccs1, the yeast Sod1 is isolated with Zn(II) in both the Zn and Cu sites. Thus, one clear role for Ccs1 may be ensuring proper metallation of the copper site.

Secondly, *in vivo* NMR analysis of human Sod1 overexpressed in HEK293T cells led to the accumulation of 360 μM Sod1 (75). At this elevated concentration, backbone atom signals from Sod1 were clearly seen and the HSQC signals could discriminate the apo-protein from a Zn-loaded protein. In the absence of co-expression of Ccs1 or added copper, the cellular Sod1 was a mixture of apo-monomer and a Zn-loaded dimeric species (75). These observations are consistent with a model that Zn(II) metalltion of Sod1 occurs from a labile Zn(II) pool.

1.7 Role of Ccs1 in Sod1 maturation

The addition of copper and the disulfide in Sod1 are linked to the Ccs1 metallochaperone. Ccs1 is a ~27kDa protein that was originally identified using a genetic approach (2). The initial screen for a Sod1 chaperone was based on the premise that a mutant lacking a Sod1-chaperone would mimic the known defects in the lysine and methionine biosynthetic pathways observed in *sod1*Δ cells. Cells lacking the *LYS7* gene were found to have same phenotype as *sod1*Δ cells. Both *lys7*Δ and *sod1*Δ cells only exhibited these phenotypes in the presence of oxygen. The *LYS7* locus was reannotated as *CCS1* and a human homologue was identified from the human proteome (2). Ccs1 is primarily localized within the cytosol and mitochondrial IMS, like Sod1. Yeast lacking

Ccs1 are largely devoid of cellular Sod1 activity, but a fraction of active Sod1 can be rescued with the addition of exogenous Cu (76,77). Yeast Sod1 is dependent on the presence of Ccs1 for activation under normal physiological conditions, yet other organisms such as *C. elegans* lack Ccs1 yet maintain a fully active Sod1. Human cells contain both a Ccs1-dependent and independent activation pathway of Sod1. The molecular details of the Ccs1-dependent maturation of Sod1 remain under investigation.

Ccs1 has a secondary role in the function of Sod1. The presence of Sod1 within the mitochondrial IMS is dependent on Ccs1 (6,7,9). Cells devoid of Ccs1 have reduced Sod1 within the IMS, and conversely, cells with elevated IMS levels of Ccs1 mediate enhanced retention of Sod1 within the mitochondrial compartment (6,7,9). Ccs1 uptake into the IMS is mediated by the oxidative folding Mia40/Erv1 pathway, whereas Sod1's retention is solely dependent on the prior presence of Ccs1 in the IMS (69,78).

The Ccs1 protein consists of three distinct domains. The N-terminal domain (domain 1, D1) shares structural homology with the Atx1 copper chaperone (79). This domain is arranged in a βαββαβ fold and contains an Atx1-like MXCXXC motif capable of stably binding one Cu(I) ion (5). Cu(I) binding to D1 of Ccs1 leads to minimal structural changes in the tertiary fold of the domain itself (80). The presence of the Atx motif suggests that D1 has a role in copper delivery to Sod1 and a direct transfer of Cu(I)-Ccs1 in which Cu(I) is present in D1 to apo-Sod1 was shown (80). Physiologically, D1 is only required for *in vivo* activation of yeast Sod1 under copper-limiting growth conditions (76). D1 also harbors two additional cysteine residues, C27 and C64. These residues are able to form a disulfide bond *in vivo* and are involved in the import of Ccs1 into the mitochondrial IMS through the Mia40/Erv1 disulfide relay system mentioned

above (69,78). Either single or double mutations of C27 and C64 result in a marked diminution of steady state levels of Ccs1 within the IMS but not as significantly attenuated in the cytoplasm (69,78). Mutation of C27 or C64 limit mitochondrial Sod1 activity, but show very little effect on cytosolic Sod1 activity (78).

Domain 2 (D2) of Ccs1 consists of an eight-stranded antiparallel β-barrel domain analogous to Sod1, and is termed the Sod1-like domain (79). This domain is necessary for the heterodimer interaction with Sod1 (5,81,82). The overall fold of D2 is very similar to Sod1, with the exception of the zinc and electrostatic loop regions. The human Ccs1 D2 contains 3 of the 4 active site histidines, but this domain fails to bind copper (83). Deletion of D2 or mutation of residues on dimer interface, disrupt the interaction with Sod1.

Domain 3 (D3), known as the activation domain, is a highly flexible domain containing an invariant CXC motif. The crystal structure of apo-Ccs1 from yeast was shown to be a dimeric conformer but only domains 1 and 2 were structurally defined. D3 was disordered and not observed (79). D3 is stabilized upon complexation with Sod1 and one of the cysteines in the essential CXC motif has been shown able to form an intermolecular disulfide with Sod1 (84). This structure was obtained from a stalled Ccs1:Sod1 heterodimer resulting from a Sod1 Cu ligand His48Phe substitution. C57 is located on the disulfide loop (loop IV) of Sod1 and forms the intermolecular disulfide with C229 of Ccs1 D3, which is observed as an extended αhelical conformation(84). A second heterodimeric structure was obtained by mutation of Sod1 copper binding ligands H46R and H48Q as well as a WEER to WAAA mutation in D3 of Ccs1 (preliminary data). In this stalled structure of Sod1:Ccs1, D3 is observed as a compact β-hairpin

conformation and C231 of Ccs1 is within 4 angstroms of C146 of Sod1.

Deletion of D3 or mutation of CXC motif impairs Sod1 activation, indicating its importance in Ccs1-mediated activation (2,76). The CXC motif has been proposed to be involved in copper transfer and/or disulfide transfer (5), but direct evidence *in vivo* has been elusive. The candidate Cu(I)-binding CXC motif in D3 has a binding affinity to Cu(I) that is roughly one order of magnitude weaker than the MXCXXC motif in D1 (85), raising questions of a purported Cu(I) handoff from D1 to D3 as has been suggested.

Mutation in the spacing of the D3 CXC motif yielding either a CC or a CXXC motif results in a largely inactive, disulfide-reduced Sod1. Both CC and CXXC motifs are well-known as Cu(I)-binding motifs (86), yet these Ccs1 variants are functionally compromised (preliminary data). However, a $C_{230}C_{231}$ Ccs1 variant supports limited Sod1 activation unlike other spacing mutants (preliminary data). This Ccs1 variant, which cannot form an intramolecular D3 disulfide, ostensibly *rule out* prior models implicating Ccs1 D3-mediated shuffling of a preformed disulfide bond to Sod1 during activation (87,88).

Ccs1 involvement in the Sod1 disulfide oxidation process has been shown *in vitro* as well as *in vivo* (5,75,88,89). The stalled intermolecular disulfide bond previously mentioned supports the role of Ccs1 in disulfide formation. However, whether Ccs1 is responsible for the introduction the disulfide, an additional upstream enzyme, or small molecule oxidant, is unresolved. The activation process in the native enzyme is oxygen-dependent, as the addition of a Cu(I)-loaded Ccs1 fails to activate yeast Sod1 *in vitro* under anaerobic conditions (88).

The role of Ccs1 in the disulfide acquisition in human Sod1 was demonstrated by *in vivo* NMR analysis of human Sod1 overexpressed in HEK293T cells (75). Efficient disulfide bond formation in Sod1 was dependent on the co-expression of Sod1 and Ccs1 along with the addition of supplemental copper salts in the growth medium (75). In the absence of co-expression of Ccs1, the supplemental copper led to a modest increase in Sod1 disulfide bond formation. Likewise, co-expression of Sod1 and Ccs1 without the addition of added copper led to partial oxidation in Sod1. Efficient disulfide bond formation in Sod1 is therefore dependent on copper, Ccs1, and oxygen.

Ccs1-mediated Cu(I) donation to Sod1 has been widely discussed. Cu-Ccs1 is able to activate Sod1 *in vitro*, however, it is not easy to distinguish copper transfer vs. disulfide oxidation *in vivo* as they appear to be linked (3). Ccs1 is critical for the maturation of Sod1 in yeast due to the presence of a proline residue (P144) in Sod1, which is absent in the human enzyme (4). Expression of human Sod1 in yeast produces ~25-50% active enzyme in the absence of Ccs1 (4). Certain organisms, such as *C. elegans*, lack Ccs1 in their proteome and Sod1 is fully activated in a Ccs1-independent manner (90). This begs the question of how the Cu(I) is inserted and the disulfide bond formed in Sod1 in these organisms. Additionally, since Sod1 is susceptible to mismetallation in the absence of Ccs1 (91), it is curious how the Ccs1-independent organisms ensure proper metallation.

1.8 Copper acquisition of Sod1

In general, copper is high regulated in the cell due to its reactivity. Cellular acquisition of copper is mediated by the high affinity Ctr1 copper transporter and low

affinity transporters, such as Fet4 in yeast (92). Ctr1 leads to the import of Cu(I) (93-95). Ctr1 is an integral membrane protein, which forms a homo-trimeric complex with 3 transmembrane helices per subunit (96). The extracellular amino terminal domain contains a methionine rich motif for Cu(I) binding (97-99). Unlike the P-type ATPases, Ctr1 lacks any known ATP hydrolysis site to facilitate Cu(I) ion uptake. Cu(I) uptake may be driven by the copper concentration gradient between the cytoplasm and extracellular fluid.

Several models have been proposed for how Cu(I) is distributed after import. In the case of Sod1 metallation, one model posits that Ccs1 is weakly associated with the plasma membrane through electrostatic interactions with the phosphate groups of the bilayer (100). This interaction involves a positively charged surface on Ccs1 composed of lysine and arginine residues. Membrane association may aid in bringing Ccs1 in proximity to the Cu(I) transporters. The known association of Ccs1 and Sod1 would then permit Sod1 activation to occur close to the membrane interface. Mutation of the mentioned basic residues in Ccs1 abolishes the interaction with the membrane, and impairs copper metallation of Sod1 *in vivo* (100). These data suggest that association of Ccs1 to the membrane bilayers is necessary for efficient activation of Sod1. This implies that Ccs1 may be able to directly acquire copper from Ctr1 for transfer to Sod1.

A second hypothesis is that the copper chaperones such as Ccs1 or Atox1, do not directly extract Cu(I) from Ctr1. Rather, the intracellular glutathione pool facilitates Cu(I) transfer from Ctr1 to the metallochaperones. Maryon et al. proposed this model in which GSH mediates Cu(I) distribution in cells (101). In their studies, initial cellular copper uptake was unaffected by either overexpression or knockdown of either Ccs1 or Atox1 in

HEK293 cells. However, depletion of GSH by treating the cells with L-buthionine-sulfoximine (BSO) caused a 50% decrease in the initial rate of Cu(I) uptake. This study suggests that GSH is important for cellular copper uptake from Ctr1. This observation has been supported by other studies (102,103).

Multiple studies have sought to delineate the process of copper transfer to Sod1. Ccs1 is intimately involved in the process, as deletion of Ccs1 results in a defect in Sod1 maturation in yeast and humans (2,4,83). Yeast Sod1 activity can be partially rescued in the absence of Ccs1 with addition of copper salts (76,77). As mentioned, *in vitro* studies using copper-loaded Ccs1 are sufficient to transfer copper and oxidize the disulfide bond in Sod1 (5,88). As previously mentioned, Ccs1 has two Cu(I) binding motifs, the D1 MXCXXC motif and the D3 CXC motif. One hypothesis is that there is direct copper transfer from D1 to D3, then subsequently to Sod1. This seems unlikely since the Cu(I) affinity of D1 is ~5 x 10^{17} M^{-1} at pH 7.5 and the affinity for D3 is ~6 x10^{16} M^{-1} (85).

Elegant *in vitro* studies using Cu(I)-loaded Ccs1 and its domains demonstrated that Cu(I) transfer and Sod1 activation occurred using full-length Ccs1, but not Cu(I)-loaded Ccs1 D1 (5). However, a Ccs1 truncate containing only D1 and D2 was able to mediate Cu(I) transfer to Sod1 *in vitro*, but the enzyme lacked the critical disulfide. Curiously, a Cu(I)-Ccs1 truncate lacking D1 showed heterocomplex formation with Sod1 but no Cu(I) transfer. The reduced affinity of Cu(I) associated with D3 may compromise such transfer. Cu(I) transfer to Sod1 was dependent on prior occupancy of the Zn(II) site in Sod1 (5).

Cu(I) acquisition to Sod1 clearly involved the Ccs1 D1 in mammalian cells and yeast under conditions of copper limitation. The observed copper-activation of *ccs1*Δ

yeast cells (77) demonstrates that Sod1 can access a labile cellular Cu(I) pool, such that in the absence of the availability of Cu(I)-loaded Ccs1, Sod1 is able to acquire Cu(I). The *in vitro* Cu(I) transfer studies also question the role of Ccs1 D3 in Cu(I) presentation to Sod1. However, D3 is essential for acquisition of the Sod1 disulfide bond.

The acquisition of Cu(I) by Sod1 appears to involve the Sod1 disulfide cysteines (80). The *in vitro* Cu(I) transfer from full-length Cu(I)-Ccs1 to Sod1 was attenuated with Sod1 alleles containing either C57A or C146A substitutions (80). These substitutions do not attenuate Cu(I) loading when Cu(I) was presented as a Cu(I)-acetonitrile complex. Thus, Ccs1 mediated activation of Sod1 may require Cu(I) entry through the Sod1 thiolates as an intermediate to translocation to the active site.

We confirmed the importance of Cys57 and Cys146 in the copper loading of Sod1 in yeast. Purification of Sod1 from yeast followed by metal analysis revealed that a C57S or C146S variant were impaired in copper loading. Copper levels in these mutants were ~.07 and .19 g atoms Cu/mol protein, respectively (preliminary data). The more severe copper defect in Sod1 C57S could be a result of this cysteine being involved as an initial copper ligand in a transfer reaction. In the absence of electrostatic guidance, the Sod1 Arg143Glu mutant, although inactive, is ~40% copper metallated *in vivo* (preliminary data).

We have validated this mode of Cu(I) entry. X-ray absorption spectroscopy studies reveal a thiol-bound Cu(I) site in Sod1 when the active site Sod1 copper ligands His46 and His48 are mutated to Arg and Gln, respectively (preliminary data). The entry site is a novel trigonal Cu(I) ion coordinated by $(Cys)_2His$ ligands **(Figure 1.2)**. The thiolates may be contributed exclusively by the Sod1 cysteines that form the disulfide, or

a combination of Sod1 and the Ccs1 CXC motif. The His residue is likely either His120 or His48 from the copper active site. Cu(I) binding to this putative "entry site" is likely an intermediate prior to reaching the His_4 active site. In this model, Ccs1 acts as a protein chaperone stabilizes a nascent conformation of Sod1 exposing a Cu(I) entry site. Presumably, this entry site holds copper until the disulfide bond is formed, where copper is pushed into the native active site (**Figure 1.3**).

1.9 Oxygen dependence of Sod1 activation

The cell is dependent on oxygen as the final electron acceptor in cellular respiration through the electron transport chain. Despite this, oxygen can be deleterious to the cell by modifying proteins and lipids (104,105). However, in order to properly mature, Sod1 is dependent on the abundance of oxygen. Early studies on superoxide dismutase showed that yeast grown in pure oxygen vs. nitrogen showed a ~6 fold greater activity that is attributed to Sod1 (106).

In vitro assays first explored the mechanism by which oxygen is necessary for Sod1 activation. It has been established that Cu(I)-loaded Ccs1 is able to react with apo-Sod1 *in vitro* and facilitate Cu transfer and disulfide formation in the presence of oxygen (3,5,88). In this experiment, a characteristic Cu(II) signal was seen by EPR after incubation of Cu(I)-Ccs1 with apo-Sod1 for 1 hr in oxygen at 37°C (3). However, the same experiment has been performed in the absence of oxygen, and Ccs1 failed to activate Sod1, or give a signature Cu(II) EPR signal (3). These experiments demonstrated the importance of oxygen *in vitro* and are consistent with a model in which Cu(I) → Cu(II) turnover may be an important aspect of Sod1 maturation.

Additionally, yeast cells grown in the absence of oxygen lacked Sod1 activity, but the mitochondrial Mn-Sod2 was largely unaffected. However, after lysis under anaerobic condition, exposure of the lysates to oxygen resulted in a response where Sod1 protein levels and overall activity increased in a time and oxygen dependent manor (3). A similar experiment was performed where cells were treated with cyclohexamide, which inhibits new protein synthesis, in anaerobic conditions prior to air exposure. Upon air exposure cells treated with cyclohexamide showed a significant increase in Sod1 activity, but steady state levels were unaffected (3). These results taken together demonstrate that there is a rapid response, both transcriptional and post-translational, to increase Sod1 activity during increased oxidative stress.

Prolonged incubation of wild-type Sod1 under anaerobic conditions led to loss of enzymatic activity (107). In contrast, a Pro144Ser mutant retains enzymatic activity when shifted to an anaerobic environment. Under these conditions, the level of Sod1 activity shows an inverse relationship with the level of phosphorylation of Ser38, where a greater abundance of phosphorylation was found after prolonged anaerobic exposure. The Pro144Ser substitution, which permits Ccs1-independent activation, resulted in decreased levels of Sod1 phosphorylation when compared to WT Sod1 under anaerobic conditions.

1.10 Introduction of the disulfide bond

Disulfide bonds confer stability to a myriad of proteins. In Sod1, the disulfide bond between C57 and C146 is normally critical for enzyme activity. Careful analysis of Sod1 mutants lacking one of the disulfide cysteines revealed limited catalytic activity (91). This disulfide is unique in that a bulk of Sod1 is found in the highly reducing

environment of the cytosol. Cytosolic disulfides are rare due to the reducing potential of the cytoplasm, and it is currently unknown how they are introduced.

The lumen of the endoplasmic reticulum (ER) and the mitochondrial IMS harbor a large number of disulfide-bonded proteins and have redox potentials of ~-170 to -185 mV, and ~-300 mV, respectively. The IMS is roughly as reducing as the cytosol (~-306 mV), yet is still able to harbor disulfide-bonded proteins due to limiting levels of glutaredoxin-2 (108-112). Both the ER and the IMS have dedicated disulfide relay pathways that have been characterized in detail (113-116). Both pathways employ sulfhydryl oxidases (Ero1 and Erv1) and oxidoreductases (PDI and Mia40) to transfer disulfide bonds to the substrate proteins through a disulfide relay. There are no known sulfhydryl oxidases in the cytoplasm, so the mechanism of Sod1 disulfide oxidation remains elusive.

One model of Sod1 oxidation invoked the CXC motif in domain 3 of Ccs1 as the disulfide donor (5). In this model, Ccs1 would have to acquire an intramolecular disulfide by an undefined sulfhydryl oxidase or oxidized glutaredoxin. However, this model is inconsistent with the Ccs1-independent activation pathway in humans.

An alternative hypothesis of disulfide introduction is through a peroxiredoxin-like mechanism (117). Such enzymes with an active site cysteine react with hydrogen peroxide to form a sulfenic acid intermediate that can mediate disulfide bond formation in an interacting target protein. Cysteine side chains are most reactive nucleophiles out of all amino acids under physiological pH and thus, free thiols in the cell can undergo a variety of modifications which include glutathionylation, nitrosylation, and sulfenylation (118-120). Sulfenic acid modifications are unique in that the formal oxidation state of the

sulfur is 0, which can lead to reactivity as either a nucleophile or electrophile (121).

Protein sulfenic acid is generally an unstable reversible intermediate, but additional reaction with hydrogen peroxide can yield irreversible sulfinic and sulfonic oxidation states (121,122). While sulfenic acids have been known to be involved in stress response and modulating enzymatic activity, it was not until recently that its role in disulfide bond formation was observed (123). The peroxiredoxin Gpx3 is involved in an oxidative stress response-signaling pathway (124). Upon sensing an elevated level of oxidative stress, the active site cysteine of Gpx3, C36, is able to react with hydrogen peroxide to form a sulfenic acid intermediate. The sulfenic acid modified Gpx3 interacts with the transcription factor Yap1, and forms an intermolecular disulfide bond through a nucleophilic attack from a thiolate in Yap1. The intermolecular disulfide bond is resolved by a second thiolate in Yap1, and the oxidized Yap1 can then translocate to the nucleus where it initiates its transcriptional response (124). This mechanism has now been defined in multiple other systems (125).

We propose a related mechanism for the activation of Sod1 with a copper-mediated sulfenylation reaction. We observed copper-mediated sulfenylation of Sod1 in yeast cultures (preliminary data). A model to account for this observation suggests that Cu(I) presented by Ccs1 D1 or alternatively from a labile Cu(I) cellular complex transiently binds to an entry site in Sod1 consisting of the Sod1 thiolates Cys57 and Cys146 along with a histidine ligand. Cu(I) bound in the entry site is adjacent to an electropositive hole created by the association of Ccs1 with apo-Sod1. The electropositive hole in Sod1 attracts either a superoxide anion of hydrogen peroxide anion. Attraction of a superoxide anion to the bound Cu(I) ion would allow for a single

turnover event generating peroxide that can mediate Sod1 sulfenylation leaving Cu(II) in the entry site. The Ccs1 D3 thiolates trigger disulfide exchange reactions leading to formation of the Sod1 C57-C146 disulfide bond. In the process, Cu(II) is chased into the active site for catalysis. Alternatively, attraction of a peroxyl anion to the electropositive hole would allow sulfenylation without concomitant Cu(I) oxidation. In this case, disulfide bond formation may drive Cu(I) to the active site.

The sulfenic acid modification seems to be preferentially on Cys146, since a C146S variant attenuates this modification. In a recent crystal structure of the Ccs1/Sod1 heterodimer, Cys146 of Sod1 is ~ 4 Å away from C231 of the CXC motif in Ccs1. This presents the possibility of a disulfide exchange reaction involving the CXC motif in Ccs1. Additionally, the crystal structure showed a salt bridge formed between Arg143 and Cys57 of Sod1. Stabilization of thiolates by salt bridge or hydrogen bonds can increase the nucleophilicity of the residue, suggesting that a nucleophilic attack of Cys57 to the sulfenylated C146 may drive disulfide bond formation (126). This mechanism is supported by the importance of Ccs1 in disulfide bond formation especially in yeast and the oxygen-dependency on the process.

1.11 Ccs1-independent mechanism of Sod1 activation

As mentioned, human Sod1 is capable of limited activation in cells lacking Ccs1 (47). This is unlike the yeast protein that exhibits a more rigid dependency on Ccs1. The question arises as to the mechanism of the Ccs1-independent pathway. This pathway is dominant in *C. elegans* (90). One study addressing the Ccs1-independent pathway demonstrated that both the Ccs1-dependent and Ccs1-independent pathways are

dependent on the same source of intracellular copper (47). In contrast, the two pathways diverge with regards to the requirement for copper and oxygen in the disulfide bond formation. Expression of the *C. elegans* Sod1 in a yeast *sod1*Δ strain resulted in oxidation of the worm Sod1 independent of the copper status of cells (47). This is in marked contrast to yeast Sod1. The Ccs1-independent process of human Sod1 activation is partially dependent on copper and oxygen. Substitution of Pro144 in yeast Sod1 by a serine permits limited Ccs1-independent Sod1 activation and the disulfide bond formation proceeds in copper-deficient cells. The redox potential of the Sod1 cysteines in human Sod1 were reported to be ~ -248 mV, but considering that the cytoplasmic redox potential is closer to ~ -300 mV, this process would be inefficient.

The Ccs1-independent pathway appears to depend on glutathione. The Ccs1-independent activation of human Sod1 was found to be dependent on GSH (4). Attenuation of glutathione by deletion of γ-glutamyl cysteine synthase 1 (Gsh1), results in impaired human Sod1 activation in the absence of Ccs1. Sod1 was able to be activated in *ghs1*Δ cells in cells containing Ccs1. Similar results were found using immortalized fibroblasts from mice (4). Additional experiments suggest that the Ccs1-independent pathway needs reduced glutathione. Deletion of glutathione reductase null (*glr1*Δ), which causes the accumulation of oxidized glutathione, resulted in an attenuation in Sod1 activity.

1.12 Conclusions and perspectives

Cu,Zn superoxide dismutase is one of the most abundant enzymes in the eukaryotic cell, and its diverse roles are being continually updated. Where there has been

considerable attention focused on the role of Sod1 in ALS, the fundamental processes in the *in vivo* activation process have not been completely defined. Of the two pathways for Sod1 activation, the Ccs1-independent process exhibits less dependency on copper and oxygen than the Ccs1-dependent process. Clearly, the most efficient process is the Ccs1-dependent process for human and yeast Sod1. In this process, copper and oxygen are key components of the activation process. The nature of the oxygen dependency has not been addressed.

Recent observations support a model in which Cu(I) derived from either Ccs1 D3 or a labile Cu(I) pool initially binds to an entry site in Sod1 prior to its translocation to the active site (preliminary data). This entry site Cu(I) is characterized by a trigonal Cys_2His environment, presumably by the cysteines of Sod1, or a combination of cysteines from Sod1 and domain 3 of Ccs1, and on histidine residue from the native active site. Superoxide anions produced from normal cellular respiration and the cytosolic NADPH oxidases appear to be recruited to this entry site Sod1 intermediate by virtue of an exposed electropositive hole adjacent to the entry site. Electrostatic attraction of either a superoxide anion or peroxyl anion to the entry site Cu(I) leads to either a Cu(I)-catalyzed generation of hydrogen peroxide leading to sulfenylation of a Sod1 thiolate, presumably Cys146. Binding of a peroxyl anion may directly mediate sulfenylation of Cys146. Sulfenic acid modifications are facile, and can resolve readily into inter- or intramolecular disulfide bonds, releasing H_2O in the process. Ccs1 likely mediates the disulfide exchange reactions leading to the mature Cys57-Cys146 disulfide in Sod1. This model is consistent with the copper- and oxygen-dependencies of the activation process. According to this model, oxygen, and particularly superoxide, is a modulator of Sod1

activity.

Recently, numerous proteins in the cytosol have been shown to contain either transient or stable disulfide bonds. Clearly, many of these proteins are oxidized in response to oxidants that may involve sulfenylation chemistry (127,128). It remains unclear whether Cu(I) mediates the oxidation of proteins other than Sod1. Transient binding of Cu(I) may contribute to the oxidation process. Copper is an abundant trace element and is tightly regulated due to its redox properties. Could cells have evolved a mechanism to utilize the redox properties of this potentially toxic ion to form necessary disulfide bonds as a stress response?

Sod1 has also been implicated in diverse roles in the cell, including that of a transcription factor (60). It is also established that peroxide is utilized as a signaling molecule to mediate differentiation, cell proliferation, and apoptosis (16,67). Since Sod1 is one of the most abundant enzymes in the cell, as well as a major producer of endogenous peroxide, Sod1 may have a role in mediating cell signaling through its native reaction as is known to be the case with the yeast Yck1. This may occur in microenvironments during normal cellular growth. Future studies will shed further insights into these potential mechanisms.

1.13 References

1. McCord, J.M. and Fridovich, I. (1969) Superoxide dismutase. An enzymic function for erythrocuprein (hemocuprein). *J. Biol. Chem.*, **244**, 6049-6055.

2. Culotta, V.C., Klomp, L.W., Strain, J., Casareno, R.L., Krems, B. and Gitlin, J.D. (1997) The copper chaperone for superoxide dismutase. *J. Biol. Chem.*, **272**, 23469-23472.

3. Brown, N.M., Torres, A.S., Doan, P.E. and O'Halloran, T.V. (2004) Oxygen and

the copper chaperone CCS regulate posttranslational activation of Cu,Zn superoxide dismutase. *Proc. Natl. Acad. Sci. U. S. A.*, **101**, 5518-5523.

4. Carroll, M.C., Girouard, J.B., Ulloa, J.L., Subramaniam, J.R., Wong, P.C., Valentine, J.S. and Culotta, V.C. (2004) Mechanisms for activating Cu- and Zn-containing superoxide dismutase in the absence of the CCS Cu chaperone. *Proc. Natl. Acad. Sci. U. S. A.*, **101**, 5964-5969.

5. Banci, L., Bertini, I., Cantini, F., Kozyreva, T., Massagni, C., Palumaa, P., Rubino, J.T. and Zovo, K. (2012) Human superoxide dismutase 1 (hSOD1) maturation through interaction with human copper chaperone for SOD1 (hCCS). *Proc. Natl. Acad. Sci. U. S. A.*, **109**, 13555-13560.

6. Field, L.S., Furukawa, Y., O'Halloran, T.V. and Culotta, V.C. (2003) Factors controlling the uptake of yeast copper/zinc superoxide dismutase into mitochondria. *J. Biol. Chem.*, **278**, 28052-28059.

7. Kawamata, H. and Manfredi, G. (2008) Different regulation of wild-type and mutant Cu,Zn superoxide dismutase localization in mammalian mitochondria. *Hum. Mol. Genet.*, **17**, 3303-3317.

8. Okado-Matsumoto, A. and Fridovich, I. (2001) Subcellular distribution of superoxide dismutases (SOD) in rat liver: Cu,Zn-SOD in mitochondria. *J. Biol. Chem.*, **276**, 38388-38393.

9. Sturtz, L.A., Diekert, K., Jensen, L.T., Lill, R. and Culotta, V.C. (2001) A fraction of yeast Cu,Zn-superoxide dismutase and its metallochaperone, CCS, localize to the intermembrane space of mitochondria. A physiological role for SOD1 in guarding against mitochondrial oxidative damage. *J. Biol. Chem.*, **276**, 38084-38089.

10. Islinger, M., Li, K.W., Seitz, J., Volkl, A. and Luers, G.H. (2009) Hitchhiking of Cu/Zn superoxide dismutase to peroxisomes--evidence for a natural piggyback import mechanism in mammals. *Traffic*, **10**, 1711-1721.

11. Gardner, P.R. and Fridovich, I. (1991) Superoxide sensitivity of the Escherichia coli aconitase. *J. Biol. Chem.*, **266**, 19328-19333.

12. Flint, D.H., Tuminello, J.F. and Emptage, M.H. (1993) The inactivation of Fe-S cluster containing hydro-lyases by superoxide. *J. Biol. Chem.*, **268**, 22369-22376.

13. Farr, S.B., D'Ari, R. and Touati, D. (1986) Oxygen-dependent mutagenesis in Escherichia coli lacking superoxide dismutase. *Proc. Natl. Acad. Sci. U. S. A.*, **83**, 8268-8272.

14. Gutteridge, J.M. (1984) Lipid peroxidation initiated by superoxide-dependent

hydroxyl radicals using complexed iron and hydrogen peroxide. *FEBS Lett.*, **172**, 245-249.

15. Quinlan, C.L., Goncalves, R.L., Hey-Mogensen, M., Yadava, N., Bunik, V.I. and Brand, M.D. (2014) The 2-oxoacid dehydrogenase complexes in mitochondria can produce superoxide/hydrogen peroxide at much higher rates than complex I. *J. Biol. Chem.*, **289**, 8312-8325.

16. Foreman, J., Demidchik, V., Bothwell, J.H., Mylona, P., Miedema, H., Torres, M.A., Linstead, P., Costa, S., Brownlee, C., Jones, J.D. *et al.* (2003) Reactive oxygen species produced by NADPH oxidase regulate plant cell growth. *Nature*, **422**, 442-446.

17. Weisiger, R.A. and Fridovich, I. (1973) Mitochondrial superoxide simutase. Site of synthesis and intramitochondrial localization. *J. Biol. Chem.*, **248**, 4793-4796.

18. Weisiger, R.A. and Fridovich, I. (1973) Superoxide dismutase. Organelle specificity. *J. Biol. Chem.*, **248**, 3582-3592.

19. Renton, A.E., Chio, A. and Traynor, B.J. (2014) State of play in amyotrophic lateral sclerosis genetics. *Nat. Neurosci.*, **17**, 17-23.

20. Valentine, J.S., Doucette, P.A. and Zittin Potter, S. (2005) Copper-zinc superoxide dismutase and amyotrophic lateral sclerosis. *Annu. Rev. Biochem.*, **74**, 563-593.

21. Sheng, Y., Chattopadhyay, M., Whitelegge, J. and Valentine, J.S. (2012) SOD1 aggregation and ALS: role of metallation states and disulfide status. *Curr. Top. Med. Chem.*, **12**, 2560-2572.

22. Banci, L., Bertini, I., Boca, M., Girotto, S., Martinelli, M., Valentine, J.S. and Vieru, M. (2008) SOD1 and amyotrophic lateral sclerosis: mutations and oligomerization. *PLoS One*, **3**, e1677.

23. Gurney, M.E., Pu, H., Chiu, A.Y., Dal Canto, M.C., Polchow, C.Y., Alexander, D.D., Caliendo, J., Hentati, A., Kwon, Y.W., Deng, H.X. *et al.* (1994) Motor neuron degeneration in mice that express a human Cu,Zn superoxide dismutase mutation. *Science*, **264**, 1772-1775.

24. Bruijn, L.I., Houseweart, M.K., Kato, S., Anderson, K.L., Anderson, S.D., Ohama, E., Reaume, A.G., Scott, R.W. and Cleveland, D.W. (1998) Aggregation and motor neuron toxicity of an ALS-linked SOD1 mutant independent from wild-type SOD1. *Science*, **281**, 1851-1854.

25. Cozzolino, M., Pesaresi, M.G., Amori, I., Crosio, C., Ferri, A., Nencini, M. and Carri, M.T. (2009) Oligomerization of mutant SOD1 in mitochondria of

motoneuronal cells drives mitochondrial damage and cell toxicity. *Antioxid. Redox Signal.*, **11**, 1547-1558.

26. Liu, J., Lillo, C., Jonsson, P.A., Vande Velde, C., Ward, C.M., Miller, T.M., Subramaniam, J.R., Rothstein, J.D., Marklund, S., Andersen, P.M. *et al.* (2004) Toxicity of familial ALS-linked SOD1 mutants from selective recruitment to spinal mitochondria. *Neuron*, **43**, 5-17.

27. Son, M., Leary, S.C., Romain, N., Pierrel, F., Winge, D.R., Haller, R.G. and Elliott, J.L. (2008) Isolated cytochrome c oxidase deficiency in G93A SOD1 mice overexpressing CCS protein. *J. Biol. Chem.*, **283**, 12267-12275.

28. Son, M., Puttaparthi, K., Kawamata, H., Rajendran, B., Boyer, P.J., Manfredi, G. and Elliott, J.L. (2007) Overexpression of CCS in G93A-SOD1 mice leads to accelerated neurological deficits with severe mitochondrial pathology. *Proc. Natl. Acad. Sci. U. S. A.*, **104**, 6072-6077.

29. Rodriguez, J.A., Shaw, B.F., Durazo, A., Sohn, S.H., Doucette, P.A., Nersissian, A.M., Faull, K.F., Eggers, D.K., Tiwari, A., Hayward, L.J. *et al.* (2005) Destabilization of apoprotein is insufficient to explain Cu,Zn-superoxide dismutase-linked ALS pathogenesis. *Proc. Natl. Acad. Sci. U. S. A.*, **102**, 10516-10521.

30. Rakhit, R., Robertson, J., Vande Velde, C., Horne, P., Ruth, D.M., Griffin, J., Cleveland, D.W., Cashman, N.R. and Chakrabartty, A. (2007) An immunological epitope selective for pathological monomer-misfolded SOD1 in ALS. *Nat. Med.*, **13**, 754-759.

31. Ho, Y.S., Gargano, M., Cao, J., Bronson, R.T., Heimler, I. and Hutz, R.J. (1998) Reduced fertility in female mice lacking copper-zinc superoxide dismutase. *J. Biol. Chem.*, **273**, 7765-7769.

32. Wang, X., Vatamaniuk, M.Z., Roneker, C.A., Pepper, M.P., Hu, L.G., Simmons, R.A. and Lei, X.G. (2011) Knockouts of SOD1 and GPX1 exert different impacts on murine islet function and pancreatic integrity. *Antioxid. Redox Signal.*, **14**, 391-401.

33. Huang, T.T., Yasunami, M., Carlson, E.J., Gillespie, A.M., Reaume, A.G., Hoffman, E.K., Chan, P.H., Scott, R.W. and Epstein, C.J. (1997) Superoxide-mediated cytotoxicity in superoxide dismutase-deficient fetal fibroblasts. *Arch. Biochem. Biophys.*, **344**, 424-432.

34. Muller, F.L., Song, W., Liu, Y., Chaudhuri, A., Pieke-Dahl, S., Strong, R., Huang, T.T., Epstein, C.J., Roberts, L.J., 2nd, Csete, M. *et al.* (2006) Absence of CuZn superoxide dismutase leads to elevated oxidative stress and acceleration of age-dependent skeletal muscle atrophy. *Free Radic. Biol. Med.*, **40**, 1993-2004.

35. Turner, B.J. and Talbot, K. (2008) Transgenics, toxicity and therapeutics in rodent models of mutant SOD1-mediated familial ALS. *Prog. Neurobiol.*, **85**, 94-134.

36. Reaume, A.G., Elliott, J.L., Hoffman, E.K., Kowall, N.W., Ferrante, R.J., Siwek, D.F., Wilcox, H.M., Flood, D.G., Beal, M.F., Brown, R.H., Jr. *et al.* (1996) Motor neurons in Cu/Zn superoxide dismutase-deficient mice develop normally but exhibit enhanced cell death after axonal injury. *Nat. Genet.*, **13**, 43-47.

37. Keithley, E.M., Canto, C., Zheng, Q.Y., Wang, X., Fischel-Ghodsian, N. and Johnson, K.R. (2005) Cu/Zn superoxide dismutase and age-related hearing loss. *Hear. Res.*, **209**, 76-85.

38. Perry, J.J., Shin, D.S., Getzoff, E.D. and Tainer, J.A. (2010) The structural biochemistry of the superoxide dismutases. *Biochim. Biophys. Acta*, **1804**, 245-262.

39. Tainer, J.A., Getzoff, E.D., Richardson, J.S. and Richardson, D.C. (1983) Structure and mechanism of copper, zinc superoxide dismutase. *Nature*, **306**, 284-287.

40. Richardson, J., Thomas, K.A., Rubin, B.H. and Richardson, D.C. (1975) Crystal structure of bovine Cu,Zn superoxide dismutase at 3 A resolution: chain tracing and metal ligands. *Proc. Natl. Acad. Sci. U. S. A.*, **72**, 1349-1353.

41. Tainer, J.A., Getzoff, E.D., Beem, K.M., Richardson, J.S. and Richardson, D.C. (1982) Determination and analysis of the 2 A-structure of copper, zinc superoxide dismutase. *J. Mol. Biol.*, **160**, 181-217.

42. Banci, L., Benedetto, M., Bertini, I., Del Conte, R., Piccioli, M. and Viezzoli, M.S. (1998) Solution structure of reduced monomeric Q133M2 copper, zinc superoxide dismutase (SOD). Why is SOD a dimeric enzyme? *Biochemistry*, **37**, 11780-11791.

43. Hart, P.J., Balbirnie, M.M., Ogihara, N.L., Nersissian, A.M., Weiss, M.S., Valentine, J.S. and Eisenberg, D. (1999) A structure-based mechanism for copper-zinc superoxide dismutase. *Biochemistry*, **38**, 2167-2178.

44. Hough, M.A. and Hasnain, S.S. (2003) Structure of fully reduced bovine copper zinc superoxide dismutase at 1.15 A. *Structure*, **11**, 937-946.

45. Forman, H.J. and Fridovich, I. (1973) On the stability of bovine superoxide dismutase. The effects of metals. *J. Biol. Chem.*, **248**, 2645-2649.

46. Roe, J.A., Butler, A., Scholler, D.M., Valentine, J.S., Marky, L. and Breslauer, K.J. (1988) Differential scanning calorimetry of Cu,Zn-superoxide dismutase, the apoprotein, and its zinc-substituted derivatives. *Biochemistry*, **27**, 950-958.

47. Leitch, J.M., Jensen, L.T., Bouldin, S.D., Outten, C.E., Hart, P.J. and Culotta, V.C. (2009) Activation of Cu,Zn-superoxide dismutase in the absence of oxygen and the copper chaperone CCS. *J. Biol. Chem.*, **284**, 21863-21871.

48. Ostergaard, H., Tachibana, C. and Winther, J.R. (2004) Monitoring disulfide bond formation in the eukaryotic cytosol. *J. Cell Biol.*, **166**, 337-345.

49. Arnesano, F., Banci, L., Bertini, I., Martinelli, M., Furukawa, Y. and O'Halloran, T.V. (2004) The unusually stable quaternary structure of human Cu,Zn-superoxide dismutase 1 is controlled by both metal occupancy and disulfide status. *J. Biol. Chem.*, **279**, 47998-48003.

50. Hornberg, A., Logan, D.T., Marklund, S.L. and Oliveberg, M. (2007) The coupling between disulphide status, metallation and dimer interface strength in Cu/Zn superoxide dismutase. *J. Mol. Biol.*, **365**, 333-342.

51. Banci, L., Bertini, I., Cantini, F., D'Amelio, N. and Gaggelli, E. (2006) Human SOD1 before harboring the catalytic metal: solution structure of copper-depleted, disulfide-reduced form. *J. Biol. Chem.*, **281**, 2333-2337.

52. Klug, D., Rabani, J. and Fridovich, I. (1972) A direct demonstration of the catalytic action of superoxide dismutase through the use of pulse radiolysis. *J. Biol. Chem.*, **247**, 4839-4842.

53. Polticelli, F., Battistoni, A., O'Neill, P., Rotilio, G. and Desideri, A. (1998) Role of the electrostatic loop charged residues in Cu,Zn superoxide dismutase. *Protein Sci.*, **7**, 2354-2358.

54. Beyer, W.F., Jr., Fridovich, I., Mullenbach, G.T. and Hallewell, R. (1987) Examination of the role of arginine-143 in the human copper and zinc superoxide dismutase by site-specific mutagenesis. *J. Biol. Chem.*, **262**, 11182-11187.

55. Getzoff, E.D., Tainer, J.A., Weiner, P.K., Kollman, P.A., Richardson, J.S. and Richardson, D.C. (1983) Electrostatic recognition between superoxide and copper, zinc superoxide dismutase. *Nature*, **306**, 287-290.

56. Corson, L.B., Strain, J.J., Culotta, V.C. and Cleveland, D.W. (1998) Chaperone-facilitated copper binding is a property common to several classes of familial amyotrophic lateral sclerosis-linked superoxide dismutase mutants. *Proc. Natl. Acad. Sci. U. S. A.*, **95**, 6361-6366.

57. Reddi, A.R. and Culotta, V.C. (2013) SOD1 integrates signals from oxygen and glucose to repress respiration. *Cell*, **152**, 224-235.

58. Liu, Z., Thornton, J., Spirek, M. and Butow, R.A. (2008) Activation of the SPS amino acid-sensing pathway in Saccharomyces cerevisiae correlates with the

phosphorylation state of a sensor component, Ptr3. *Mol. Cell. Biol.*, **28**, 551-563.

59. Moriya, H. and Johnston, M. (2004) Glucose sensing and signaling in Saccharomyces cerevisiae through the Rgt2 glucose sensor and casein kinase I. *Proc. Natl. Acad. Sci. U. S. A.*, **101**, 1572-1577.

60. Tsang, C.K., Liu, Y., Thomas, J., Zhang, Y. and Zheng, X.F. (2014) Superoxide dismutase 1 acts as a nuclear transcription factor to regulate oxidative stress resistance. *Nat. Commun.*, **5**, 3446.

61. Juarez, J.C., Manuia, M., Burnett, M.E., Betancourt, O., Boivin, B., Shaw, D.E., Tonks, N.K., Mazar, A.P. and Donate, F. (2008) Superoxide dismutase 1 (SOD1) is essential for H2O2-mediated oxidation and inactivation of phosphatases in growth factor signaling. *Proc. Natl. Acad. Sci. U. S. A.*, **105**, 7147-7152.

62. Kamata, H., Honda, S., Maeda, S., Chang, L., Hirata, H. and Karin, M. (2005) Reactive oxygen species promote TNFalpha-induced death and sustained JNK activation by inhibiting MAP kinase phosphatases. *Cell*, **120**, 649-661.

63. Denu, J.M. and Tanner, K.G. (1998) Specific and reversible inactivation of protein tyrosine phosphatases by hydrogen peroxide: evidence for a sulfenic acid intermediate and implications for redox regulation. *Biochemistry*, **37**, 5633-5642.

64. Lee, S.R., Kwon, K.S., Kim, S.R. and Rhee, S.G. (1998) Reversible inactivation of protein-tyrosine phosphatase 1B in A431 cells stimulated with epidermal growth factor. *J. Biol. Chem.*, **273**, 15366-15372.

65. Lee, S.R., Yang, K.S., Kwon, J., Lee, C., Jeong, W. and Rhee, S.G. (2002) Reversible inactivation of the tumor suppressor PTEN by H2O2. *J. Biol. Chem.*, **277**, 20336-20342.

66. Meng, T.C., Fukada, T. and Tonks, N.K. (2002) Reversible oxidation and inactivation of protein tyrosine phosphatases in vivo. *Mol. Cell*, **9**, 387-399.

67. Holmstrom, K.M. and Finkel, T. (2014) Cellular mechanisms and physiological consequences of redox-dependent signalling. *Nat. Rev. Mol. Cell Biol.*, **15**, 411-421.

68. Reddehase, S., Grumbt, B., Neupert, W. and Hell, K. (2009) The disulfide relay system of mitochondria is required for the biogenesis of mitochondrial Ccs1 and Sod1. *J. Mol. Biol.*, **385**, 331-338.

69. Gross, D.P., Burgard, C.A., Reddehase, S., Leitch, J.M., Culotta, V.C. and Hell, K. (2011) Mitochondrial Ccs1 contains a structural disulfide bond crucial for the import of this unconventional substrate by the disulfide relay system. *Mol. Biol. Cell*, **22**, 3758-3767.

70. Suzuki, Y., Ali, M., Fischer, M. and Riemer, J. (2013) Human copper chaperone for superoxide dismutase 1 mediates its own oxidation-dependent import into mitochondria. *Nat. Commun.*, **4**, 2430.

71. Outten, C.E. and O'Halloran, T.V. (2001) Femtomolar sensitivity of metalloregulatory proteins controlling zinc homeostasis. *Science*, **292**, 2488-2492.

72. MacDiarmid, C.W., Gaither, L.A. and Eide, D. (2000) Zinc transporters that regulate vacuolar zinc storage in Saccharomyces cerevisiae. *EMBO J.*, **19**, 2845-2855.

73. Suhy, D.A., Simon, K.D., Linzer, D.I. and O'Halloran, T.V. (1999) Metallothionein is part of a zinc-scavenging mechanism for cell survival under conditions of extreme zinc deprivation. *J. Biol. Chem.*, **274**, 9183-9192.

74. Sea, K.W., Sheng, Y., Lelie, H.L., Kane Barnese, L., Durazo, A., Valentine, J.S. and Gralla, E.B. (2013) Yeast copper-zinc superoxide dismutase can be activated in the absence of its copper chaperone. *J. Biol. Inorg. Chem.*, **18**, 985-992.

75. Banci, L., Barbieri, L., Bertini, I., Luchinat, E., Secci, E., Zhao, Y. and Aricescu, A.R. (2013) Atomic-resolution monitoring of protein maturation in live human cells by NMR. *Nat. Chem. Biol.*, **9**, 297-299.

76. Schmidt, P.J., Rae, T.D., Pufahl, R.A., Hamma, T., Strain, J., O'Halloran, T.V. and Culotta, V.C. (1999) Multiple protein domains contribute to the action of the copper chaperone for superoxide dismutase. *J. Biol. Chem.*, **274**, 23719-23725.

77. Rae, T.D., Schmidt, P.J., Pufahl, R.A., Culotta, V.C. and O'Halloran, T.V. (1999) Undetectable intracellular free copper: the requirement of a copper chaperone for superoxide dismutase. *Science*, **284**, 805-808.

78. Kloppel, C., Suzuki, Y., Kojer, K., Petrungaro, C., Longen, S., Fiedler, S., Keller, S. and Riemer, J. (2011) Mia40-dependent oxidation of cysteines in domain I of Ccs1 controls its distribution between mitochondria and the cytosol. *Mol. Biol. Cell*, **22**, 3749-3757.

79. Lamb, A.L., Wernimont, A.K., Pufahl, R.A., Culotta, V.C., O'Halloran, T.V. and Rosenzweig, A.C. (1999) Crystal structure of the copper chaperone for superoxide dismutase. *Nat. Struct. Biol.*, **6**, 724-729.

80. Banci, L., Cantini, F., Kozyreva, T. and Rubino, J.T. (2013) Mechanistic aspects of hSOD1 maturation from the solution structure of Cu(I) -loaded hCCS domain 1 and analysis of disulfide-free hSOD1 mutants. *Chembiochem.*, **14**, 1839-1844.

81. Lamb, A.L., Wernimont, A.K., Pufahl, R.A., O'Halloran, T.V. and Rosenzweig, A.C. (2000) Crystal structure of the second domain of the human copper

chaperone for superoxide dismutase. *Biochemistry*, **39**, 1589-1595.

82. Lamb, A.L., Torres, A.S., O'Halloran, T.V. and Rosenzweig, A.C. (2000) Heterodimer formation between superoxide dismutase and its copper chaperone. *Biochemistry*, **39**, 14720-14727.

83. Schmidt, P.J., Ramos-Gomez, M. and Culotta, V.C. (1999) A gain of superoxide dismutase (SOD) activity obtained with CCS, the copper metallochaperone for SOD1. *J. Biol. Chem.*, **274**, 36952-36956.

84. Lamb, A.L., Torres, A.S., O'Halloran, T.V. and Rosenzweig, A.C. (2001) Heterodimeric structure of superoxide dismutase in complex with its metallochaperone. *Nat. Struct. Biol.*, **8**, 751-755.

85. Allen, S., Badarau, A. and Dennison, C. (2012) Cu(I) affinities of the domain 1 and 3 sites in the human metallochaperone for Cu,Zn-superoxide dismutase. *Biochemistry*, **51**, 1439-1448.

86. Robinson, N.J. and Winge, D.R. (2010) Copper metallochaperones. *Annu. Rev. Biochem.*, **79**, 537-562.

87. Rae, T.D., Torres, A.S., Pufahl, R.A. and O'Halloran, T.V. (2001) Mechanism of Cu,Zn-superoxide dismutase activation by the human metallochaperone hCCS. *J. Biol. Chem.*, **276**, 5166-5176.

88. Furukawa, Y., Torres, A.S. and O'Halloran, T.V. (2004) Oxygen-induced maturation of SOD1: a key role for disulfide formation by the copper chaperone CCS. *EMBO J.*, **23**, 2872-2881.

89. Wong, P.C., Waggoner, D., Subramaniam, J.R., Tessarollo, L., Bartnikas, T.B., Culotta, V.C., Price, D.L., Rothstein, J. and Gitlin, J.D. (2000) Copper chaperone for superoxide dismutase is essential to activate mammalian Cu/Zn superoxide dismutase. *Proc. Natl. Acad. Sci. U. S. A.*, **97**, 2886-2891.

90. Jensen, L.T. and Culotta, V.C. (2005) Activation of CuZn superoxide dismutases from Caenorhabditis elegans does not require the copper chaperone CCS. *J. Biol. Chem.*, **280**, 41373-41379.

91. Sea, K., Sohn, S.H., Durazo, A., Sheng, Y., Shaw, B.F., Cao, X., Taylor, A.B., Whitson, L.J., Holloway, S.P., Hart, P.J. *et al.* (2015) Insights into the role of the unusual disulfide bond in copper-zinc superoxide dismutase. *J. Biol. Chem.*, **290**, 2405-2418.

92. Portnoy, M.E., Schmidt, P.J., Rogers, R.S. and Culotta, V.C. (2001) Metal transporters that contribute copper to metallochaperones in Saccharomyces cerevisiae. *Mol. Genet. Genomics*, **265**, 873-882.

93. Zhou, B. and Gitschier, J. (1997) hCTR1: a human gene for copper uptake identified by complementation in yeast. *Proc. Natl. Acad. Sci. U. S. A.*, **94**, 7481-7486.

94. Hassett, R. and Kosman, D.J. (1995) Evidence for Cu(II) reduction as a component of copper uptake by Saccharomyces cerevisiae. *J. Biol. Chem.*, **270**, 128-134.

95. Georgatsou, E., Mavrogiannis, L.A., Fragiadakis, G.S. and Alexandraki, D. (1997) The yeast Fre1p/Fre2p cupric reductases facilitate copper uptake and are regulated by the copper-modulated Mac1p activator. *J. Biol. Chem.*, **272**, 13786-13792.

96. De Feo, C.J., Aller, S.G., Siluvai, G.S., Blackburn, N.J. and Unger, V.M. (2009) Three-dimensional structure of the human copper transporter hCTR1. *Proc. Natl. Acad. Sci. U. S. A.*, **106**, 4237-4242.

97. Puig, S., Lee, J., Lau, M. and Thiele, D.J. (2002) Biochemical and genetic analyses of yeast and human high affinity copper transporters suggest a conserved mechanism for copper uptake. *J. Biol. Chem.*, **277**, 26021-26030.

98. Eisses, J.F. and Kaplan, J.H. (2002) Molecular characterization of hCTR1, the human copper uptake protein. *J. Biol. Chem.*, **277**, 29162-29171.

99. Guo, Y., Smith, K., Lee, J., Thiele, D.J. and Petris, M.J. (2004) Identification of methionine-rich clusters that regulate copper-stimulated endocytosis of the human Ctr1 copper transporter. *J. Biol. Chem.*, **279**, 17428-17433.

100. Pope, C.R., De Feo, C.J. and Unger, V.M. (2013) Cellular distribution of copper to superoxide dismutase involves scaffolding by membranes. *Proc. Natl. Acad. Sci. U. S. A.*, **110**, 20491-20496.

101. Maryon, E.B., Molloy, S.A. and Kaplan, J.H. (2013) Cellular glutathione plays a key role in copper uptake mediated by human copper transporter 1. *Am. J. Physiol. Cell Physiol.*, **304**, C768-779.

102. Ciriolo, M.R., Desideri, A., Paci, M. and Rotilio, G. (1990) Reconstitution of Cu,Zn-superoxide dismutase by the Cu(I).glutathione complex. *J. Biol. Chem.*, **265**, 11030-11034.

103. Ciriolo, M.R., Battistoni, A., Falconi, M., Filomeni, G. and Rotilio, G. (2001) Role of the electrostatic loop of Cu,Zn superoxide dismutase in the copper uptake process. *Eur. J. Biochem.*, **268**, 737-742.

104. Davies, M.J. (2016) Protein oxidation and peroxidation. *Biochem. J.*, **473**, 805-825.

105. Johnson, D.R. and Decker, E.A. (2015) The role of oxygen in lipid oxidation reactions: a review. *Annu. Rev. Food Sci. Technol.*, **6**, 171-190.

106. Gregory, E.M., Goscin, S.A. and Fridovich, I. (1974) Superoxide dismutase and oxygen toxicity in a eukaryote. *J. Bacteriol.*, **117**, 456-460.

107. Leitch, J.M., Li, C.X., Baron, J.A., Matthews, L.M., Cao, X., Hart, P.J. and Culotta, V.C. (2012) Post-translational modification of Cu/Zn superoxide dismutase under anaerobic conditions. *Biochemistry*, **51**, 677-685.

108. Kojer, K., Bien, M., Gangel, H., Morgan, B., Dick, T.P. and Riemer, J. (2012) Glutathione redox potential in the mitochondrial intermembrane space is linked to the cytosol and impacts the Mia40 redox state. *EMBO J.*, **31**, 3169-3182.

109. Morgan, B., Sobotta, M.C. and Dick, T.P. (2011) Measuring E(GSH) and H2O2 with roGFP2-based redox probes. *Free. Radic. Biol. Med.*, **51**, 1943-1951.

110. Hu, J., Dong, L. and Outten, C.E. (2008) The redox environment in the mitochondrial intermembrane space is maintained separately from the cytosol and matrix. *J. Biol. Chem.*, **283**, 29126-29134.

111. Hwang, C., Sinskey, A.J. and Lodish, H.F. (1992) Oxidized redox state of glutathione in the endoplasmic reticulum. *Science*, **257**, 1496-1502.

112. Kojer, K., Peleh, V., Calabrese, G., Herrmann, J.M. and Riemer, J. (2015) Kinetic control by limiting glutaredoxin amounts enables thiol oxidation in the reducing mitochondrial intermembrane space. *Mol. Biol. Cell*, **26**, 195-204.

113. Allen, S., Balabanidou, V., Sideris, D.P., Lisowsky, T. and Tokatlidis, K. (2005) Erv1 mediates the Mia40-dependent protein import pathway and provides a functional link to the respiratory chain by shuttling electrons to cytochrome c. *J. Mol. Biol.*, **353**, 937-944.

114. Banci, L., Bertini, I., Cefaro, C., Cenacchi, L., Ciofi-Baffoni, S., Felli, I.C., Gallo, A., Gonnelli, L., Luchinat, E., Sideris, D. *et al.* (2010) Molecular chaperone function of Mia40 triggers consecutive induced folding steps of the substrate in mitochondrial protein import. *Proc. Natl. Acad. Sci. U. S. A.*, **107**, 20190-20195.

115. Mesecke, N., Terziyska, N., Kozany, C., Baumann, F., Neupert, W., Hell, K. and Herrmann, J.M. (2005) A disulfide relay system in the intermembrane space of mitochondria that mediates protein import. *Cell*, **121**, 1059-1069.

116. Laboissiere, M.C., Sturley, S.L. and Raines, R.T. (1995) The essential function of protein-disulfide isomerase is to unscramble non-native disulfide bonds. *J. Biol. Chem.*, **270**, 28006-28009.

117. Delaunay, A., Pflieger, D., Barrault, M.B., Vinh, J. and Toledano, M.B. (2002) A thiol peroxidase is an H2O2 receptor and redox-transducer in gene activation. *Cell*, **111**, 471-481.

118. Dalle-Donne, I., Rossi, R., Colombo, G., Giustarini, D. and Milzani, A. (2009) Protein S-glutathionylation: a regulatory device from bacteria to humans. *Trends Biochem. Sci.*, **34**, 85-96.

119. Hess, D.T., Matsumoto, A., Kim, S.O., Marshall, H.E. and Stamler, J.S. (2005) Protein S-nitrosylation: purview and parameters. *Nat. Rev. Mol. Cell Biol.*, **6**, 150-166.

120. Lo Conte, M. and Carroll, K.S. (2013) The redox biochemistry of protein sulfenylation and sulfinylation. *J. Biol. Chem.*, **288**, 26480-26488.

121. Gupta, V. and Carroll, K.S. (2014) Sulfenic acid chemistry, detection and cellular lifetime. *Biochim. Biophys. Acta.*, **1840**, 847-875.

122. van Bergen, L.A., Roos, G. and De Proft, F. (2014) From thiol to sulfonic acid: modeling the oxidation pathway of protein thiols by hydrogen peroxide. *J. Phys. Chem. A.*, **118**, 6078-6084.

123. Rehder, D.S. and Borges, C.R. (2010) Cysteine sulfenic acid as an intermediate in disulfide bond formation and nonenzymatic protein folding. *Biochemistry*, **49**, 7748-7755.

124. Paulsen, C.E. and Carroll, K.S. (2009) Chemical dissection of an essential redox switch in yeast. *Chem. Biol.*, **16**, 217-225.

125. Sobotta, M.C., Liou, W., Stocker, S., Talwar, D., Oehler, M., Ruppert, T., Scharf, A.N. and Dick, T.P. (2015) Peroxiredoxin-2 and STAT3 form a redox relay for H2O2 signaling. *Nat. Chem. Biol.*, **11**, 64-70.

126. Conte, M.L. and Carroll, K.S. (2013) In Jakob, U. and Reichmann, D. (eds.), *Oxidative Stress and Redox Regulation*. Springer Netherlands, Dordrecht, pp. 1-42.

127. Brandes, N., Reichmann, D., Tienson, H., Leichert, L.I. and Jakob, U. (2011) Using quantitative redox proteomics to dissect the yeast redoxome. *J. Biol. Chem.*, **286**, 41893-41903.

128. Godon, C., Lagniel, G., Lee, J., Buhler, J.M., Kieffer, S., Perrot, M., Boucherie, H., Toledano, M.B. and Labarre, J. (1998) The H2O2 stimulon in Saccharomyces cerevisiae. *J. Biol. Chem.*, **273**, 22480-22489.

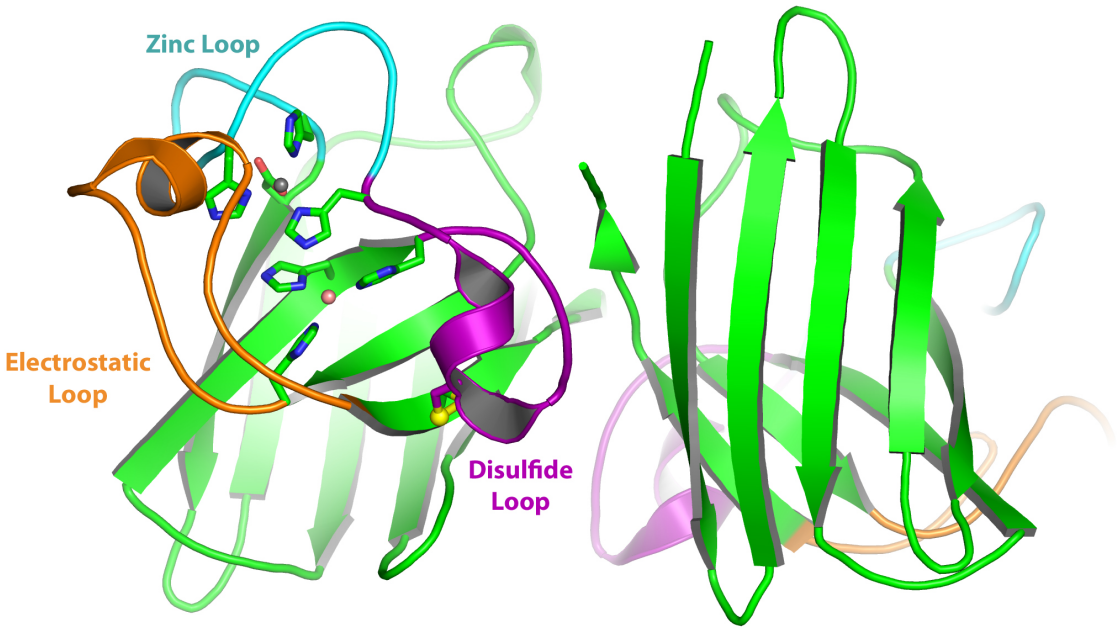

Figure 1.1 The crystal structure of the holo, homodimeric human Sod1.

The backbone barrel domain is shown in green. The zinc ion is shown in grey, while the copper ion is shown in orange. The zinc loop and the electrostatic loop are shown in cyan and orange, respectively, while the disulfide loop is shown in purple.

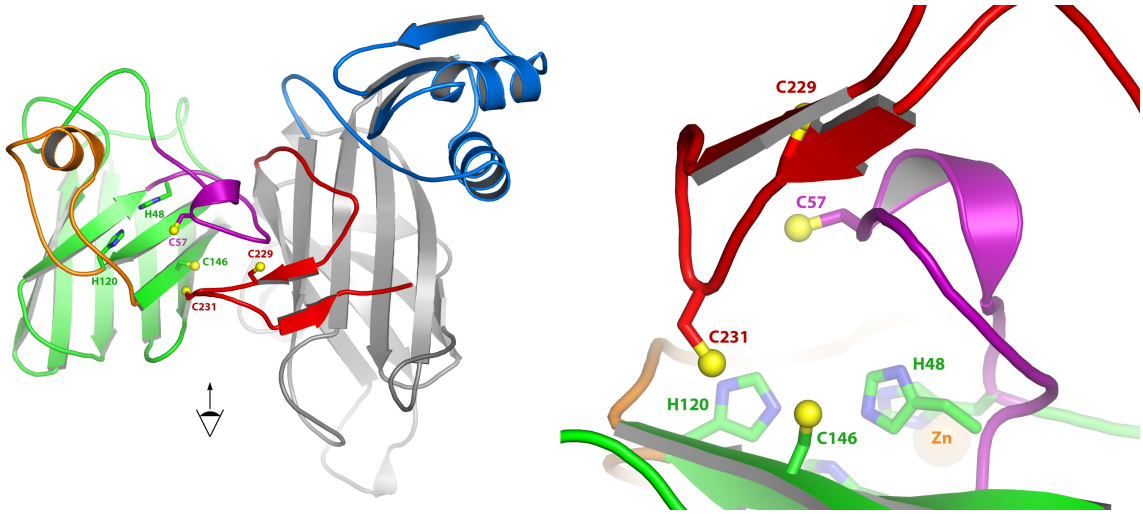

Figure 1.2 Crystal structure of the heterodimeric Sod1/Ccs1 stalled complex.

Left, the crystal structure of the complex where Sod1 is present in green with the electrostatic loop highlighted in orange and the disulfide loop is shown in purple. Copper binding ligands His 48 and His120 of Sod1 are shown as well as the two cysteine residues (C57 and C146). Ccs1 domain 1 is highlight in blue, domain 2 in grey, and domain 3 in red. Right, the dimer interface has been rotated ~180 degrees and zoomed. Shows the proposed entry site ligands of Ccs1(red) and Sod1(purple and green).

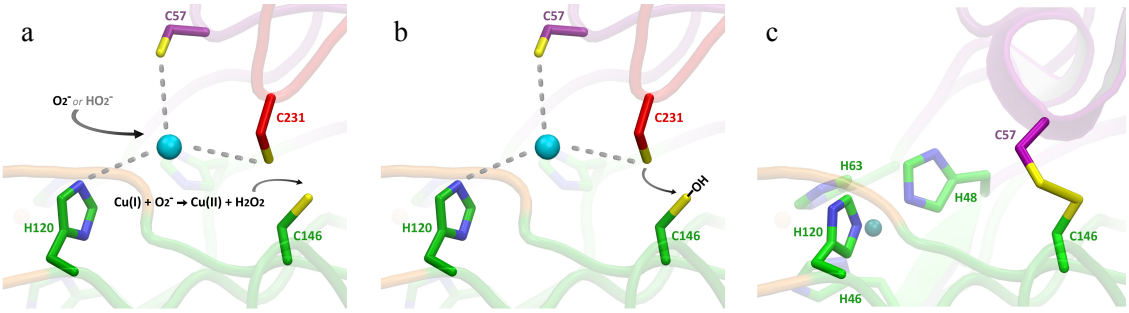

Figure 1.3 Model of the Ccs1 dependent activation of Sod1.

a) Ccs1 is able to stabilize a conformation that allows for copper to bind in a Cys2His entry site. Superoxide is funneled to the copper through electrostatic guidance created at the dimer interface between Sod1 and Ccs1. Cu(I) reacts with superoxide at the entry site to produce hydrogen peroxide which then reacts with the closest thiol (Cys146) to form a sulfenic acid. **b)** The sulfenic acid formed on C146 of Sod1 undergoes a nucleophilic attack from the C231 thiolate of Ccs1. This form a intermolecular disulfide bond, which is resolved by subsequent nucleophilic attacks from the other cys residues in the relay. **c)** The disulfide relay is capped off by formation of a disulfide between C57 and C146 of Sod1. The disulfide formation pushes Cu(II) into the native active site and Ccs1 dissociates.

CHAPTER 2

COPPER-ZINC SUPEROXIDE DISMUTASE IS ACTIVATED THROUGH A SULFENIC ACID INTERMEDIATE AT A COPPER-ION ENTRY SITE

Morgan M. Fetherolf,[1] Stefanie B. Sneed,[2] Alexander B. Taylor,[3,4] Ninian J. Blackburn,[6] Dennis R. Winge,[1] P. John Hart,[3,4,5] and Duane D. Winkler[2*]

[1]Department of Medicine, University of Utah Health Sciences Center School of Medicine, 30 North 1900 East, Salt Lake City, UT 84132-2408, USA; Department of Biochemistry, University of Utah, 15 North Medical Drive East, Salt Lake City, UT 84112-5650, USA.

[2]Department of Biological Sciences, University of Texas at Dallas, 800 W. Campbell Road, Richardson, TX 75080, USA.

[3]Department of Biochemistry and [4]*X-ray Crystallography Core Laboratory*, University of Texas Health Science Center at San Antonio, 7703 Floyd Curl Drive, San Antonio, TX 78229, USA; [5]Geriatric Research, Education, and Clinical Center, Department of Veterans Affairs, South Texas Veterans Health Care System, University of Texas Health Science Center at San Antonio, San Antonio, TX 78229, USA.

[6]Institute of Environmental Health, Oregon Health and Science University, 3181 Southwest Sam Jackson Park Road, Portland, Oregon 97239, USA.

2.1 Abstract

Metallo-chaperones are a diverse family of trafficking molecules that provide metal ions to protein targets for use as cofactors. The copper chaperone for Sod1 (Ccs1) activates immature copper-zinc superoxide dismutase (Sod1) by delivering copper and catalyzing the oxidation of the Sod1 intramolecular disulfide bond. Here, we present structural, spectroscopic, and cell-based data supporting a novel copper-induced mechanism for Sod1 activation. Ccs1 binding exposes an electropositive cavity and proposed "entry site" for copper ion delivery on immature Sod1. Copper-mediated turnover of superoxide at this site produces hydrogen peroxide and Cu(II). Local peroxide generation leads to a sulfenic acid intermediate that eventually resolves to form the Sod1 disulfide bond with concomitant release of copper into the Sod1 active site. Sod1 is the predominant disulfide bond requiring enzyme in the cytoplasm and this copper-induced mechanism of disulfide bond formation obviates the need for a thiol/disulfide oxidoreductase in that compartment.

2.2 Significance

We demonstrate with a novel structure of a complex between Cu,Zn-superoxide dismutase and its chaperone Ccs1 and molecular studies that the Ccs1-mediated activation of Sod1 proceeds through a copper-mediated sulfenylation intermediate that resolves to form the essential Sod1 disulfide bond. The structure of Ccs1 bound to an immature form of Sod1 at 2.35 Å reveals a previously unobserved b-hairpin conformation of Ccs1 that creates an electropositive hole adjacent to a Cu(I) binding entry site. Attraction of a superoxide anion towards the electropositive hole leads

to a single catalytic turnover generating Cu(II) and hydrogen peroxide that mediates Sod1 sulfenylation as an intermediate in disulfide bond formation. This mechanism is a novel copper-mediated disulfide process in the highly reducing cytoplasm.

2.3 Introduction

The copper chaperone for superoxide dismutase (Ccs1) activates newly translated copper-zinc superoxide dismutase (Sod1) proteins (1). Sod1 is a critical antioxidant enzyme that detoxifies superoxide, a byproduct of cellular respiration, through redox cycling at its catalytic copper ion [$2O_2^- + 2H^+ \rightarrow H_2O_2 + O_2$] (2). Nascent Sod1 is inactive and monomeric (3-7), but is converted to its active homodimeric form through its interaction with Ccs1 (1,6,8). Yeast lacking Ccs1 are devoid of Sod1 enzymatic activity unless exogenous copper is added to the culture medium (9,10). Like *ccs1*Δ yeast, *Drosophila melanogaster* deficient in Ccs1 lack Sod1 activity and are hypersensitive to oxidative stress (11). Expression of human Sod1 in yeast *ccs1*Δ cells results in limited Sod1 activity (~25%) through the ability of a subset of hSod1 proteins to acquire copper independent of Ccs1 (11,12).

Ccs1 proteins are comprised of three domains (D1, D2, and D3), each of which plays a specialized role in Sod1 activation (9). The N-terminal domain (D1) contains a MxCxxC copper binding motif and is required under copper-limiting growth conditions, suggesting it may participate in the acquisition of copper from the membrane transporter Ctr1 (9,13,14). The second domain (D2) possesses significant sequence and structural similarity with Sod1 that permits it to mediate interaction with the immature molecule via residues analogous to those found at the Sod1 homodimeric interface (15-18). Like D2,

the C-terminal domain (D3) is essential for Sod1 activation and contains an invariant CxC motif (1,9). Cells containing Ccs1 proteins lacking the D3 CxC motif possess Sod1 proteins devoid of copper and intra-subunit disulfide bonds (8,9,19).

Multiple studies have sought to delineate the mechanism by which Ccs1 activates Sod1. Experiments in yeast demonstrated that Ccs1 acts on newly synthesized, metal-free Sod1 to facilitate Cu(I) ion insertion and oxidation of the Sod1 intra-subunit disulfide bond (20). The presence of a disulfide bond in Sod1 is unusual for an enzyme found predominantly in the highly reducing cytosolic environment. The two major cellular compartments in eukaryotes in which disulfide oxidation is commonly observed are the lumen of the endoplasmic reticulum and the mitochondrial intermembrane space, both of which contain thiol/disulfide oxidoreductases [reviewed in (21)]. Although the mechanism of disulfide oxidation in nascent cytosolic Sod1 had been elusive until now, it was known that the disulfide bond is essential for full catalytic activity because it anchors the side chain of R_{143} adjacent to the catalytic copper ion where it helps to guide superoxide into the active site (22).

Copper ion delivery and disulfide bond oxidation appear to be linked processes. In Ccs1-containing yeast, Sod1 mutants unable to bind copper in the active site remain largely disulfide reduced (23). The addition of Cu-Ccs1 to Zn-Sod1 fails to induce oxidation of the disulfide bond anaerobically, but this process is facile in the presence of oxygen or superoxide (20). A previous yeast Sod1•Ccs1 crystal structure revealed an intermolecular disulfide between C_{57} of Sod1 and C_{229} of Ccs1, suggesting the intermolecular disulfide may be an intermediate that eventually resolves to the C_{57}-C_{146} disulfide via a disulfide exchange reaction (18).

Unlike mammalian Sod1 proteins, yeast Sod1 proteins cannot acquire copper via the Ccs1-independent pathway (10,24). The electrostatic loop of yeast Sod1 contains two proline residues that preclude the low levels of Ccs1-independent activation observed in the human and mouse enzymes (12,25). Replacement of the Pro residues (P_{142} and P_{144}) in the yeast enzyme with their cognate residues from mammalian Sod1 proteins permits yeast enzyme activation via a Ccs1-indpendent pathway (12). Likewise, ~25% of the Sod1 pool is active in *ccs1* -/- null mice (26). The activation of Sod1 proteins without Pro at these positions in *ccs1*D yeast cells (11,24) or in *ccs1* -/- null mice suggests the copper ion may be provided by labile Cu(I) complexes in the yeast cytosol (e.g., Cu-glutathione) (27,28).

Here, we present structural, biochemical, and spectroscopic data that suggest a mechanism of Sod1 activation not previously described. Crystallographic studies on a new Sod1•Ccs1 complex reveal a cavity with positive electrostatic potential exposed by a previously unobserved β-hairpin conformation of Ccs1 D3 that embraces the Sod1 "disulfide loop," displacing it from the β-barrel. Spectroscopic studies establish that Cu(I) is held at a $(Cys)_2(His)$ “entry site” adjacent to the electropositive cavity and Sod1•Ccs1 interface. *In vivo* studies of yeast Sod1 and its variants strongly suggest that the “entry site” is functionally relevant and that disulfide formation and Cu delivery into the Sod1 active site are linked processes dependent on sulfenylation of C_{146}. This new model is consistent with the vast majority of the biochemical data on Ccs1-mediated activation in the literature.

2.4 Results

2.4.1 *Role(s) of Ccs1 D3 in Sod1 Activation*

Previous studies have highlighted the importance of the CxC motif in Ccs1 D3 for Sod1 activation (9,29); however, debate continues on its exact role. Existing data suggest that the CxC motif mediates Cu(I) transfer from D1 to Sod1 (9) and/or oxidation of the Sod1 disulfide bond (8,20). We attempted to glean additional insights into the role of D3 by structurally characterizing the Sod1•Ccs1 heterocomplex and evaluating residue spacing within the CxC motif.

Previously, Lamb and colleagues determined the structure of a yeast H48F Sod1•Ccs1 heterotetramer containing two Sod1•Ccs1 heterodimers in the asymmetric unit related by two-fold noncrystallographic symmetry (NCS) (18). Heterotetramer assembly was mediated by reciprocal "swapping" interactions in which a highly conserved Ccs1 D3 $_{237}$WEER$_{240}$ a-helical motif bound to grooves on D2 of NCS-related heterodimers (**Figure S2.1**) (18). To probe the importance of the $_{237}$WEER$_{240}$ motif, we created a series of mutants targeting these residues. One variant, E$_{238}$A/E$_{239}$A/R$_{240}$A ($_{237}$WAAA$_{240}$) demonstrated ~5-fold greater yield and enhanced resistance to the trypsinolysis observed at K66 in the linker region between D2 and D3 in wild type Ccs1 (17). H$_{46}$R/H$_{48}$Q Sod1 possesses an ablated copper-binding site (23) and forms a highly stable, H$_{46}$R/H$_{48}$Q Sod1•E$_{238}$A/E$_{239}$A/R$_{240}$A Ccs1 heterocomplex useful here for structural analysis.

2.4.2 *New* S*tructure of the Sod1•Ccs1 Complex*

Structure of the $H_{46}R/H_{48}Q$ Sod1•$E_{238}A/E_{239}A/R_{240}A$ Ccs1 complex was determined by molecular replacement and refined in space group $P2_12_12$ to a resolution of 2.35 Å. **Table 2.1** provides the X-ray diffraction and structure refinement statistics. Although the asymmetric unit contains two Sod1•Ccs1 heterodimers related by noncrystallographic symmetry, the D3 conformation and heterodimeric orientations are dramatically different from the previous yeast H48F Sod1•Ccs1 heterotetramer structure (**Figure S2.1**) (18). D3 in the new structure adopts a compact β-hairpin conformation that strengthens the Sod1•Ccs1 interaction, consistent with previous data indicating that the Sod1•Ccs1 complex exists as a stable heterodimer in solution (16,23), and in contrast to the extended α-helical and/or disordered conformations of D3 observed in earlier work (17,18) (**Figure 2.1a, b**).

Multiple interactions with residues coming from Ccs1 D1 and D2 stabilize the b-hairpin conformation of Ccs1 D3 (**Figure 2.1c**). The indole ring of W_{222} stacks with the side chain of R_{105} from D2, immobilizing the residues immediately N-terminal to the β-hairpin (**Figure 2.1a, c**). The buried location of W_{222} is dramatically different from the solvent exposed environment observed in a previous Sod1•Ccs1 complex structure (**Figure 2.1b**). The invariant $_{237}WEER_{240}$ tryptophan fits nicely into a hydrophobic pocket on D2 formed by residues I_{83}, V_{100}, and L_{103} and seemingly acts as a "latch" stabilizing the D3 β-hairpin (**Figure 2.1a, c**).

Previous studies in solution reported that Ccs1 D3 is required not only for Sod1 activation, but also for robust Sod1•Ccs1 interaction (30). The Sod1•Ccs1 complex structure presented here provides a clear molecular basis for the latter observation.

Figure 2.1c highlights the interface between the Sod1 "disulfide loop" region and the Ccs1 D3 β-hairpin as a stereo-image of the representative αA electron density with coefficients 2*m*Fo-*D*Fc contoured at 1.2 σ superimposed on the refined model. The large number of interactions between Sod1 and Ccs1 (**Table S2.1**) can occur only when the Sod1 disulfide bond is reduced, consistent with previous observations of stable Sod1•Ccs1 binding only under reducing conditions (23). These interactions, together with the unanticipated intercalation of the D3 CxC motif cysteine (C_{231}) between the disulfide loop and β-barrel of Sod1, create a cysteine-rich "notch-into-groove" complementary surface (**Figure S2.2**).

2.4.3 *Spacing of D3 CxC Residues is Critical for Sod1 Activation*

By altering the spacing of the Ccs1 D3 CxC cysteines, we can begin to differentiate the roles of copper delivery and disulfide bond formation catalyzed by Ccs1. Yeast mutants lacking mature (e.g., metal bound, disulfide oxidized) Sod1 are lysine auxotrophs and exhibit impaired growth in -Lys media. Growth of the CxC variant yeast strains were largely compromised (**Figure 2.2a, b** and **S2.3**) and lysates from these cells exhibited nominal Sod1 activity (**Figure 2.2c**). However, Sod1 can be partially activated in cells expressing the $C_{230}C_{231}$ Ccs1 variant as growth was comparable to WT cells and lysates exhibited residual Sod1 activity at both 30° and 37°C (**Figure 2.2b, c**). Only minimal Sod1 activity is required for cell growth. These results suggest that two thiolates are necessary in Ccs1 D3 for Sod1 activation and that a strong positional effect is observed for both. With a dithiol configuration, only a $C_{230}C_{231}$ Ccs1 variant shows any significant Sod1 activation. The $C_{230}C_{231}$ Ccs1 variant, which cannot form an

intramolecular D3 disulfide, ostensibly *rule out* prior models implicating Ccs1 D3-mediated shuffling of a preformed disulfide bond to Sod1 during activation (8,20,31).

To assess the redox status of the Sod1 disulfide bond in these studies, thiol-specific alkylation experiments were performed. Modification of cysteines with polyethylene glycol modified N-ethyl maleimide (m-PEG) selectively adds 2 kDa per free thiol. Sod1 present in WT cells is resistant to m-PEG modification, whereas Sod1 in *ccs1*Δ cells is readily modified (**Figure 2.2d**). Likewise, Sod1 modification is similar for cells harboring Ccs1 CxC spacer mutants (**Figure 2.2d**), suggesting the bulk of cellular Sod1 in these strains exists in the disulfide reduced inactive state. However, there may be a small fraction of oxidized Sod1 in the cells expressing Ccs1 $C_{230}C_{231}$ that cannot be visualized by alkylation which gives rise to the cell viability seen on plate assays.

2.4.4 *Stalled Sod1•Ccs1 Complexes*

Previous studies have noted and our current Sod1•Ccs1 structure deciphers that immature forms of Sod1 are the primary target of Ccs1 (**Figure 2.1c**) (16,23). **Figure 2.3** shows the results from Strep-Sod1•Ccs1 pull-downs from yeast where Ccs1 does not significantly co-purify with WT Strep-Sod1 (**Figure 2.3a**). Co-purification of stalled Sod1•Ccs1 complexes was enhanced in cells expressing the Sod1 variant $C_{146}S$ and to a lesser degree with $C_{57}S$ or the catalytically inactive $R_{143}E$ mutant (**Figure 2.3a**). The Ccs1 D3 CxC variant $C_{231}S$, but not $C_{229}S$, enhanced co-purification relative to WT Ccs1 (**Figure 2.3b**). Enhancement persists when the Sod1 variant $C_{146}S$, is mixed with Ccs1 D3 CxC variants (**Figure 2.3c**). However, D3 CxC spacing mutants with C_{231} still in place did not affect complex stalling (**Figure 2.3d, e**). The positional requirement of C_{231},

but not C_{229}, posits deviating roles during the Sod1 activation process that may be explained by their relative arrangements in our Sod1•Ccs1 complex (**Figure 2.1a, c**).

2.4.5 *Sod1 Disulfide Formation Secures Copper Delivery*

Next, we strove to further examine the link between disulfide bond formation and metal delivery to Sod1. Various affinity purified heterocomplexes were assessed on non-reducing SDS-PAGE for the presence of an *inter*-molecular disulfide bond. A ~45 kDa molecular mass band containing both Sod1 and Ccs1 was not only observed in samples when C_{146}S Sod1 were utilized, but also when C_{229}S or C_{231}S Ccs1 were present (**Figure 2.4a**). Without both Ccs1 D3 CxC cysteines present, the process guiding formation of the Sod1 C_{57}-C_{146} *intra*-subunit disulfide bond likely becomes trapped as an intermolecular disulfide intermediate. Interestingly, though a high mass Sod1•Ccs1 complex was not visualized with Sod1 C_{57}S, significant levels of Ccs1 were co-purified with this Sod1 mutant (compare **Figure 2.4a** to **Figure 2.3a**). Thus, we repeated the experiments with N-ethyl maleimide (NEM) to quench possible disulfide exchange reactions. The addition of NEM resulted in all of the single mutants forming the high molecular weight complex, nonetheless at least one of the D3 CxC cysteines is necessary (**Figure S2.4**). Interestingly, a Ccs1 D3 variant lacking both Cys residues was attenuated in its interaction with Sod1 consistent with an intermolecular disulfide in the stalled Sod1-Ccs1 interaction. In order to rule out that the stalled heterocomplexes are bridged by Cu(I) coordination, the Cu(I) chelator BCS was added to the reactions and stalled complexes persisted even in the presence of excess BCS (**Figure 2.4b**).

To gauge whether Sod1 in the Ccs1 mutant cells contained bound metal ions, N-

terminally Strep-tagged Sod1 purified from cells with WT and mutant Ccs1 variants were probed for metals by ICP-OES (**Figure 2.4c**). WT Sod1 contained roughly 1 mol equiv. of both copper and zinc, whereas Sod1 purified from *ccs1*Δ cells contained essentially no copper but ~2 mol equiv. of zinc. Sod1 purified from cells containing Ccs1 D3 variants or Sod1 with a $C_{57}S$ substitution were devoid of copper. In contrast, the $C_{146}S$ Sod1 was isolated with appreciable levels (~0.3 mol equiv.) of copper relative to *ccs1*Δ cells. The difference in the copper content of $C_{57}S$ vs. $C_{146}S$ Sod1 may suggest that these two cysteines play differing roles in copper loading and/or retention. Taken together, the variant forms of Sod1 or Ccs1 that hinder efficient disulfide bond formation also hinder the ability of Sod1 to receive its full complement of copper.

2.4.6 *Cysteine Residues From Sod1 and/or Ccs1 Form a Cu(I) "Entry Site"*

Next, we wanted to address the position and coordination of copper during delivery to Sod1. WT and variant forms of Strep-Sod1 were purified from yeast cells containing either WT or mutant Ccs1. Again, the mutant Sod1 samples, but not the WT, co-purify with Ccs1. X-ray absorption spectroscopy was then utilized to probe copper coordination. Absorption edge features can distinguish Cu(I) from Cu(II) and digonal from trigonal complexes by comparison with extensive data coming from Cu(I) and Cu(II) model complexes (32). **Figure 2.5a** shows the XAS Cu K-edge for WT and mutant Sod1. The absorption edge exhibited a feature at ~8983 eV consistent with a 1s→4p transition of the Cu ion. For all three samples, the energy and intensity of this near-edge feature relative to the absorption continuum are characteristic of trigonal Cu(I) complexes (32).

Figure 2.5b shows the copper K-edge EXAFS spectra and Fourier transform of the EXAFS for WT Sod1. The Fourier transform consists of a major peak at 1.96 Å and two outer shell scatter peaks at ~3 and ~4 Å. Simulations with different ligand types reveal a best fit for the 1.96 Å peak with three N/O ligands, which agrees well with the known three histidyl ligand coordination of Cu(I) ion in the Sod1 active site (33)**.** The outer shell scatter peaks correspond to backscattering effects of the imidazole ring carbons. Analyses of the $H_{46}R/H_{48}Q$ Sod1 mutant, which cannot bind copper at the active site, was carried out after purification from yeast containing WT Ccs1 or the mutant Ccs1 containing only the D3 CxC cysteines (**Figure 2.5c** and **2.5d**, respectively). The copper K-edge feature in both samples was indistinguishable from WT Sod1, suggestive of trigonal Cu(I) coordination (**Figure 2.5a**). In contrast to WT Sod1, the EXAFS analyses of the two variant samples reveal broader first shell peaks that best fit to mixed sulfur and N/O coordination of the Cu(I) ion. Cu(I) binding to Ccs1 consists of only thiolate ligands, so the candidate nitrogen ligand is likely from Sod1. The EXAFS Fourier transform of the mutant Sod1 purified with WT Ccs1 is best fit with a model containing two sulfur ligands at 2.21 Å (2.22 Å for Cys variant Ccs1) and a single N/O at 1.92 Å (1.93 Å for Cys variant Ccs1) (**Figure 2.5c, d**). The Cu(I) site thiolate ligands are not fully distinguished, but are consistent with a model in which Cu(I) is coordinated at an "entry site" generated by the interaction between immature Sod1 and Ccs1.

2.4.7 *Ccs1 Exposes an Electropositive Cavity on Immature Sod1*

The reduced disulfide bond in Sod1 permits the intercalation of the Ccs1 D3 β-hairpin between the "disulfide loop" and β-barrel, which exposes an electropositive

cavity on the Sod1 surface inaccessible in the disulfide oxidized/mature enzyme (**Figure 2.6a, b**). The positive surface potential arises primarily through the amide nitrogen atoms of A_{60}, T_{116}, and L_{117}. The cavity is immediately adjacent to the Sg atom of C_{231} coming from the Ccs1 D3 CxC motif and Sod1 residues C_{57} and C_{146} that become oxidized to form the disulfide bond. Replacement of the glutamine residue at position 48 in this structure with the normal active site histidine suggests a structural equivalence between H_{48} and H_{120} such that either could provide a ligand in a putative $(Cys)_2His$ Cu(I) "entry site" (**Figure 2.6c** and **S2.5**). Sod1 disulfide bond formation likely drives concomitant copper delivery to the active site, as mutants where the disulfide bond is not formed are defective in copper acquisition/retention (**Figure 2.4c**). These structural details provide relevance for our hypothesis that an electropositive cavity and proximal copper ion "entry site" exposed on Ccs1-bound Sod1 link copper ion delivery and disulfide oxidation.

2.4.8 *Copper-Dependent Sulfenylation at the Sod1 "Entry Site"*

The dismutation of superoxide anions by Sod1 yields both molecular oxygen and hydrogen peroxide. Thiols are particularly prone to modification by reactive oxygen species in the cell and sulfenic acid is one product produced upon oxidation by hydrogen peroxide (34,35). Protein microenvironment contributes significantly to the stability and reactivity of cysteine sulfenic acids, and reactivity of specific thiolates cannot be completely explained by solvent exposure (36,37). The formation of sulfenic acid on glutathione peroxidase 3 is a critical precursor for the subsequent disulfide transfer to the transcriptional activator Yap1 under oxidative stress (38,39). Could redox turnover of superoxide at an exposed Sod1 "entry site" be catalyzing a similar reaction?

Purified Sod1 treated with dimedone, which specifically labels sulfenic acid modifications, was analyzed by western blot using a dimedone adduct specific antibody. A gel band visualized by this technique comigrated with a band imaged with a Sod1 antibody (**Figure 2.7a**). Notably, sulfenylation was observed on mutant Sod1 proteins purified from yeast also containing untagged WT Sod1, so the modification did not arise from a buildup of cellular reactive oxygen species. The sulfenylated adduct is detectable in all Sod1 mutants except for $C_{146}S$, advocating a preferred site for adduct formation (**Figure 2.7b**). Interestingly, the adduct is more prevalent with the $R_{143}E$ variant. Whereas, R_{143} is important for electrostatic guidance of superoxide into the catalytic site of mature Sod1, the addition of a negative charge at $R_{143}E$ mutant may help push superoxide towards the vicinal electropositive cavity and "entry site." Sod1 sulfenylation is attenuated in yeast cells that are rendered copper-deficient by inclusion of the copper chelator BCS in the growth media or selective knockout of the influx copper transporter Ctr1 (**Figure 2.7c**). This strongly suggests that sulfenylation at Sod1 C_{146} is a copper-mediated reaction. Sulfenylation at this site likely promotes C_{57}-C_{146} disulfide oxidation in Sod1, which in turn releases the now oxidized Cu(II) from its "entry site" ligands into the nearby Sod1 active site (**see Figure 2.5c**).

2.4.9 *Sod1 Activation Under Copper-Replete Conditions*

For yeast Ccs1 (but not necessarily mammalian), D1 is required only under copper limiting conditions *in vivo* (9,10,29). The conditional necessity of D1 in yeast Ccs1 suggests that the cellular environment may alter the mechanism of copper delivery. During normal cellular conditions, copper ions are present in the cytosol as small

molecule complexes with reduced glutathione (GSH) or metallothionein scavengers (40). However, presently, only mammalian cells are known to utilize Cu(I)-GSH as an alternate route for Sod1 activation (12). **Figure 2.7d** shows the results for an *in vitro* yeast Sod1 activation assay incorporating Cu(I)-GSH. Lane 1 is metal-free (apo) Sod1, which shows no detectable activity, as expected. The addition of Cu(I)-GSH to apo-Sod1 provides very little benefit, as minimal activity is observed (lane 2). Lane 3 is apo-Sod1 mixed with apo-Ccs1 as a control for background activity. Remarkably, when apo-Sod1 is mixed with apo-Ccs1 and Cu(I)-GSH, abundant Sod1 activity is detected (lane 4); a level of activity similar to apo-Sod1 mixed with Cu(I)-Ccs1 (lane 5). These data suggest that when copper is readily available, Ccs1 may simply expose the electropositive cavity and Cu(I) "entry site" on immature Sod1 to allow entry of Cu(I) from a labile source such as glutathione and then facilitating disulfide formation, as described above.

2.5 Discussion

Based upon the data presented here, Ccs1-mediated Sod1 maturation appears to proceed via a Cu-mediated sulfenylation intermediate that resolves to form the stable Sod1 disulfide bond. Our new Sod1•Ccs1 complex structure demonstrates that upon binding to immature Sod1, interactions between Ccs1 and the disulfide loop of Sod1 orient the D3 β-hairpin towards Sod1. The indole side-chain of W_{237} fits into a hydrophobic pocket on Ccs1 D2 securing the D3 β-hairpin. The intercalation of C_{231}, together with hydrogen bonding interactions between the side chain of Sod1 residue D_{52} with the indole nitrogen of W_{222}, pulls the disulfide loop away from the Sod1 b-barrel and exposes a copper ion "entry site" and adjacent electropositive cavity. A copper ion

coming from D3 or a labile Cu(I) pool can now be coordinated at the "entry site" and superoxide is attracted towards the electropositive cavity harboring Sod1 C_{146}. Copper ion oxidation (e.g., Cu(I) → Cu(II)) reduces the superoxide to hydrogen peroxide. This newly generated peroxide molecule promotes sulfenylation of a cysteine, likely Sod1 C_{146}, although sulfenylation could initially occur on a Ccs1 D3 cysteine. Sulfenylation subsequently mediates disulfide bond formation through disulfide exchange reactions involving the Ccs1 D3 cysteines. Sulfenylation of Sod1 is not dependent on Ccs1 (**Figure 2.7b**), but the resolution to a disulfide bond is dependent on Ccs1. The driving force for Cu(I) oxidation at the entry site may in part be due to stabilization of the Cu(II) product via migration into the tetra-histidine environment of the mature catalytic site. Sod1 disulfide oxidation and copper ion release into the active site expels the Ccs1 D3 β-hairpin as the formation of the disulfide bond closes the electropositive cavity and terminates interaction between Sod1 and Ccs1.

The Sod1•Ccs1 interaction during the maturation process is likely short-lived and is terminated by successful *intra*-subunit C_{57}-C_{146} disulfide bond formation in Sod1. However, this transient binding event can be trapped as an intermolecular disulfide linked intermediate in cells containing either C_{146}S Sod1 or C_{231}S Ccs1, yet substitution of both Ccs1 D3 CxC cysteines expectedly attenuates trapping. These data support a model where Ccs1-mediated disulfide exchange reactions between cysteine residues at the Cu(I) "entry site" drive Sod1 maturation to completion.

The Sod1•Ccs1 complex is stalled in Sod1 catalytic site His mutants. The reactivity of the Cu(I)NS_2 complex at the entry site of this Sod1 mutant with superoxide is expected to be diminished, since the driving force provided by subsequent Cu(II)

stabilization in the catalytic site is absent. This facilitates partial build-up of the Cu(I) intermediate. A corollary to this premise is that the resolution of the C_{146} sulfenic acid intermediate by C_{57} could also be inhibited since movement of C_{57} towards C_{146} is a consequence of reorganization of the electrostatic loop to accommodate the bound Cu(II) ion. Therefore, in the absence of the driving force supplied by cupric ion migration, resolution of the C_{146} sulfenic acid by *a Ccs1-derived thiol* may be a more favorable reaction, which in turn would generate intermolecular cross links of the type observed by Lamb et al. (41) and with the results from the present study that at least one *Ccs1-derived thiol* is required for formation of the cross-link.

Clear evidence for a Cu(I) "entry site" on immature Sod1 bound by Ccs1 is provided by X-ray absorption and related techniques. Cells harboring a Sod1 $H_{46}R/H_{48}Q$ variant unable to bind copper at the active site, coordinate Cu(I) using a $(Cys)_2His$ pseudo-trigonal planar geometry. Consistent with this geometry and ligand set, the new heterocomplex structure reveals that the Sγ atoms of C_{231}, C_{57}, and the position of Cu in the activated enzyme are co-planar, with liganding nitrogen atoms from H_{48} and H_{120} equidistant and normal to this plane (**Figure 2.6c**). Thus, the entry site may be fluxional, sampling some or all of the four possible thiolate ligands. Only one of these states might lead to proper maturation, while others could result in nonproductive cross-links. A Cu(I) resting state observed in the WT EXAFS analysis is consistent with *in vivo* NMR analysis performed on the maturation steps of Sod1(6,7). In separate *in vitro* analysis, transfer of copper from Cu(I)-Ccs1 to Sod1 in the presence of oxygen showed a stable Cu(II)-Sod1(42). The difference between these two experiments may be explained by the presence or absence of abundant superoxide anions, since we know that superoxide is a

substrate for both half reactions of the native Sod1 enzyme.

A readily accessible Cu(I) "entry site" requires direct delivery and "hand-off" by a copper ion carrier. Cu-GSH complexes have shown the ability to activate human Sod1 in the absence of Ccs1; a process not replicable for yeast Sod1 due to proline residues just upstream of C_{146} (12). Here, we show evidence that Cu-GSH can deliver copper to yeast Sod1, but requires interaction with metal-free Ccs1. Under normal cellular conditions, the major role of Ccs1 may be to pull the disulfide loop away from the Sod1 β-barrel, thereby exposing the electropositive cavity and "entry site" on immature Sod1.

We suggest the electropositive cavity flanking the Cu(I) "entry site" attracts superoxide anion in a manner analogous to the role of R_{143} during normal Sod1 catalysis. Oxidation of the copper ion bound at the "entry site" (e.g., Cu(I) → Cu(II)) reduces the superoxide to hydrogen peroxide, which in turn promotes sulfenylation of a nearby thiolate, preferably C_{146}. Sulfenylation is known to mediate disulfide bond formation in biological systems (34,35). Sulfenylated C_{146} reacts with Cu-bound C_{57} or C_{231} at the "entry site" resulting in disulfide exchange reactions that lead to eventual resolution of the stable Sod1 disulfide and concomitant release of copper into the active site. Once formed, the rigid C_{57}-C_{146} disulfide bond helps to immobilize the guanidinium moiety of R_{143} adjacent to the catalytic copper ion. An engineered Sod1 monomer in which the position of the disulfide bond is altered due to the loss of stabilizing interactions at the homodimer interface is an order of magnitude less active than the disulfide oxidized dimeric enzyme (5). In this context, the Cu(I) "entry site" and electropositive cavity are integral to normal Sod1 function.

In conclusion, our biochemical studies and Sod1•Ccs1 complex structure suggest

a novel mechanism for Sod1 maturation. Copper delivery to an exposed "entry site" on immature Sod1 and redox turnover of a single superoxide substrate are required for the initial maturation steps. Results indicate that cellular copper ion levels may dictate the delivery source for the "entry site" and under normal conditions Ccs1 may play an indirect role in copper ion delivery by facilitating access to the "entry site." Ccs1 directs Sod1 disulfide formation through sulfenylation of C_{146}, which keys disulfide exchange reactions concluding in a stable Sod1 C_{57}-C_{146} disulfide, copper ion placement in the active site, and termination of the interaction with the now mature Sod1. The maturation path is a concerted process requiring a specific conformation of thiolates in the entry complex, accompanied by coupled sulfenylation, Cu(II) migration, and resolution to disulfide, with the driving force dependent on all three molecular events. Our data and ensuing mechanism also require that Sod1 maturation is initiated by oxidative chemistry, as previously reported by the O'Halloran lab (43), and more specifically by superoxide itself. This latter conclusion is significant since it implies that Sod1 metalation and activation is *regulated* by the presence of its substrate such that its precious copper cargo is only loaded when the cell or organelle experiences oxidative stress.

2.6 Materials and methods

2.6.1 *Materials*

Monobasic and dibasic potassium phosphate, acetonitrile (Optima grade), formic acid, sodium hydroxide, yeast extract, peptone, dextrose (glucose), EDTA, sodium chloride, and sodium acetate were obtained from Fischer Scientific. Ammonium sulfate was purchased from US Biological. Polyethelyne glycol 1000 came from Fluka. Tris

was purchased from Research Products International. Primers came from Invitrogen. Agarose glycerol, DEAE Sephadex, DTT, and PMSF were obtained from Sigma. *Pfu* DNA polymerase and deoxyribonucleotides were purchased from Stratagene. Glass beads were obtained from Biospec. Crystallization screening kits and crystal growth trays were purchased from Hampton Research. Phenyl Sepharose and Sephadex G-75 came from Pharmacia. All solutions were prepared using de-ionized water passed through a Millipore ultra-purification system.

2.6.2 *Sod1 Cloning, Expression, and Purification*

DNA fragments encoding the human H46R/H48Q Sod1 double mutant were amplified by PCR and ligated into the YEP351-hSOD plasmid, where expression of the Sod1 protein is directed under the control of its own promoter. The protein was expressed, purified, and characterized, as previously described, (23) with the addition of a DEAE-Sephadex chromatography step between the hydrophobic interaction chromatography and gel filtration column steps. The metal content of purified Sod1 and Ccs1 proteins was determined using inductively coupled plasma mass spectrometry (ICP-MS) at the Chemical Analysis Laboratory at the University of Georgia.

2.6.3 *Ccs1 Cloning, Expression, and Purification*

DNA fragments encoding yCcs1 were generated by polymerase chain reaction (PCR) from plasmids generously supplied by J.S. Valentine (UCLA). Ccs1 constructs were cloned into a pkA6H vector, which contains an inducible *lacZ* promoter, a 6x-N-terminal His-tag, and a tobacco etch virus (TEV) cleavage site. Residues ^{237}WEER^{240} in

D3 were substituted to ^{237}WAAA^{240} via quick-change mutagenesis and these substitutions dramatically enhanced the overall yield of recombinant Ccs1 (~5-fold) while simultaneously obviating the instability and proteolysis observed in wild type Ccs1 otherwise identically prepared. Yeast Ccs1 was expressed in *Escherichia coli* BL21 (DE3). Transformed cells were grown in LB media at 37^{o} C to an OD_{600} of 0.6 to 0.8. After induction with 0.1 mM IPTG, the cells were transferred to 30^{o} C for an additional 4 hr before being harvested. Ccs1 was purified using a HisTrap HP Ni^{2+} affinity column purchased from GE. After purification, the hexa-His-tag was removed by digestion overnight with TEV protease produced in-house and engineered to contain its own non-cleavable hexa-His tag. After digestion, the cleaved His tag and TEV protease was removed from the Ccs1 sample by a final pass through the nickel column. This procedure leaves a two residue (Gly-His) extension on the Ccs1 N-terminus.

2.6.4 *Crystallization, Structure Determination, and Refinement*

The H46R/H48Q Sod1• E238A/E239A/R239 Ccs1 complex was prepared in solution, as previously described (23). All crystals were grown at room temperature using the hanging drop vapor diffusion method. Purified Sod1•Ccs1 complex at 20 mg/mL in 50 mM MES, pH 6.5, 150 mM sodium chloride, 10 mM TCEP, and 50 μM $ZnSO_4$ was mixed with an equal volume of reservoir solution containing 100 mM Bis-Tris, pH 6.5, 200 mM Ammonimum Sulfate, and 25% w/v PEG 3350. Rectangular crystals grew in space group $P2_12_12$ within two weeks at room temperature. Suitable specimens were soaked in a cryoprotectant consisting of reservoir solution made 10% (v/v) in ethylene glycol before flash-cooling by plunging into liquid nitrogen. X-ray

diffraction data were measured to a resolution of 2.5 Å resolution at the Argonne National Laboratory NE-CAT beamline 24-ID-E, which is equipped with microfocus MD-E microdiffractometer. All diffraction data were processed using the HKL2000 program suite (44). The structure was determined by molecular replacement with the program MOLREP (45) using the structures of human S134N Sod1 [PDB: 1OZU (46)] and yCcs1 D2 [PDB: 1JK9 (18)] as the search models. The Sod1 component was positioned in the unit cell first, then yeast Ccs1 DII followed by rigid body refinement using the program PHENIX (47). The model was refined iteratively in PHENIX without noncrystallographic symmetry restraints, invoking simulated annealing in the early rounds of refinement and alternating with manual model adjustment into σ_A-weighted electron density map using the program COOT (48). No stereochemical restraints were applied to the metal-ligand distances or bond angles. All structural figures were created using the PyMOL Molecular Graphics System, Version 1.8 Schrödinger, LLC.

2.6.5 *Yeast Growth, Strains, and Plasmids*

S. cerevisiae strains were grown in SC-glucose (dextrose) (SCD) media at 30°C unless otherwise noted. BY4741 *ccs1*Δ::KanMX knockout was generously provided by Dr. Val Culotta. The *sod1*Δ mutant in BY4741 as well as in the *ccs1*Δ::KanMX background was generated with a *URA3* disruption. Dr. Culotta generously provided both pRS313-*CCS1* and YEP351-y*SOD1* plasmid for *in vivo* and EXAFS experiments. N-terminal Strep tag (WSHPQFEK) with a 2 Gly linker and all subsequent mutations in y*SOD1* were generated by Phusion mutagenesis PCR.

2.6.6 *Analysis of Sod1 Disulfide Redox State and Activity Measurements*

*ccs1*Δ were transformed with *CCS1*-containing plasmids harboring specific spacing mutations. 50 mL cultures were harvested at OD_{600nm}~1. Pellets were resuspended in 8M Urea, 3mM EDTA, .5% Triton X-100, 50 mM Tris, pH 8.0 and split into 2 aliquots containing or lacking mPEG-Mal (PEG Maleimide, MW 2000) purchased from NANOCS. The cells were lysed by bead beating and centrifuged at 12,000 x g for 10 min. The supernatant was placed at 37°C for 1 hr and ~ 30 µg of lysate was analyzed by western blot. Sod1 activity was measured using the SOD assay kit purchased from Sigma.

2.6.7 *Sod1 Purification*

For Strep-tag affinity purification, *ccs1*Δ*sod1*Δ cells were co-transformed with vectors encoding Sod1-Strep and Ccs1 variants and grown to OD_{600nm}~1 in SCD media. Cells were resuspended in 50 mM NaH_2PO_4, 300 mM NaCl, pH 8.0 with Roche cOmplete protease inhibitor cocktail tablets. Cells were lysed by bead beating and centrifuged at 12,000 x g for 10 min. One mg of supernatant was diluted to 500 µl of buffer and 50 µl bead volume of Strep-Tactin Superflow plus, purchased from Qiagen, was added and incubated for either 4 hr or overnight. For nonreducing alkylation experiments, 20 mM N-ethyl maleimide (NEM) was added to overnight incubation of lysates. To test whether copper was involved in heterodimer complex, 500 µM BCS was added to lysates in overnight incubation. Eluates were then analyzed by western blot analysis. For purification of Sod1 $H_{46}R$ $H_{48}Q$, cells were lysed by French pressure cell press and centrifuged at 10,000 x g to clarify lysates. Ammonium sulfate was added to

lysates at 4°C while stirring to a final concentration of 60%. Upon reaching 60% saturation, an equal volume of methanol was added to the solution and stirred vigorously for 10 min. The supernatant was centrifuged at 10,000 x g for 30 min and the supernatant was dialyzed overnight into 50 mM phosphate buffer, 150 mM NaCl, pH 7.0. Following dialysis, the eluate was loaded onto a Superdex 75 FPLC column and the major peak containing Sod1 was dialyzed into 20 mM Tris, pH 8.0.

2.6.8 *Sod1 Metal Analysis*

Sod1-Strep tagged constructs were grown in SCD media to OD_{600nm} 1.5 and harvested. Cells were lysed by French pressure cell press and centrifuged at 50,000 x g for 1 hr at 4°C. The protein was purified using Strep-Tactin Superflow plus resin. Eluted proteins were dialyzed overnight in 20 mM Tris pH 8.0 and analyzed by inductively coupled plasma optical emission spectrometry (ICP-OES) for metal content.

2.6.9 *Sod1 Sulfenylation*

Sod1 was purified as described above. 5,5-dimethyl-1,3-cyclohexanedione (dimedone), purchased from Sigma Aldrich, was added to a final concentration of 20 mM to the eluate or to lysates. The protein was incubated at 37°C for 1 hr, and analyzed by western blot analysis using an anti-cysteine sulfenic antibody purchased from EMD Millipore which reacts with cysteine sulfenic acids derivatized with dimedone.

2.6.10 *X-ray Absorption Data Collection and Analysis*

Copper K-edge (8.9 KeV) extended X-ray absorption fine structure (EXAFS) and X-ray absorption near edge structure (XANES) data were measured at the Stanford Synchrotron Radiation Lightsource operating at 3 GeV with currents between 300 and 500 mA operated in continuous top-up mode. Samples were measured on beamline 7-3 using a Si[220] monochromator and an upstream Rh-coated mirror with 13 keV energy cutoff in order to reject harmonics. Data were collected in fluorescence mode using a Canberra 30-element Ge array detector with maximum count rates per array element set to less than 120 kHz. A Z-1 nickel (NiO) filter and Soller slit assembly inserted in front of the detector were used to reduce elastic scattering relative to the Cu Kα fluorescence. Four scans of a buffer blank were averaged and subtracted from the averaged data for each protein sample to remove the Ni K_β fluorescence and produce a flat pre-edge baseline. Samples were measured as aqueous glasses in 20% ethylene glycol at 10K. Data reduction and background subtractions were performed using the program modules of EXAFSPAK (49). Spectral simulation was carried out using EXCURVE version 9.2 (50,51) as described previously (52-54). The best fit of the simulations of the EXAFS data supported a mixed-shell coordination model consisting of imidazole from histidine and sulfur from cysteine coordination where appropriate. The threshold energy, E0, was chosen at 8985 eV, and refinement of structural parameters included distances (R), coordination numbers (N), and Debye-Waller factors ($2\sigma^2$), and included multiple scattering contributions from outer-shell atoms of imidazole ring.

2.7 Acknowledgements

We thank Dr. Val Culotta for generously providing numerous reagents. M.F. was supported by training grant T32 DK007115 from the National Institutes of Health. This research was supported in part by grants R01 GM110755, R01 GM054803, R01 NS39112, and R01 GM120252 from the National Institutes of Health awarded to D.R.W., N.B., P.J.H., and D.D.W. respectively, and in part by U.S. Dept. of Veterans Affairs Merit Review Award I01 BX002580 (P.J.H.) and Robert A. Welch Foundation grant AQ-1399 (P.J.H.). Support for Northeastern Collaborative Access Team beamline 24-ID-E is provided by National Institutes of Health Grant P41 GM103403 and U.S. Department of Energy Grant DE-AC02–06CH11357. The X-Ray Crystallography Core Laboratory at the University of Texas Health Science Center at San Antonio is supported in part by the Office of the Vice President for Research and by San Antonio Cancer Institute Grant P30 CA054174." Use of the Stanford Synchrotron Radiation Lightsource, SLAC National Accelerator Laboratory, is supported by the U.S. Department of Energy, Office of Science, Office of Basic Energy Sciences under Contract No. DE-AC02-76SF00515. The SSRL Structural Molecular Biology Program is supported by the DOE Office of Biological and Environmental Research, and by the National Institutes of Health, National Institute of General Medical Sciences (including P41GM103393).

2.8 References

1. Culotta, V.C., Klomp, L.W., Strain, J., Casareno, R.L., Krems, B. and Gitlin, J.D. (1997) The copper chaperone for superoxide dismutase. *J. Biol. Chem.*, **272**, 23469-23472.

2. Fridovich, I. (1989) Superoxide dismutases. An adaptation to a paramagnetic gas. *J. Biol. Chem.*, **264**, 7761-7764.

3. Arnesano, F., Banci, L., Bertini, I., Martinelli, M., Furukawa, Y. and O'Halloran, T.V. (2004) The unusually stable quaternary structure of human Cu,Zn-superoxide dismutase 1 is controlled by both metal occupancy and disulfide status. *J. Biol. Chem.*, **279**, 47998-48003.

4. Doucette, P.A., Whitson, L.J., Cao, X., Schirf, V., Demeler, B., Valentine, J.S., Hansen, J.C. and Hart, P.J. (2004) Dissociation of human copper-zinc superoxide dismutase dimers using chaotrope and reductant. Insights into the molecular basis for dimer stability. *J. Biol. Chem.*, **279**, 54558-54566.

5. Lindberg, M.J., Normark, J., Holmgren, A. and Oliveberg, M. (2004) Folding of human superoxide dismutase: disulfide reduction prevents dimerization and produces marginally stable monomers. *Proc. Natl. Acad. Sci. U. S. A.*, **101**, 15893-15898.

6. Banci, L., Barbieri, L., Bertini, I., Luchinat, E., Secci, E., Zhao, Y. and Aricescu, A.R. (2013) Atomic-resolution monitoring of protein maturation in live human cells by NMR. *Nat. Chem. Biol.*, **9**, 297-299.

7. Luchinat, E., Barbieri, L., Rubino, J.T., Kozyreva, T., Cantini, F. and Banci, L. (2014) In-cell NMR reveals potential precursor of toxic species from SOD1 fALS mutants. *Nat. Commun.*, **5**, 5502.

8. Banci, L., Bertini, I., Cantini, F., Kozyreva, T., Massagni, C., Palumaa, P., Rubino, J.T. and Zovo, K. (2012) Human superoxide dismutase 1 (hSOD1) maturation through interaction with human copper chaperone for SOD1 (hCCS). *Proc. Natl. Acad. Sci. U. S. A.*, **109**, 13555-13560.

9. Schmidt, P.J., Rae, T.D., Pufahl, R.A., Hamma, T., Strain, J., O'Halloran, T.V. and Culotta, V.C. (1999) Multiple protein domains contribute to the action of the copper chaperone for superoxide dismutase. *J. Biol. Chem.*, **274**, 23719-23725.

10. Rae, T.D., Schmidt, P.J., Pufahl, R.A., Culotta, V.C. and O'Halloran, T.V. (1999) Undetectable intracellular free copper: the requirement of a copper chaperone for superoxide dismutase. *Science*, **284**, 805-808.

11. Kirby, K., Jensen, L.T., Binnington, J., Hilliker, A.J., Ulloa, J., Culotta, V.C. and Phillips, J.P. (2008) Instability of superoxide dismutase 1 of Drosophila in mutants deficient for its cognate copper chaperone. *J. Biol. Chem.*, **283**, 35393-35401.

12. Carroll, M.C., Girouard, J.B., Ulloa, J.L., Subramaniam, J.R., Wong, P.C., Valentine, J.S. and Culotta, V.C. (2004) Mechanisms for activating Cu- and Zn-containing superoxide dismutase in the absence of the CCS Cu chaperone. *Proc. Natl. Acad. Sci. U. S. A.*, **101**, 5964-5969.

13. Dancis, A., Haile, D., Yuan, D.S. and Klausner, R.D. (1994) The Saccharomyces cerevisiae copper transport protein (Ctr1p). Biochemical characterization, regulation by copper, and physiologic role in copper uptake. *J. Biol. Chem.*, **269**, 25660-25667.

14. Pope, C.R., De Feo, C.J. and Unger, V.M. (2013) Cellular distribution of copper to superoxide dismutase involves scaffolding by membranes. *Proc.Natl. Acad. Sci. U. S. A.*, **110**, 20491-20496.

15. Lamb, A.L., Wernimont, A.K., Pufahl, R.A., O'Halloran, T.V. and Rosenzweig, A.C. (2000) Crystal structure of the second domain of the human copper chaperone for superoxide dismutase. *Biochemistry*, **39**, 1589-1595.

16. Lamb, A.L., Torres, A.S., O'Halloran, T.V. and Rosenzweig, A.C. (2000) Heterodimer formation between superoxide dismutase and its copper chaperone. *Biochemistry*, **39**, 14720-14727.

17. Lamb, A.L., Wernimont, A.K., Pufahl, R.A., Culotta, V.C., O'Halloran, T.V. and Rosenzweig, A.C. (1999) Crystal structure of the copper chaperone for superoxide dismutase. *Nat. Struct. Biol.*, **6**, 724-729.

18. Lamb, A.L., Torres, A.S., O'Halloran, T.V. and Rosenzweig, A.C. (2001) Heterodimeric structure of superoxide dismutase in complex with its metallochaperone. *Nat. Struct. Biol.*, **8**, 751-755.

19. Proescher, J.B., Son, M., Elliott, J.L. and Culotta, V.C. (2008) Biological effects of CCS in the absence of SOD1 enzyme activation: implications for disease in a mouse model for ALS. *Hum. Mol. Genet.*, **17**, 1728-1737.

20. Furukawa, Y., Torres, A.S. and O'Halloran, T.V. (2004) Oxygen-induced maturation of SOD1: a key role for disulfide formation by the copper chaperone CCS. *EMBO J.*, **23**, 2872-2881.

21. Lopez-Mirabal, H.R. and Winther, J.R. (2008) Redox characteristics of the eukaryotic cytosol. *Biochim. Biophys. Acta*, **1783**, 629-640.

22. Ferraroni, M., Rypniewski, W., Wilson, K.S., Viezzoli, M.S., Banci, L., Bertini, I. and Mangani, S. (1999) The crystal structure of the monomeric human SOD mutant F50E/G51E/E133Q at atomic resolution. The enzyme mechanism revisited. *J. Mol. Biol.*, **288**, 413-426.

23. Winkler, D.D., Schuermann, J.P., Cao, X., Holloway, S.P., Borchelt, D.R., Carroll, M.C., Proescher, J.B., Culotta, V.C. and Hart, P.J. (2009) Structural and biophysical properties of the pathogenic SOD1 variant H46R/H48Q. *Biochemistry*, **48**, 3436-3447.

24. Jensen, L.T. and Culotta, V.C. (2005) Activation of CuZn superoxide dismutases from Caenorhabditis elegans does not require the copper chaperone CCS. *J. Biol. Chem.*, **280**, 41373-41379.

25. Leitch, J.M., Jensen, L.T., Bouldin, S.D., Outten, C.E., Hart, P.J. and Culotta, V.C. (2009) Activation of Cu,Zn-superoxide dismutase in the absence of oxygen and the copper chaperone CCS. *J. Biol. Chem.*, **284**, 21863-21871.

26. Wong, P.C., Waggoner, D., Subramaniam, J.R., Tessarollo, L., Bartnikas, T.B., Culotta, V.C., Price, D.L., Rothstein, J. and Gitlin, J.D. (2000) Copper chaperone for superoxide dismutase is essential to activate mammalian Cu/Zn superoxide dismutase. *Proc. Natl. Acad. Sci. U. S. A.*, **97**, 2886-2891.

27. Ciriolo, M.R., Desideri, A., Paci, M. and Rotilio, G. (1990) Reconstitution of Cu,Zn-superoxide dismutase by the Cu(I).glutathione complex. *J. Biol. Chem.*, **265**, 11030-11034.

28. Ascone, I., Longo, A., Dexpert, H., Ciriolo, M.R., Rotilio, G. and Desideri, A. (1993) An X-ray absorption study of the reconstitution process of bovine Cu,Zn superoxide dismutase by Cu(I)-glutathione complex. *FEBS Lett.*, **322**, 165-167.

29. Caruano-Yzermans, A.L., Bartnikas, T.B. and Gitlin, J.D. (2006) Mechanisms of the copper-dependent turnover of the copper chaperone for superoxide dismutase. *J. Biol. Chem.*, **281**, 13581-13587.

30. Schmidt, P.J., Kunst, C. and Culotta, V.C. (2000) Copper activation of superoxide dismutase 1 (SOD1) in vivo. Role for protein-protein interactions with the copper chaperone for SOD1. *J. Biol. Chem.*, **275**, 33771-33776.

31. Rae, T.D., Torres, A.S., Pufahl, R.A. and O'Halloran, T.V. (2001) Mechanism of Cu,Zn-superoxide dismutase activation by the human metallochaperone hCCS. *J. Biol. Chem.*, **276**, 5166-5176.

32. Pickering, I.J., George, G.N., Dameron, C.T., Kurz, B., Winge, D.R. and Dance, I.G. (1993) X-ray Absoption Spectroscopy of Cuprous-Thiolate Clusters in Proteins and Model Systems. *J. Am. Chem. Soc.*, **115**, 9498-9505.

33. Richardson, J., Thomas, K.A., Rubin, B.H. and Richardson, D.C. (1975) Crystal structure of bovine Cu,Zn superoxide dismutase at 3 A resolution: chain tracing and metal ligands. *Proc. Natl. Acad. Sci. U. S. A.*, **72**, 1349-1353.

34. Klomsiri, C., Nelson, K.J., Bechtold, E., Soito, L., Johnson, L.C., Lowther, W.T., Ryu, S.E., King, S.B., Furdui, C.M. and Poole, L.B. (2010) Use of dimedone-based chemical probes for sulfenic acid detection evaluation of conditions affecting probe incorporation into redox-sensitive proteins. *Methods Enzymol.*, **473**, 77-94.

35. Leonard, S.E., Reddie, K.G. and Carroll, K.S. (2009) Mining the thiol proteome for sulfenic acid modifications reveals new targets for oxidation in cells. *ACS Chem. Biol.*, **4**, 783-799.

36. Conte, M.L. and Carroll, K.S. (2013) In Jakob, U. and Reichmann, D. (eds.), *Oxidative Stress and Redox Regulation*. Springer Netherlands, Dordrecht, pp. 1-42.

37. Ferrer-Sueta, G., Manta, B., Botti, H., Radi, R., Trujillo, M. and Denicola, A. (2011) Factors affecting protein thiol reactivity and specificity in peroxide reduction. *Chem. Res. Toxicol.*, **24**, 434-450.

38. Paulsen, C.E. and Carroll, K.S. (2009) Chemical dissection of an essential redox switch in yeast. *Chem. Biol.*, **16**, 217-225.

39. Delaunay, A., Pflieger, D., Barrault, M.B., Vinh, J. and Toledano, M.B. (2002) A thiol peroxidase is an H2O2 receptor and redox-transducer in gene activation. *Cell*, **111**, 471-481.

40. Luk, E., Jensen, L.T. and Culotta, V.C. (2003) The many highways for intracellular trafficking of metals. *J. Biol. Inorg. Chem.*, **8**, 803-809.

41. Lamb, A.L., Torres, A.S., O'Halloran, T.V. and Rosenzweig, A.C. (2001) Heterodimeric structure of superoxide dismutase in complex with its metallochaperone. *Nat. Struct. Biol.*, **8**, 751-755.

42. Brown, N.M., Torres, A.S., Doan, P.E. and O'Halloran, T.V. (2004) Oxygen and the copper chaperone CCS regulate posttranslational activation of Cu,Zn superoxide dismutase. *Proc. Natl. Acad. Sci. U. S. A.*, **101**, 5518-5523.

43. Furukawa, Y., Torres, A.S. and O'Halloran, T.V. (2004) Oxygen-induced maturation of SOD1: a key role for disulfide formation by the copper chaperone CCS. *EMBO J.*, **23**, 2872-2881.

44. Otwinowski, Z. and Minor, W. (1997) In Carter, C. W. and Sweet, R. M. (eds.), *Methods Enzymol*. Academic Press, New York, Vol. 276, pp. 307-326.

45. Vagin, A.A. and Teplyakov, A. (1997) MOLREP: an automated program for molecular replacement. *J. Appl. Cryst.*, **30**, 1022-1025.

46. Elam, J.S., Taylor, A.B., Strange, R., Antonyuk, S., Doucette, P.A., Rodriguez, J.A., Hasnain, S.S., Hayward, L.J., Valentine, J.S., Yeates, T.O. *et al.* (2003) Amyloid-like filaments and water-filled nanotubes formed by SOD1 mutant proteins linked to familial ALS. *Nat. Struct. Biol.*, **10**, 461-467.

47. Adams, P.D., Grosse-Kunstleve, R.W., Hung, L.W., Ioerger, T.R., McCoy, A.J.,

Moriarty, N.W., Read, R.J., Sacchettini, J.C., Sauter, N.K. and Terwilliger, T.C. (2002) PHENIX: building new software for automated crystallographic structure determination. *Acta Crystallogr. D Biol. Crystallogr.*, **58**, 1948-1954.

48. Emsley, P. and Cowtan, K. (2004) Coot: model-building tools for molecular graphics. *Acta Crystallogr. D Biol. Crystallogr.*, **60**, 2126-2132.

49. George, G.N. (1995). Stanford Radiation Laboratory, Menlo Park, CA.

50. Binsted, N. and Hasnain, S.S. (1996) State-of-the-Art Analysis of Whole X-ray Absorption Spectra. *J. Synchrotron Radiat.*, **3**, 185-196.

51. Gurman, S.J. (1995) Interpretation of EXAFS Data. *J. Synchrotron Radiat.*, **2**, 56-63.

52. Eisses, J.F., Stasser, J.P., Ralle, M., Kaplan, J.H. and Blackburn, N.J. (2000) Domains I and III of the human copper chaperone for superoxide dismutase interact via a cysteine-bridged Dicopper(I) cluster. *Biochemistry*, **39**, 7337-7342.

53. Bauman, A.T., Broers, B.A., Kline, C.D. and Blackburn, N.J. (2011) A copper-methionine interaction controls the pH-dependent activation of peptidylglycine monooxygenase. *Biochemistry*, **50**, 10819-10828.

54. Blackburn, N.J., Hasnain, S.S., Binsted, N., Diakun, G.P., Garner, C.D. and Knowles, P.F. (1984) An extended-X-ray-absorption-fine-structure study of bovine erythrocyte superoxide dismutase in aqueous solution. Direct evidence for three-co-ordinate Cu(I) in reduced enzyme. *Biochem. J.*, **219**, 985-990.

Figure 2.1 Structures of Sod1•Ccs1 complexes

In all panels, the Sod1 β-barrel is shown in green with the electrostatic loop orange and disulfide loop purple, Ccs1 D1 is marine, D2 is grey, and D3 is red. The Sod1 zinc ions are shown as orange spheres. **a)** The heterodimeric complex between human $H_{46}R/H_{48}Q$ Sod1 and yeast $E_{238}A/E_{239}A/R_{240}A$ Ccs1 determined in the present work. The reduced disulfide bond of $H_{46}R/H_{48}Q$ Sod1 between C_{57} and C_{146} permits the displacement of the disulfide loop from the Sod1 β-barrel where it interacts extensively with residues coming from Ccs1 D2 and D3. **b)** The heterodimeric complex between yeast $H_{48}F$ Sod1 and yeast Ccs1 [pdb 1JK9] (18). Note the difference in the positions of W_{222}, W_{237}, and the overall conformation of D3 relative to that shown in panel **a)**. **c)** A stereo-image of the representative αA electron density with coefficients 2*m*Fo-*D*Fc is contoured at 1.2 σ superimposed on the refined Sod1•Ccs1 model. Atoms coming from D3 residues 217-224 interact extensively with atoms coming from residues 68-71 in the linker region connecting D1 and D2 and residues from the displaced disulfide loop of Sod1 (residues 50-62). Stabilizing hydrogen bonds and salt-links are shown as dotted lines.

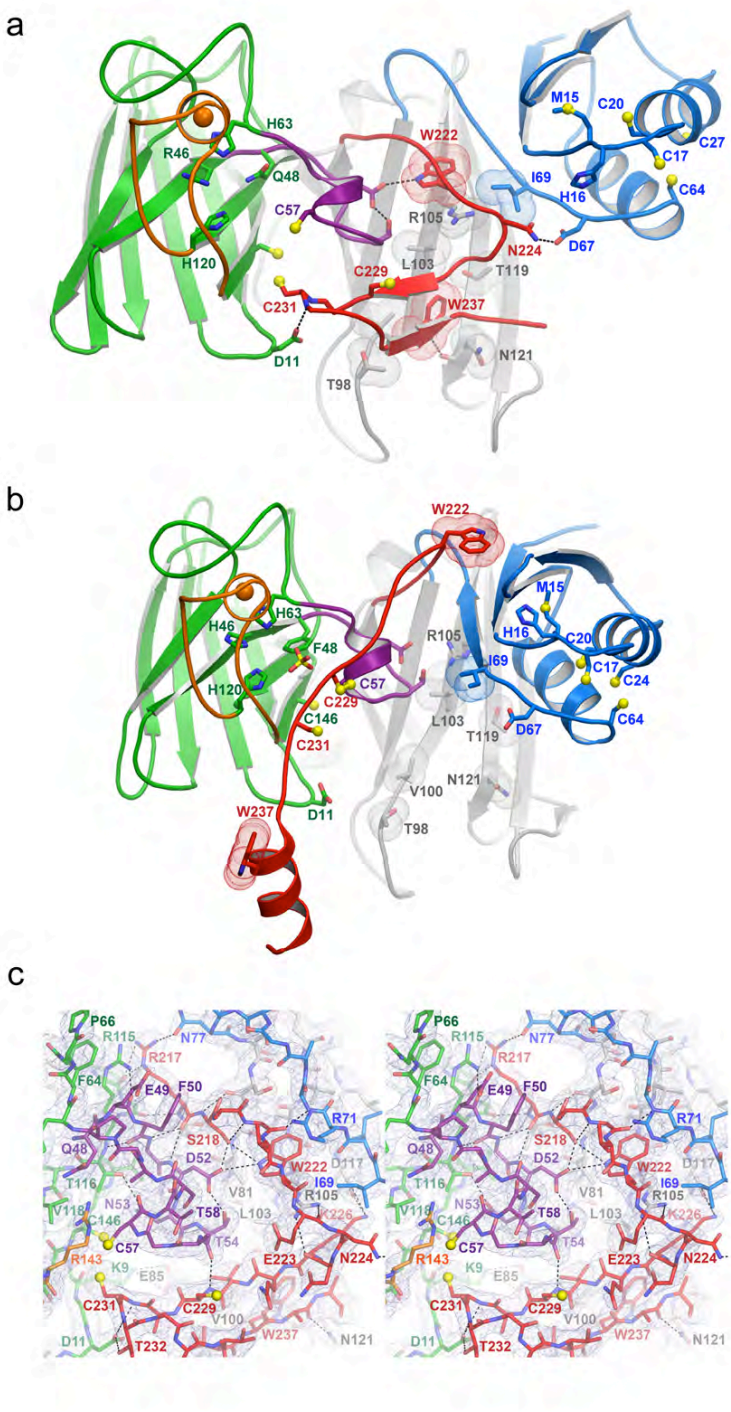
a
H63
R46
Q48
C57
H120
D11
W222
M15
C20
C27
C17
I69
H16
C64
R105
N224
D67
L103
T119
C229
C231
W237
N121
T98
b
W222
M15
H63
H46
F48
R105
H16
C20
I69
C17
C24
C57
H120
C229
C146
C231
L103
T119
D67
C64
V100
N121
W237
D11
T98
c
P66
R115
N77
R217
F64
E49
F50
R71
S218
Q48
D52
W222
D117
T116
I69
V81
R105
V118
N53
T58
L103
K226
C146
C57
T54
R143
K9
E223
N224
E85
C231
C229
V100
D11
T232
W237
N121

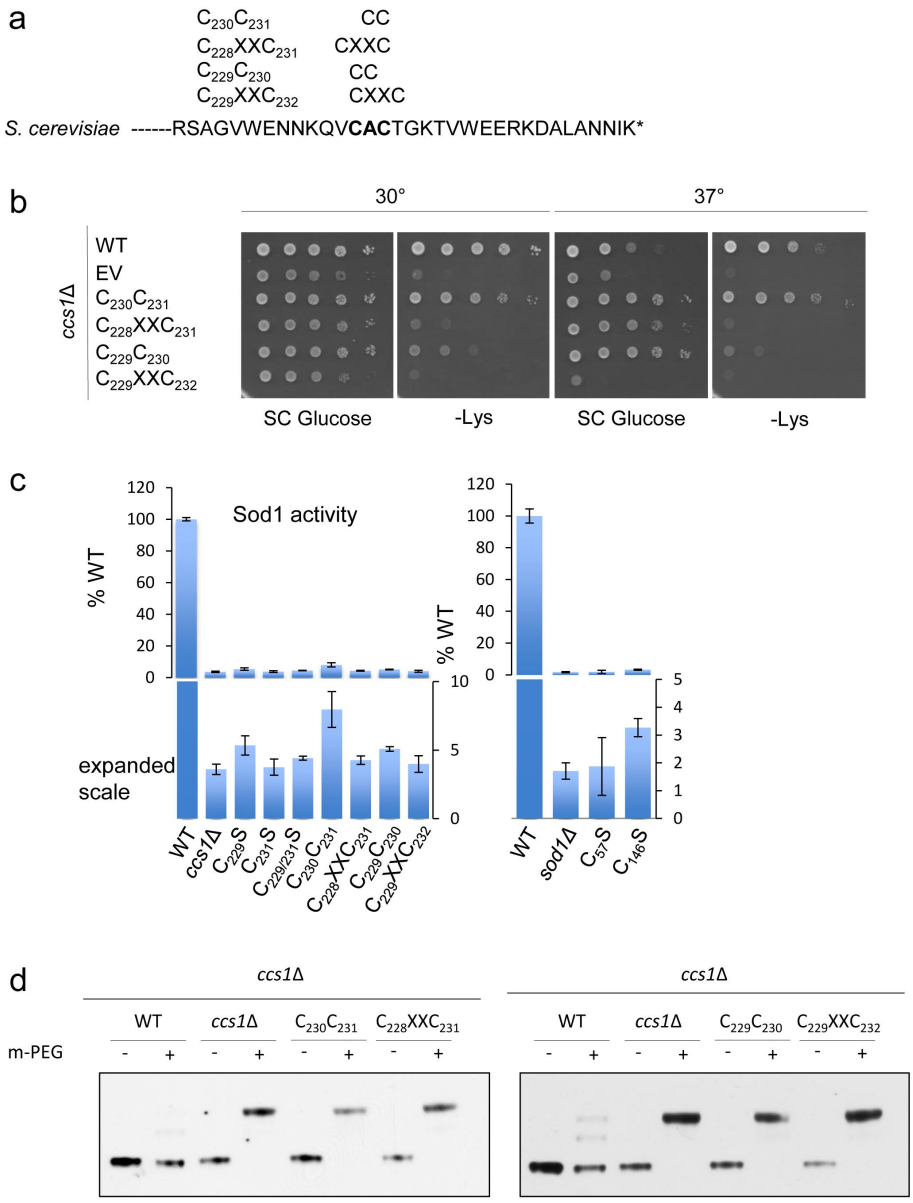

Figure 2.2 The spacing of the D3 CxC Cys residues is critical for Sod1 activation

a) Mutations were made in the CxC motif of Ccs1 to alter the spacing to either a CC or a CxxC motif without disrupting downstream residues. **b)** Viability tests were performed by plating cells on synthetic complete media with or without lysine at 30°C or 37°C. **c)** Sod1 activity for various Ccs1 mutants was quantified. **d)** The status of the disulfide bond was visualized by lysing cells in the presence of a PEG-maleimide alkylating agent that selectively reacts with free thiols.

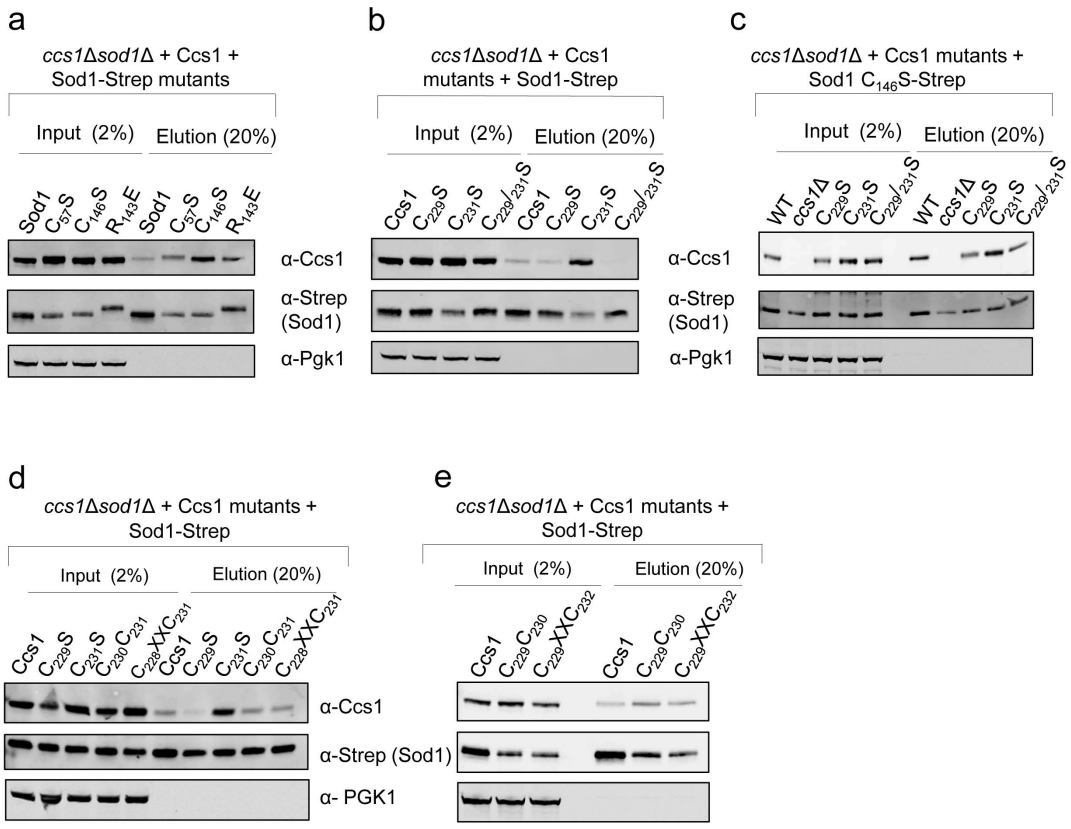

Figure 2.3 Stalled Sod1•Ccs1 complexes

a) Lysates from *sod1*Δ transformed with Sod1-Strep mutants were subject to affinity purification using Strep-Tactin resin **b)** Strep affinity purification from *ccs1*Δ cells harboring Ccs1 CxC motif mutants **c)** Strep affinity purification from *ccs1*Δ *sod1*Δ cells harboring Sod1 C_{146}S-Strep and co-transformed with vectors encoding various Ccs1 CxC mutants **d)** and **e)** Strep affinity purification from lysates containing Ccs1 CxC spacing mutants coexpressing Sod1-Strep.

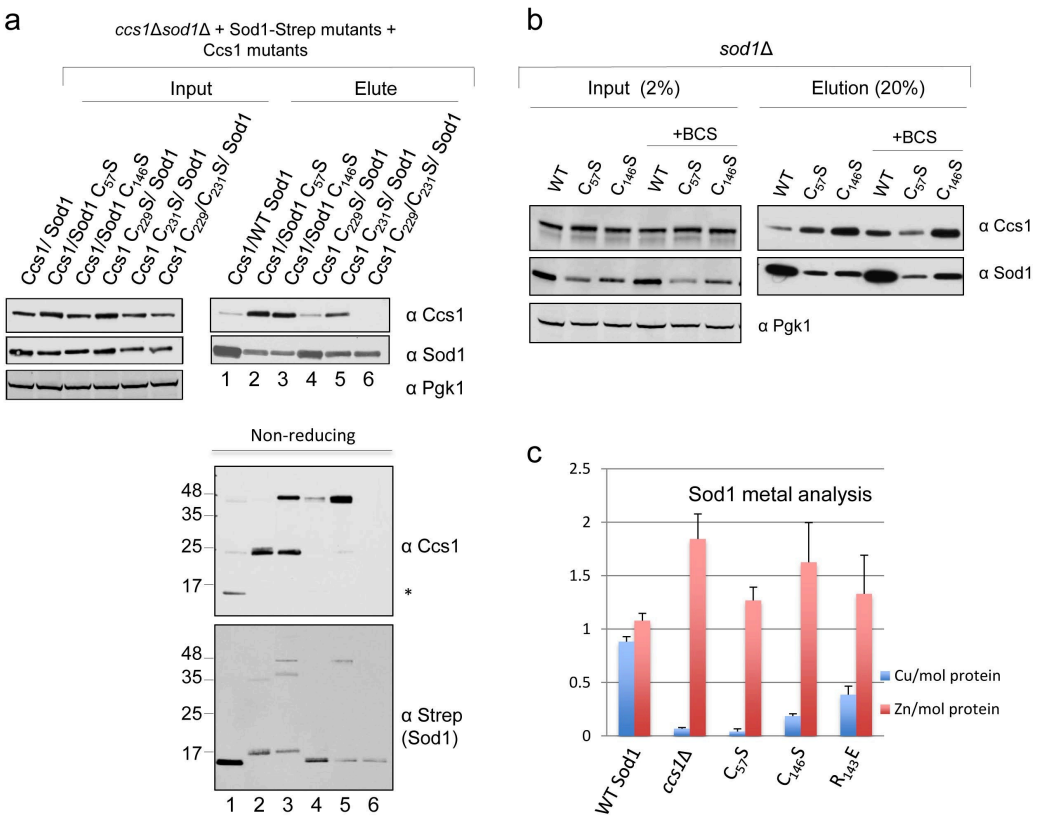

Figure 2.4 Sod1 can form an intermolecular disulfide with Ccs1

a) Cell lysates from *ccs1*Δ *sod1*Δ co-transformed with WT or Ccs1 CxC mutants and WT Sod1-Strep or Sod1-Strep mutants were subject to affinity purification. Reducing SDS PAGE gels were run (top) as well as nonreducing SDS-PAGE gel (bottom) and blotted for Sod1 or Ccs1. **b)** WT Sod1-Strep or mutants were purified in the presence or absence of 500 μM bathocuproinedisulfonic acid (BCS) and analyzed for Ccs1 interaction. **c)** Sod1-Strep (WT) or containing various Sod1 mutations were affinity purified and metal ratios were determined by ICP-OES.

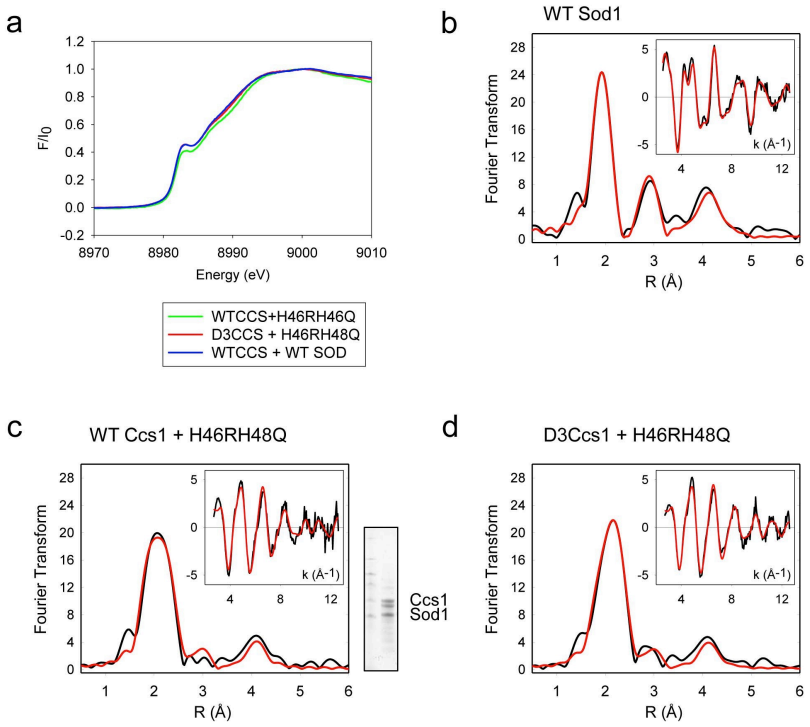

Figure 2.5 Cysteine residues from Sod1 and/or Ccs1 form a novel Cu(I) "entry site" Sod1 was purified from yeast lysates containing the indicated Sod1 and Ccs1 mutations. X-ray absorption spectroscopy was employed to determine the Cu coordination environment of Sod1. **a)** The Cu K edge of WT samples along with WT Ccs1 + Sod1 $H_{46}R$ $H_{48}Q$ and Ccs1 $C_{17/20/27/64/159}S$ + Sod1 $H_{46}R$ $H_{48}Q$, **b)** EXAFS region for WT samples, **c)** EXAFS region for sample containing WT Ccs1 + Sod1 $H_{46}R$ $H_{48}Q$, **d)** EXAFS region for sample containing $C_{17/20/27/64/159}S$ + Sod1 $H_{46}R$ $H_{48}Q$.

Figure 2.6 Electropositive cavity and copper ion "entry site" on immature Sod1

a) WT Sod1 (colored as in **Figure 2.1** and **S2.2**) shown in its disulfide oxidized mature conformation (left). The electrostatic surface is contoured at ± 4 kT (right). **b)** The disulfide reduced, copper-free Sod1 molecule from the current Sod1•Ccs1 complex with residues 46 and 48 exchanged back to histidine for demonstrative purposes. The box in the right panel highlights an electropositive cavity on Sod1 made accessible through the intercalation of the Ccs1 D3 β-hairpin. **c)** The Cu(I) "entry site" on immature Sod1 (solid black lines), as shown here, contains two cysteine sulfhydryl groups (C_{57}, C_{146} from Sod1) and one histidyl side chain from H_{48} or H_{120}. The left panel shows a semitransparent electrostatic surface covering the "entry site" from the view of the Ccs1 D3 β-hairpin. The right panel is rotated back and counterclockwise (both ~90^{o}) from the left panel and now the electropositive cavity surface is shown to emphasize its depth an positioning with regard to the "entry site" ligands.

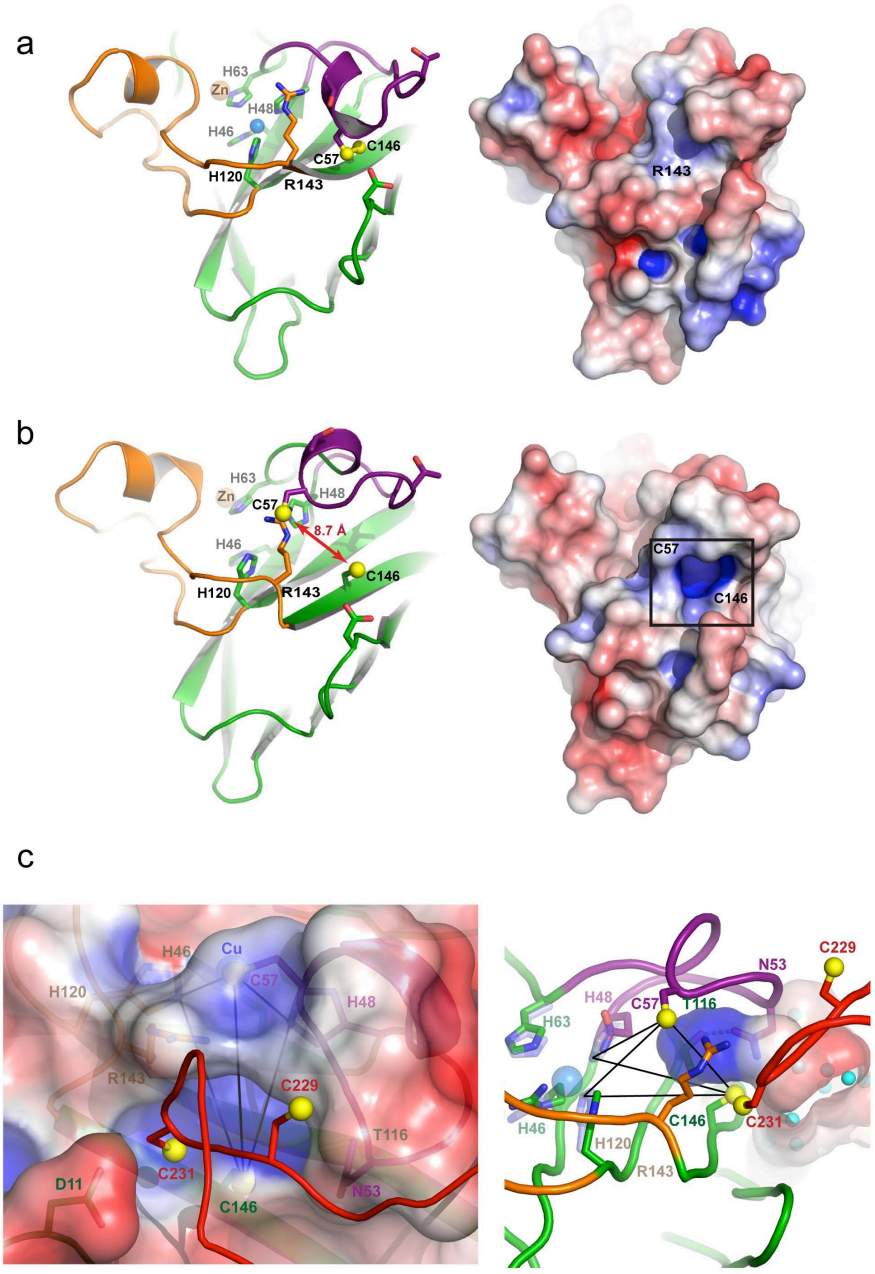
a
H63
Zn
H48
H46
C57
C146
H120
R143
R143
b
H63
Zn
C57
H48
8.7 Å
H46
C146
H120
R143
C57
C146
c
H46
Cu
C57
H120
H48
R143
C229
T116
D11
C231
C146
N53
C229
N53
H48
C57
T116
H63
H46
C146
C231
H120
R143

Figure 2.7 Copper-dependent sulfenylation at the Sod1 "entry site" and a role for reduced glutathione (GSH)

a) WT Sod1-Strep purified from yeast cells and treated with DMSO vehicle or dimedone to a final concentration of 20 mM. Coomassie stain of the purified Sod1 samples are on left panel and western blot using a cysteine sulfenic acid antibody or Sod1 antibody on the panels on the right. **b)** Purified Sod1 with various mutations were reacted with dimedone and visualized by western blot analysis. **c)** WT cells or *ctr1*Δ cells were transformed with a Sod1-Strep-encoding plasmid. The cells were grown in the absence or presence of 150 μM BCS and subject to Strep-Tactin affinity purification. **d)** *Lane 1* - Immature (metal-free, disulfide reduced) yeast Sod1 cannot scavenge superoxide (e.g., no white band). *Lane 2* – Immature ySod1 + copper bound glutathione (Cu-GSH) or a metal-free (apo) form of yCcs1 *(Lane 3)*. *Lane 4* – Cu-GSH + immature ySod1 + apo-yCcs1. *Lane 5* – immature ySod1 + Cu-yCcs1.

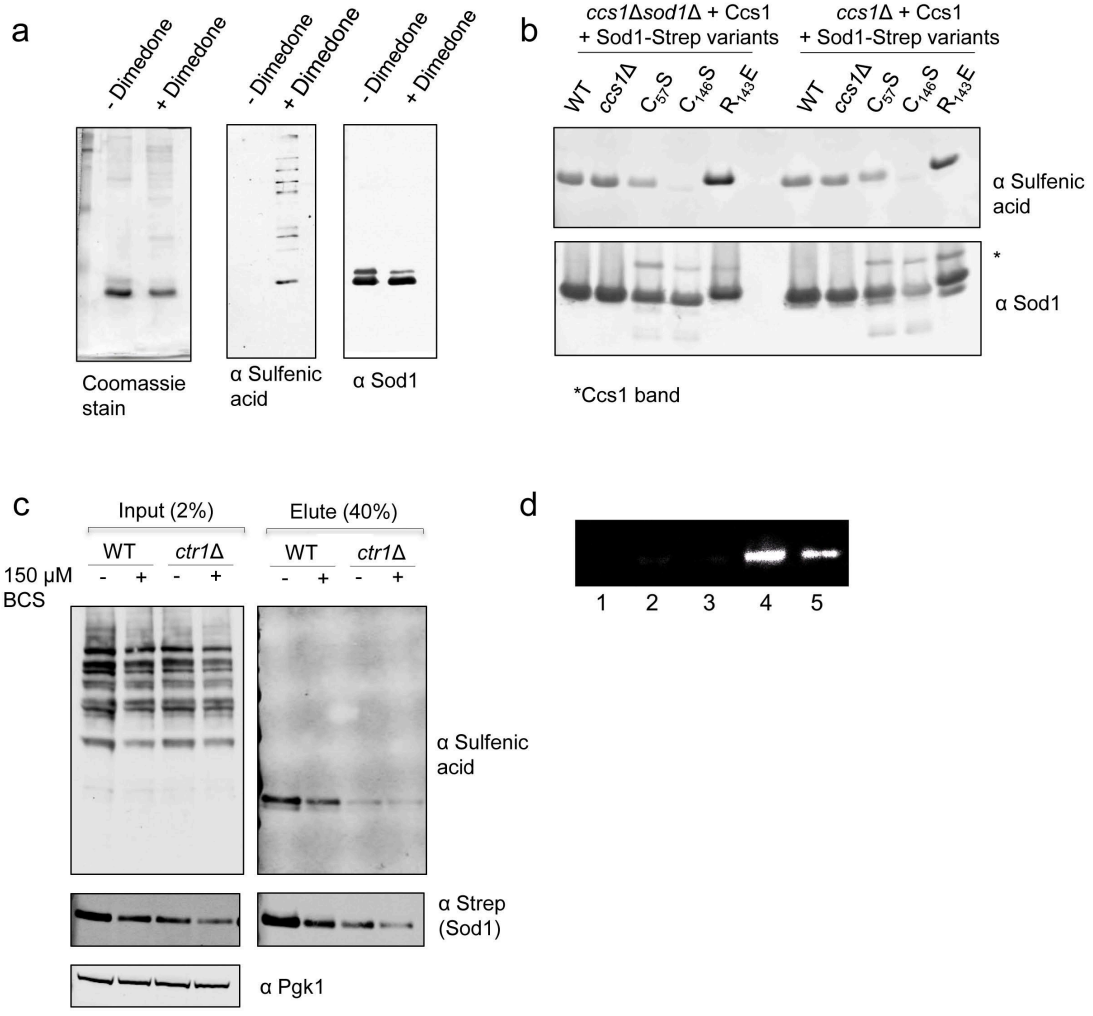
a
- Dimedone
+ Dimedone
- Dimedone
+ Dimedone
- Dimedone
+ Dimedone
Coomassie stain
α Sulfenic acid
α Sod1
b
ccs1Δsod1Δ + Ccs1 + Sod1-Strep variants
ccs1Δ + Ccs1 + Sod1-Strep variants
WT
ccs1Δ
C57S
C146S
R143E
WT
ccs1Δ
C57S
C146S
R143E
α Sulfenic acid
*
α Sod1
*Ccs1 band
c
Input (2%)
Elute (40%)
WT
ctr1Δ
WT
ctr1Δ
150 μM BCS
- + - + - + - +
α Sulfenic acid
α Strep (Sod1)
α Pgk1
d
1 2 3 4 5

Table 2.1 Data collection, phasing, and refinement statistics

Data collection, phasing and refinement statistics

Data collection	
Space group	$P2_12_12$
Cell dimensions	
a, *b*, *c* (Å)	99.1, 184.4, 48.5
α, β, γ (°)	90, 90, 90
Wavelength (Å)	0.97918
Resolution (Å)	48.51-2.35 (2.48-2.35)*
R_{sym}	0.112 (1.125)
R_{pim}	0.051 (0.480)
Mean ($I / \sigma I$)	13.8 (2.0)
Completeness (%)	99.9 (100)
Redundancy	7.0 (7.3)
Refinement	
Resolution (Å)	46.92-2.35
No. reflections	37,948
R_{work} / R_{free}	0.186/0.235
No. atoms	
Protein	5,734
Ligand	3 Zn^{2+}
Solvent	120
B-factors	
Protein	57.4
Ligand	73.0
Solvent	42.9
R.m.s deviations	
Bond lengths (Å)	0.009
Bond angles (°)	1.142
Ramachandran statistics	
Favored, allowed, outliers (%)	98.7, 1.3, 0.0

*Values in parentheses are for the highest-resolution shell.

Figure S2.1 Contents of the asymmetric units

a) The human $H_{46}R/H_{48}Q$ Sod1•yeast $E_{238}A/E_{239}A/R_{240}A$ Ccs1 complex structure determined in this study, and **b)** the yeast $H_{48}F$ Sod1•yeast Ccs1 complex structure determined previously [pdb code 1JK9 (18)]. In both panels, Sod1 is shown in green, zinc ions are shown as orange spheres, Ccs1 D1 is cyan, D2 is light blue, and D3 is red. The MxCxxC copper-binding motifs in D1 are shown in magenta. In panel **b)**, note the formation of an intermolecular disulfide bond between Sod1 C_{57} and Ccs1 C_{229} and the "swapping" of the α-helical $_{237}WEER_{240}$ motif to form a heterotetrameric complex. This $_{237}WEER_{240}$-mediated swapping interaction suggested a functional Sod1•Ccs1 heterotetramer and was targeted for mutagenesis in this work.

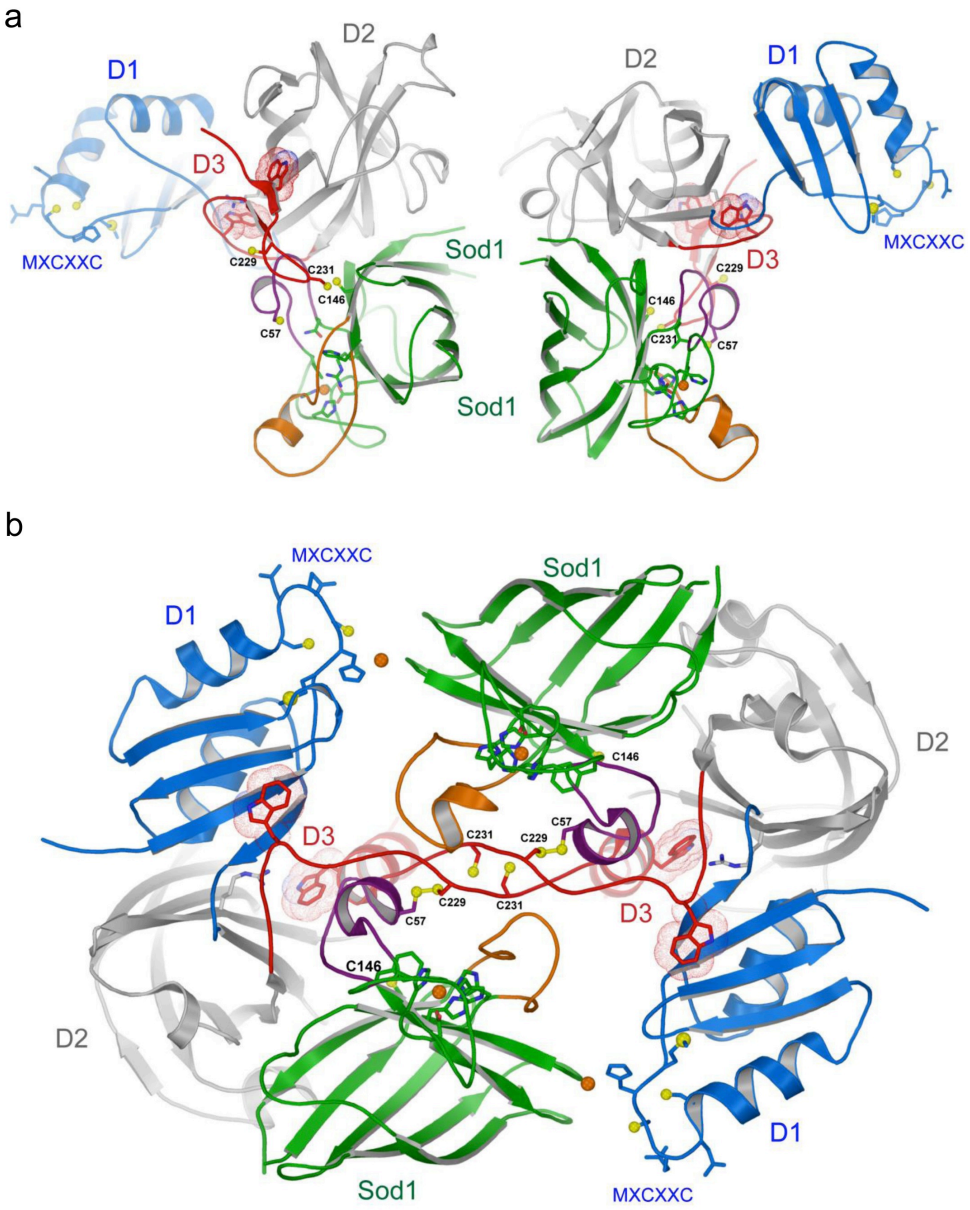
a
D1
D2
D3
MXCXXC
C229
C231
C146
C57
Sod1
Sod1
D2
D1
D3
MXCXXC
C229
C146
C231
C57
b
MXCXXC
D1
Sod1
D2
C146
D3
C231
C229
C57
C57
C229
C231
C146
D3
D2
D1
Sod1
MXCXXC

Figure S2.2 Space-filling notch-into-groove interaction of Ccs1 D3 at the Sod1•Ccs1 interface

The colors mimic that of **Figure 1.1 a)** Critical cysteine residues involved in Sod1 activation are displayed as yellow spheres. The β-hairpin of Ccs1 D3 displaces the Sod1 disulfide loop (purple) to gain access to the cysteine residues of the "entry site." **b)** Intercalation of the D3 β-hairpin between the Sod1 β-barrel and disulfide loop. Sod1 is shown as an electrostatic surface contoured at ± 4 kT. The reduced C_{57}-C_{146} Sod1 disulfide bond exposes an electropositive "hole" near C_{146}. Domains 1 (marine) and 2 (grey) of Ccs1 are shown as surfaces. The stabilizing positioning of the conserved Ccs1 tryptophan residues W_{222} and W_{237} from D3 are highlighted.

a

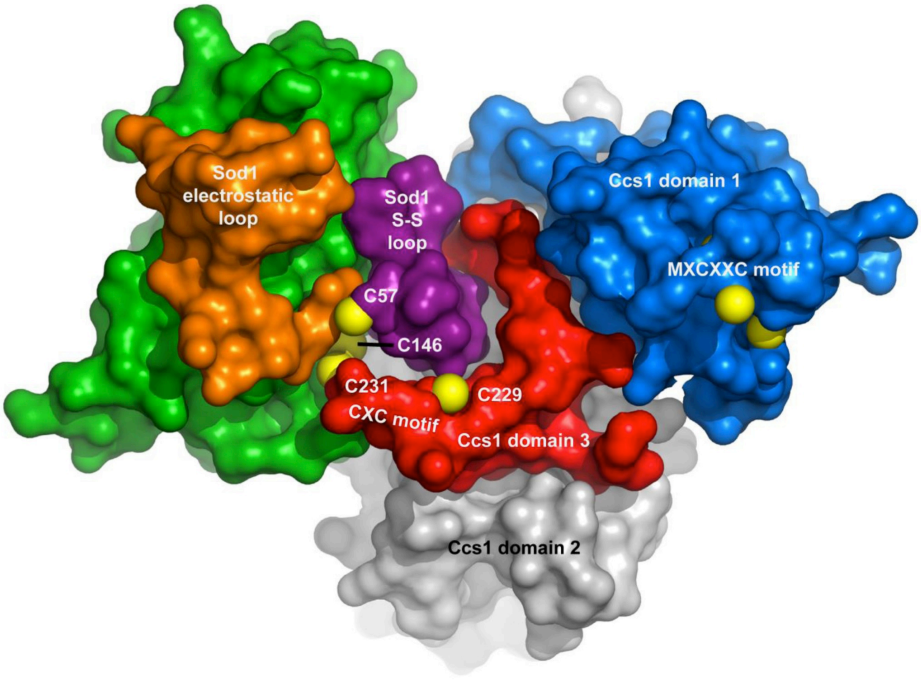
Sod1
electrostatic
loop
Sod1
S-S
loop
Ccs1 domain 1
MXCXXC motif
C57
C146
C231
CXC motif
C229
Ccs1 domain 3
Ccs1 domain 2

b

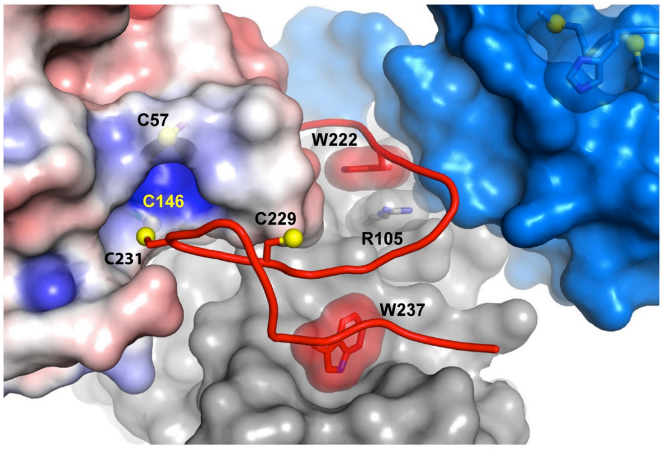
C57
W222
C146
C229
R105
C231
W237

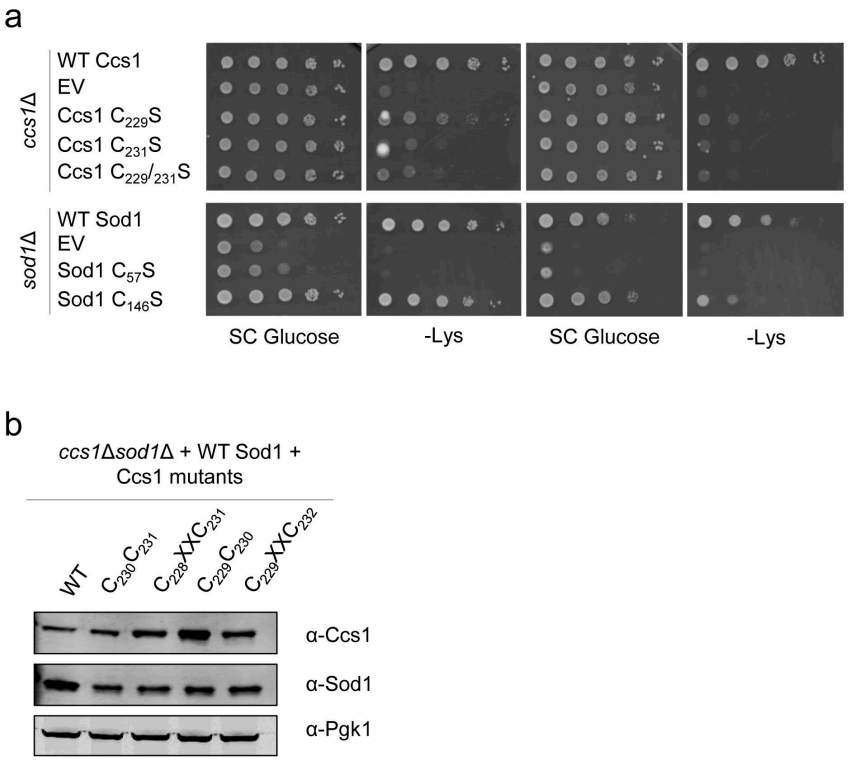

Figure S2.3 The D3 CxC and Sod1 disulfide cysteine residues are essential for Sod1 activation

a) Yeast viability assays performed by plating serial dilutions of cells on synthetic complete media with or without lysine at 30°C. **b)** 30 μg of total cell lysates were analyzed by western blot. The cytosolic marker PGK1 was used as a loading control.

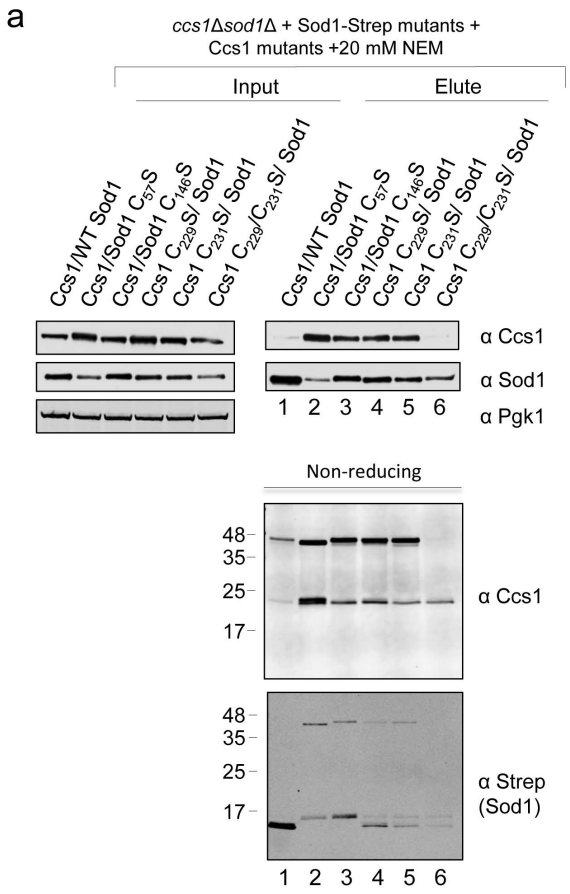

Figure S2.4 Hindered disulfide shuffling stalls the Sod1•Ccs1 interaction

a) Cell lysates from *ccs1*Δ *sod1*Δ co-transformed with WT or Ccs1 CxC mutants and WT Sod1-Strep or Sod1-Strep mutants were subject to affinity purification. The addition of 20 mM NEM was added after lysis to overnight pull downs to deter disulfide exchange reactions. Reducing SDS-PAGE gels were run (top) as well as nonreducing SDS-PAGE gel (bottom) and blotted for Sod1 or Ccs1.

Figure S2.5 Detailed views of the electropositive cavity

a) The Sod1•Ccs1 complex is displayed as an electrostatic surface contoured at ± 4 kT. The 90^{o} rotation relating the left and right panels carries throughout the figure. **b)** The electropositive cavity is clearly solvent accessible and large enough for a superoxide molecule. Ordered water molecules that likely facilitate superoxide movement towards the electropositive cavity are shown as cyan spheres. **c)** Same view as in panel B, but without the electrostatic surface. **d)** Again, same view as in panels B and C, but the actual cavity is shown as the surface to highlight its overall shape and charge distribution.

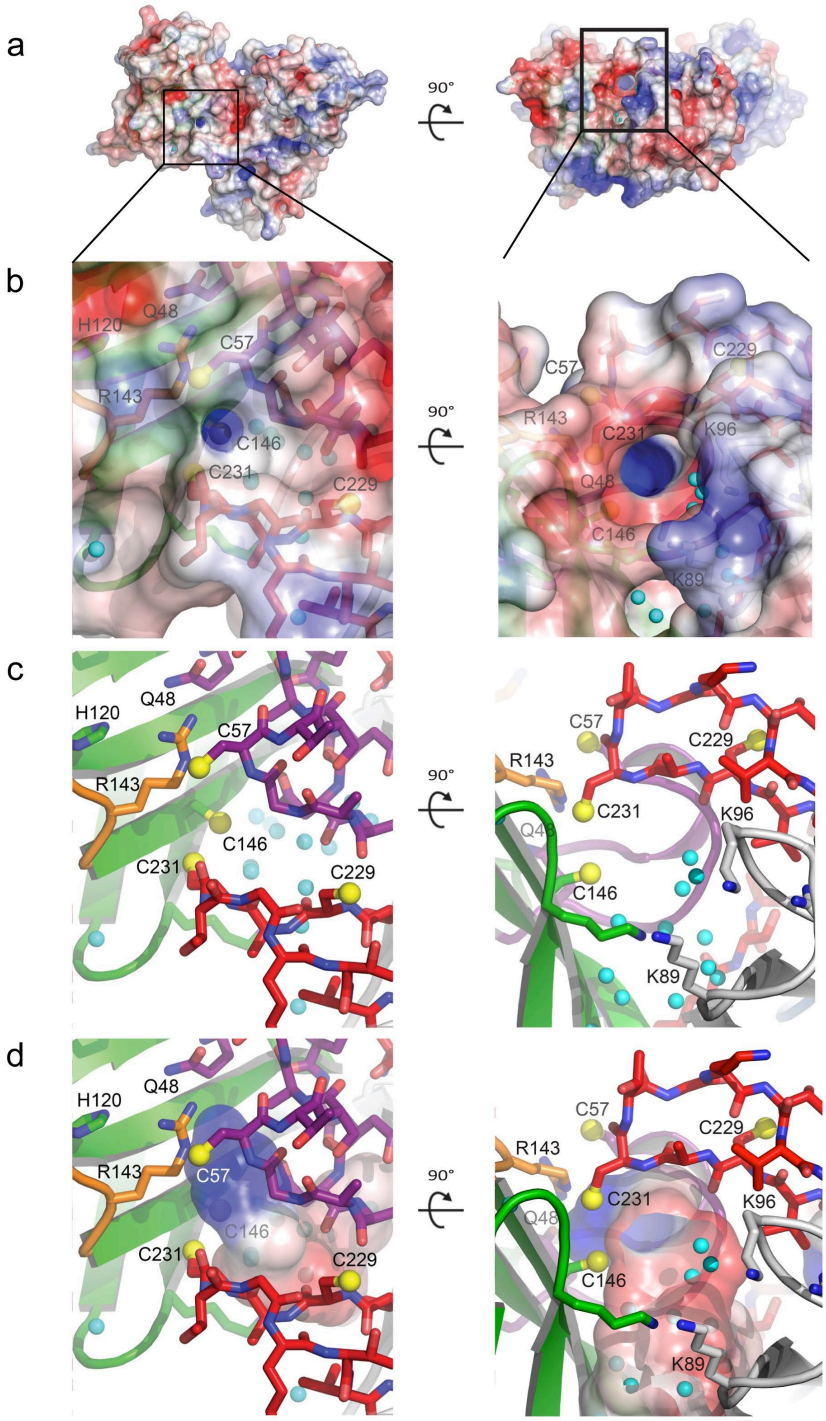
a
90°
b
H120
Q48
C57
R143
C146
C231
C229
90°
C57
C229
R143
C231
K96
Q48
C146
K89
c
H120
Q48
C57
R143
C146
C231
C229
90°
C57
C229
R143
C231
K96
Q48
C146
K89
d
H120
Q48
R143
C57
C146
C231
C229
90°
C57
C229
R143
C231
K96
Q48
C146
K89

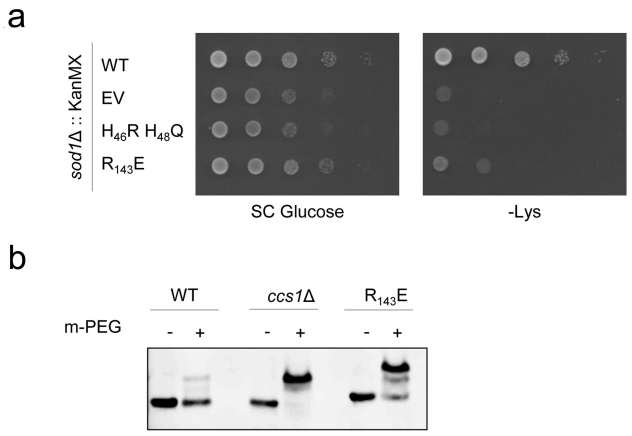

Figure S2.6 R_{143} plays a critical role in Sod1 activation.

a) Yeast viability assays performed by plating serial dilutions of cells on synthetic complete media with or without lysine at 30°C. **b)** The status of the disulfide bond in WT, ccs1Δ, and $R_{143}E$ cells was visualized by lysing cells in the presence of a PEG-maleimide alkylating agent that selectively reacts with free thiols.

Table S2.1 Interactions between Sod1 and Ccs1

Sod1 – Chain A		Ccs1 – Chain B		
Residue	Atom	Residue	Atom	Distance (Å)
5(VAL)	CG1	138(ASP)	CG	3.47
		138(ASP)	OD2	3.7
		138(ASP)	OD1	3.84
		138(ASP)	CA	3.75
		138(ASP)	CB	3.58
7(VAL)	CG1	140(SER)	N	3.72
		140(SER)	CA	3.77
		140(SER)	CB	3.93
9(LYS)	CE	85(GLU)	CD	3.95
		85(GLU)	OE1	3.35
		85(GLU)	OE2	3.86
9(LYS)	NZ	85(GLU)	CD	3.15
		85(GLU)	OE1	2.95
		85(GLU)	OE2	2.68
11(ASP)	CG	230(ALA)	CB	3.88
11(ASP)	OD1	230(ALA)	CB	3.66
11(ASP)	OD2	230(ALA)	C	3.97
		231(CYS)	N	3.23
		231(CYS)	CA	3.66
		231(CYS)	C	3.86
		231(CYS)	CB	3.41
		230(ALA)	CB	3.38
		232(THR)	N	3.2
		232(THR)	CB	3.99
		232(THR)	OG1	3.11
50(PHE)	CA	217(ARG)	O	3.81
50(PHE)	C	217(ARG)	O	3.86
50(PHE)	CB	217(ARG)	O	3.36
50(PHE)	CD	218(SER)	N	3.9
		218(SER)	CA	3.74
		218(SER)	C	3.58
		219(ALA)	N	3.52
50(PHE)	CE	218(SER)	C	3.74
		219(ALA)	N	3.47
		219(ALA)	CA	3.72
		219(ALA)	CB	3.93
50(PHE)	CZ	219(ALA)	CA	3.95
		219(ALA)	CB	3.63
51(GLY)	N	217(ARG)	C	3.97
		217(ARG)	O	2.99
51(GLY)	CA	216(ALA)	CB	3.7
		217(ARG)	O	3.8
51(GLY)	C	216(ALA)	CB	3.39
		217(ARG)	O	3.81
51(GLY)	O	216(ALA)	CB	3.33
52(ASP)	N	216(ALA)	CB	3.94
		217(ARG)	O	3.16
52(ASP)	CA	81(VAL)	CG1	3.76
		217(ARG)	O	3.86
52(ASP)	CB	81(VAL)	CG1	3.79
		217(ARG)	O	3.51
		218(SER)	CB	3.76
		218(SER)	OG	3.84
52(ASP)	CG	81(VAL)	CG1	3.46
		218(SER)	CB	3.87
		218(SER)	OG	3.55
52(ASP)	OD	81(VAL)	CG1	3.59
52(ASP)	OD	81(VAL)	CG1	3.78
		218(SER)	CB	3.13
		218(SER)	OG	2.49
		222(TRP)	NE1	3.45
53(ASN)	C	83(ILE)	CD1	3.56
53(ASN)	O	229(CYS)	O	3.92
		83(ILE)	CD1	3.76
53(ASN)	CB	83(ILE)	CD1	3.95
54(THR)	N	83(ILE)	CD1	3.68
54(THR)	C	229(CYS)	N	3.85
54(THR)	O	228(VAL)	CA	3.58
		228(VAL)	C	3.59
		229(CYS)	N	2.75
		229(CYS)	CA	3.67
		229(CYS)	CB	3.53
		229(CYS)	SG	3.69
54(THR)	CB	227(GLN)	O	3.76
54(THR)	CG	103(LEU)	CD1	3.98
		83(ILE)	CD1	3.9
111(CYS)	SG	217(ARG)	NH2	3.59
113(ILE)	C	217(ARG)	NE	3.95
113(ILE)	O	186(ILE)	CG2	3.64
		217(ARG)	NH2	3.32
		217(ARG)	CD	3.78
		217(ARG)	NE	2.75
		217(ARG)	CZ	3.46
113(ILE)	CG	187(GLY)	CA	3.63
114(GLY)	CA	186(ILE)	CG2	3.79
114(GLY)	C	217(ARG)	N	3.92
114(GLY)	O	217(ARG)	CB	3.5
		217(ARG)	CG	3.45
		216(ALA)	CA	3.75
		216(ALA)	C	3.79
		216(ALA)	CB	3.94
		217(ARG)	N	2.91
		217(ARG)	CA	3.76
		217(ARG)	CD	3.82
115(ARG)	CG	217(ARG)	CD	3.76
		217(ARG)	NE	3.98
115(ARG)	CZ	217(ARG)	CD	3.73
		217(ARG)	NE	3.69
		217(ARG)	CZ	3.94
115(ARG)	NH	217(ARG)	CD	3.45
		217(ARG)	NE	3.91
115(ARG)	NH	217(ARG)	NE	3.84
		217(ARG)	CZ	3.63
		217(ARG)	NH1	3.71
148(VAL)	CB	214(VAL)	CB	3.86
		214(VAL)	CG1	3.99
148(VAL)	CG	214(VAL)	CG1	3.62
		216(ALA)	CB	3.57
148(VAL)	CG	216(ALA)	CB	3.93
150(GLY)	CA	137(GLY)	O	3.57
		187(GLY)	O	3.54
150(GLY)	C	187(GLY)	O	3.73
151(ILE)	N	187(GLY)	C	3.93
		187(GLY)	O	2.96
151(ILE)	CA	187(GLY)	O	3.95
151(ILE)	C	137(GLY)	N	3.9
151(ILE)	O	136(LYS)	CG	3.99
		136(LYS)	CA	3.51
		136(LYS)	C	3.62
		136(LYS)	CB	3.34
		137(GLY)	N	2.92
		137(GLY)	CA	3.79
		137(GLY)	C	3.8
		138(ASP)	N	3.8
151(ILE)	CB	187(GLY)	O	3.83
151(ILE)	CG	187(GLY)	O	3.8
151(ILE)	CD	188(ARG)	NH1	3.88
		186(ILE)	O	3.9
152(ALA)	C	136(LYS)	CD	3.84
152(ALA)	O	136(LYS)	CD	3.42
153(GLN)	CG	136(LYS)	CD	3.71
153(GLN)	NE	136(LYS)	NZ	3.79

Table S2.1 Continued

Sod1 - Chain C		Ccs1 – Chain D		
Residue	Atom	Residue	Atom	Distance (Å)
5(VAL)	CG1	137(GLY)	O	3.83
		138(ASP)	CA	3.62
		138(ASP)	CB	3.61
		138(ASP)	CG	3.67
7(VAL)	CG	140(SER)	N	3.73
		140(SER)	CA	3.82
9(LYS)	CE	85(GLU)	OE1	3.65
9(LYS)	NZ	85(GLU)	CD	3.47
		85(GLU)	OE1	3.33
		85(GLU)	OE2	2.93
11(ASP)	CG	230(ALA)	CB	3.72
11(ASP)	OD	230(ALA)	CB	3.39
11(ASP)	OD	232(THR)	CB	3.9
		230(ALA)	C	3.9
		231(CYS)	N	3.22
		231(CYS)	CA	3.68
		231(CYS)	C	3.82
		232(THR)	N	3.11
		230(ALA)	CB	3.34
		231(CYS)	CB	3.58
		232(THR)	OG1	3.08
17(ILE)	CD	140(SER)	CB	3.75
50(PHE)	CA	217(ARG)	O	3.78
50(PHE)	C	217(ARG)	O	3.76
50(PHE)	CB	217(ARG)	O	3.39
50(PHE)	CD	219(ALA)	N	3.62
		218(SER)	N	3.98
		218(SER)	CA	3.89
		218(SER)	C	3.67
50(PHE)	CE	219(ALA)	N	3.67
		219(ALA)	CA	3.83
		218(SER)	C	3.9
50(PHE)	CE	219(ALA)	CB	3.84
50(PHE)	CZ	219(ALA)	CA	3.93
		219(ALA)	CB	3.64
51(GLY)	N	217(ARG)	C	3.86
		217(ARG)	O	2.83
51(GLY)	CA	217(ARG)	O	3.61
		216(ALA)	CB	3.64
51(GLY)	C	217(ARG)	O	3.66
		216(ALA)	CB	3.34
51(GLY)	O	216(ALA)	CB	3.21
52(ASP)	N	217(ARG)	O	3.13
		216(ALA)	CB	3.96
52(ASP)	CA	81(VAL)	CG1	3.7
		217(ARG)	O	3.94
52(ASP)	CB	81(VAL)	CG1	3.86
		217(ARG)	O	3.84
		218(SER)	CB	3.8
		218(SER)	OG	3.7
52(ASP)	CG	81(VAL)	CG1	3.54
		218(SER)	CB	3.97
		218(SER)	OG	3.45
52(ASP)	OD	81(VAL)	CG1	3.53
52(ASP)	OD	222(TRP)	CD1	3.85
		222(TRP)	NE1	3.36
		81(VAL)	CG1	3.96
		218(SER)	CB	3.37
		218(SER)	OG	2.5
53(ASN)	C	83(ILE)	CD1	3.54
53(ASN)	O	229(CYS)	O	3.95
		83(ILE)	CD1	3.59
53(ASN)	CB	83(ILE)	CD1	3.9
54(THR)	N	83(ILE)	CD1	3.78
54(THR)	O	227(GLN)	O	3.89
		229(CYS)	SG	3.72
		228(VAL)	CA	3.66
		228(VAL)	C	3.77
		229(CYS)	N	2.94
		229(CYS)	CA	3.8
		229(CYS)	CB	3.56
54(THR)	CB	227(GLN)	O	3.8
54(THR)	CG	81(VAL)	CG2	3.92
		103(LEU)	CD1	3.83
111(CYS)	SG	217(ARG)	NH2	3.71
113(ILE)	O	217(ARG)	CD	3.75
		217(ARG)	NE	2.74
		217(ARG)	CZ	3.44
		217(ARG)	NH2	3.26
		186(ILE)	CG2	3.55
113(ILE)	CG	187(GLY)	CA	3.63
114(GLY)	CA	186(ILE)	CG2	3.63
114(GLY)	C	217(ARG)	N	3.93
114(GLY)	O	217(ARG)	N	2.91
		217(ARG)	CA	3.73
		217(ARG)	CB	3.49
		217(ARG)	CG	3.45
		217(ARG)	CD	3.85
		216(ALA)	CA	3.75
		216(ALA)	C	3.8
115(ARG)	NE	217(ARG)	NE	3.98
115(ARG)	CZ	217(ARG)	CD	3.57
		217(ARG)	NE	3.59
		217(ARG)	CZ	3.94
115(ARG)	NH	217(ARG)	CD	3.29
		217(ARG)	NE	3.82
115(ARG)	NH	217(ARG)	NE	3.68
		217(ARG)	CZ	3.56
		217(ARG)	NH1	3.68
146(CYS)	SG	231(CYS)	SG	3.89
148(VAL)	CB	214(VAL)	CB	3.84
148(VAL)	CG	216(ALA)	CB	3.7
		214(VAL)	CG1	3.65
150(GLY)	N	137(GLY)	O	3.93
150(GLY)	CA	137(GLY)	O	3.39
		187(GLY)	O	3.33
		214(VAL)	CG1	3.79
150(GLY)	C	137(GLY)	O	3.84
		187(GLY)	O	3.52
151(ILE)	N	137(GLY)	N	3.75
		137(GLY)	CA	3.94
		187(GLY)	C	3.74
		187(GLY)	O	2.77
151(ILE)	CA	187(GLY)	O	3.76
151(ILE)	C	137(GLY)	N	3.76
151(ILE)	O	136(LYS)	C	3.45
		137(GLY)	N	2.75
		136(LYS)	CA	3.36
		137(GLY)	CA	3.64
		137(GLY)	C	3.7
		136(LYS)	CB	3.25
		136(LYS)	CG	3.9
		138(ASP)	N	3.73
151(ILE)	CB	187(GLY)	O	3.67
151(ILE)	CG	187(GLY)	C	3.92
		187(GLY)	O	3.58
151(ILE)	CD	186(ILE)	O	3.55
		188(ARG)	CG	3.88
		187(GLY)	C	3.9
152(ALA)	C	136(LYS)	CD	3.74
152(ALA)	O	136(LYS)	CD	3.21

CHAPTER 3

CONCLUSION

The accumulation of reactive oxygen species in the cell has been shown to be deleterious by causing lipid peroxidation, DNA damage, and oxidation of Fe-S clusters (1-4). Cu, Zn Superoxide dismutase 1 (Sod1) is a highly abundant intracellular protein that helps protect the cell from harmful reactive oxygen species. Sod1 is localized primarily to the cytosol and the mitochondrial intermembrane space, but has been found in the nucleus and peroxisomes(5-9). Sod1 harbors an unusually stable disulfide bond in the highly reducing cytosolic environment where formation of disulfides is typically thought to be unfavorable. Currently, there is no known disulfide transfer system present in the cytosolic compartment.

Sod1 utilizes redox cycling of its catalytic copper to convert two superoxide anions to hydrogen peroxide and water(10). The maturation of Sod1 involves insertion of a structural zinc ion, a catalytic copper ion, disulfide bond oxidation, and dimerization. Insertion of the zinc ion is achieved by an unknown mechanism, but could be accomplished through a diffusion-based mechanism. Insertion of the catalytic copper and disulfide oxidation was thought to be achieved via the interaction with Ccs1; however, the exact role has remained elusive (11-14).

In addition reactive oxygen scavenging, Sod1 has been characterized to be involved in several other cellular processes including glucose sensing, as a transcription factor, and production of hydrogen peroxide for signaling purposes(15-17). Mutations in Sod1 have been characterized to be involved in the familial for of amyotrophic lateral sclerosis (fALS). There have been over 150 mutations characterized to date, which display a variety of issues such as protein aggregation(18). Characterization of mutations in Sod1 associated with ALS continues to be a major focus in the field. Thus,

understanding the maturation process of Sod1 has broad implications in cellular defense/signaling, oxidative folding, and in the molecular basis of disease.

Over the last several years, we have discovered several discrete steps in the maturation process of Sod1. Work described in Chapter 2 supports a novel mechanism for the Ccs1 dependent activation of Sod1. The model described earlier suggests that Cu(I) originating from either Ccs1 domain 3 or a labile Cu(I)-GSH pool initially binds to an Sod1 "entry site" prior to translocation to the native active site. The presence of domain 3 of Ccs1, and particularly the cysteine residues, are necessary to stabilize the proposed entry site to allow copper coordination. The Cu(I) entry site is coordinated in a trigonal environment, characterized by a Cys_2His ligand set as shown by x-ray absorption spectroscopy. The cysteine residues may be contributed entirely by Sod1 (Cys57 and Cys146), or a combination of residues from Sod1 and the CXC motif in domain 3 of Ccs1. His120 likely contributes the histidine ligand in our studies, however, under conditions where mutations in Sod1 are not present, it is presumed that His48 could also act as a ligand also.

Superoxide anions appear to be involved in the maturation of Sod1 and are likely recruited to the Sod1 entry site Cu(I) via an exposed electropositive hole adjacent to the entry site that is formed from the interaction with Ccs1. The proposed electropositive hole seems to function in a mechanism analogous to the native electrostatic guidance of superoxide anions in the mature enzyme. Electrostatic guidance of a superoxide anion to the entry site Cu(I) leads to a Cu(I)-catalyzed generation of hydrogen peroxide. The reaction of hydrogen peroxide with a Sod1 thiolate, presumably Cys146, leads to sulfenic acid formation. Depending on the microenvironment and the pKa of the cysteine, sulfenic

acid modifications can readily undergo nucleophilic attacks from thiolates in close proximity to form inter- or intramolecular disulfide bonds, while releasing H_2O in the process (19,20). Sufenic acid formation was detected on Sod1 isolated from cells containing WT, *ccs1*Δ, Sod1 C57S, and Sod1 R143E mutants, but very little was detected on the Sod1 C146S mutant. Importantly, sulfenic acid formation is diminished upon growth and purification under copper chelating conditions. One important aspect of this experiment is the detection of sulfenic acid formation in ccs1Δ cells. Traditionally, it was thought that Ccs1 was responsible for the copper transfer to Sod1(11,14,21). This result indicates that copper is able to bind to Sod1 in the absence of Ccs1 to perform this initial superoxide turnover. These data suggest that the role of Ccs1 in Sod1 maturation is not for copper acquisition, but for resolution of the disulfide bond.

Domain 3 of Ccs1 likely mediates the disulfide exchange reaction, either directly or indirectly, leading to a Cys57-Cys146 disulfide bond in the mature enzyme. Purification of Sod1-Strep from cells containing a Ccs1 C229S or C231S mutant results in an enhanced stalling of the Sod1/Ccs1 heterodimeric species. Analysis of these mutants under nonreducing conditions shows an intermolecular disulfide bond between Ccs1 and Sod1. The heterodimer can be further enhanced by purification in the presence of the thiol alkylating agent, N-ethyl maleimide (NEM). Additionally, the spacing of the CXC motif in domain 3 of Ccs1 is critical for the activation of Sod1. Mutation or alteration of the spacing of this motif results in an inactive Sod1.

The model described is consistent with the copper- and oxygen-dependencies of the Ccs1 dependent activation process. Oxygen, and particularly superoxide, is a modulator of Sod1 activation. The data presented in Chapter 2 supports the notion that

Sod1 can be actively modulated post-translationally, by the abundance of its native substrate, and can rapidly respond to the accumulation of reactive oxygen species.

The research presented in Chapter 2 exposes several questions about the maturation process of Sod1, and alternative functions of Sod1 in the cell. One question that is obvious from the work, is whether the Ccs1 dependent, and Ccs1 independent pathways employ a similar mechanism of sulfenic acid intermediate? One key difference between the pathways is that the Ccs1 independent pathway is dependent on the presence of glutathione, where as the Ccs1 dependent pathway is not. This might simply be explained by GSH delivering copper to Sod1, however, conclusive experiments have not been performed. It seems feasible that the sulfenic acid intermediate could be a common trait between both pathways.

The recent literature has described additional proteins that exist in the cytosol with either a stable or transient disulfide bond(22). This could lead to the possibility of a general mechanism where Cu(I) is involved in generating hydrogen peroxide in a mechanism similar to what we described, or potentially that peroxide generated via Sod1 could be used for disulfide formation through a sulfenic acid intermediate. Copper is an abundant trace element, and has been described to be highly regulated and highly reactive intracellularly. This leads to the possibility that the cell could harness the inherently reactive nature or Cu(I) to form disulfide bonds.

Sod1 is involved in a diverse set of roles in the cell in addition to its role in reactive oxygen scavenging. These include in roles in glucose repression, as a transcription factor, and signaling(15-17). Sod1 is one of the most abundant enzymes in the cell, yet only a small percent of overall activity is necessary for the dismutation of

superoxide anions(23). As mentioned earlier, the native Sod1 reaction produces hydrogen peroxide. Hydrogen peroxide is particularly reactive towards cysteine residues, and can oxidize thiols to for sulfenic, sulfinic, or sulfonic acids(24,25). The latter two are irreversible reactions. One possibility to be explored is the role of peroxide generated from Sod1 for signaling purposes. Sod1 derived peroxide could be important for signaling under oxidative stressed and normal physiological conditions by modifying free tholates reversibly or irreversibly to modulate enzyme activity.

We have contributed additional details pertaining to the understanding of the maturation process of Ccs1 dependent Sod1 maturation. Studies involving the activation process of Sod1 are important not only for the development of therapeutics to combat the role of the protein in ALS, but also in the discovery of novel functions in the cell. While much is known about the maturation process, it is not a complete story and additional roles for Sod1 in the cell are still a possibility.

3.1 References

1. Gardner, P.R. and Fridovich, I. (1991) Superoxide sensitivity of the Escherichia coli aconitase. *J. Biol. Chem.*, **266**, 19328-19333.

2. Flint, D.H., Tuminello, J.F. and Emptage, M.H. (1993) The inactivation of Fe-S cluster containing hydro-lyases by superoxide. *J. Biol. Chem.*, **268**, 22369-22376.

3. Farr, S.B., D'Ari, R. and Touati, D. (1986) Oxygen-dependent mutagenesis in Escherichia coli lacking superoxide dismutase. *Proc. Natl. Acad. Sci. U. S. A.*, **83**, 8268-8272.

4. Gutteridge, J.M. (1984) Lipid peroxidation initiated by superoxide-dependent hydroxyl radicals using complexed iron and hydrogen peroxide. *FEBS Lett.*, **172**, 245-249.

5. Field, L.S., Furukawa, Y., O'Halloran, T.V. and Culotta, V.C. (2003) Factors controlling the uptake of yeast copper/zinc superoxide dismutase into

mitochondria. *J. Biol. Chem.*, **278**, 28052-28059.

6. Kawamata, H. and Manfredi, G. (2008) Different regulation of wild-type and mutant Cu,Zn superoxide dismutase localization in mammalian mitochondria. *Hum. Mol. Genet.*, **17**, 3303-3317.

7. Okado-Matsumoto, A. and Fridovich, I. (2001) Subcellular distribution of superoxide dismutases (SOD) in rat liver: Cu,Zn-SOD in mitochondria. *J. Biol. Chem.*, **276**, 38388-38393.

8. Sturtz, L.A., Diekert, K., Jensen, L.T., Lill, R. and Culotta, V.C. (2001) A fraction of yeast Cu,Zn-superoxide dismutase and its metallochaperone, CCS, localize to the intermembrane space of mitochondria. A physiological role for SOD1 in guarding against mitochondrial oxidative damage. *J. Biol. Chem.*, **276**, 38084-38089.

9. Islinger, M., Li, K.W., Seitz, J., Volkl, A. and Luers, G.H. (2009) Hitchhiking of Cu/Zn superoxide dismutase to peroxisomes--evidence for a natural piggyback import mechanism in mammals. *Traffic*, **10**, 1711-1721.

10. McCord, J.M. and Fridovich, I. (1969) Superoxide dismutase. An enzymic function for erythrocuprein (hemocuprein). *J. Biol. Chem.*, **244**, 6049-6055.

11. Culotta, V.C., Klomp, L.W., Strain, J., Casareno, R.L., Krems, B. and Gitlin, J.D. (1997) The copper chaperone for superoxide dismutase. *J. Biol. Chem.*, **272**, 23469-23472.

12. Brown, N.M., Torres, A.S., Doan, P.E. and O'Halloran, T.V. (2004) Oxygen and the copper chaperone CCS regulate posttranslational activation of Cu,Zn superoxide dismutase. *Proc. Natl. Acad. Sci. U. S. A.*, **101**, 5518-5523.

13. Carroll, M.C., Girouard, J.B., Ulloa, J.L., Subramaniam, J.R., Wong, P.C., Valentine, J.S. and Culotta, V.C. (2004) Mechanisms for activating Cu- and Zn-containing superoxide dismutase in the absence of the CCS Cu chaperone. *Proc. Natl. Acad. Sci. U. S. A.*, **101**, 5964-5969.

14. Banci, L., Bertini, I., Cantini, F., Kozyreva, T., Massagni, C., Palumaa, P., Rubino, J.T. and Zovo, K. (2012) Human superoxide dismutase 1 (hSOD1) maturation through interaction with human copper chaperone for SOD1 (hCCS). *Proc. Natl. Acad. Sci. U. S. A.*, **109**, 13555-13560.

15. Reddi, A.R. and Culotta, V.C. (2013) SOD1 integrates signals from oxygen and glucose to repress respiration. *Cell*, **152**, 224-235.

16. Tsang, C.K., Liu, Y., Thomas, J., Zhang, Y. and Zheng, X.F. (2014) Superoxide dismutase 1 acts as a nuclear transcription factor to regulate oxidative stress

resistance. *Nat. Commun.*, **5**, 3446.

17. Juarez, J.C., Manuia, M., Burnett, M.E., Betancourt, O., Boivin, B., Shaw, D.E., Tonks, N.K., Mazar, A.P. and Donate, F. (2008) Superoxide dismutase 1 (SOD1) is essential for H2O2-mediated oxidation and inactivation of phosphatases in growth factor signaling. *Proc. Natl. Acad. Sci. U. S. A.*, **105**, 7147-7152.

18. Renton, A.E., Chio, A. and Traynor, B.J. (2014) State of play in amyotrophic lateral sclerosis genetics. *Nat. Neurosci.*, **17**, 17-23.

19. Ferrer-Sueta, G., Manta, B., Botti, H., Radi, R., Trujillo, M. and Denicola, A. (2011) Factors affecting protein thiol reactivity and specificity in peroxide reduction. *Chem. Res. Toxicol.*, **24**, 434-450.

20. Conte, M.L. and Carroll, K.S. (2013) In Jakob, U. and Reichmann, D. (eds.), *Oxidative Stress and Redox Regulation*. Springer Netherlands, Dordrecht, pp. 1-42.

21. Rae, T.D., Schmidt, P.J., Pufahl, R.A., Culotta, V.C. and O'Halloran, T.V. (1999) Undetectable intracellular free copper: the requirement of a copper chaperone for superoxide dismutase. *Science*, **284**, 805-808.

22. Le Moan, N., Clement, G., Le Maout, S., Tacnet, F. and Toledano, M.B. (2006) The Saccharomyces cerevisiae proteome of oxidized protein thiols: contrasted functions for the thioredoxin and glutathione pathways. *J. Biol. Chem.*, **281**, 10420-10430.

23. Corson, L.B., Strain, J.J., Culotta, V.C. and Cleveland, D.W. (1998) Chaperone-facilitated copper binding is a property common to several classes of familial amyotrophic lateral sclerosis-linked superoxide dismutase mutants. *Proc. Natl. Acad. Sci. U. S. A.*, **95**, 6361-6366.

24. Lo Conte, M. and Carroll, K.S. (2013) The redox biochemistry of protein sulfenylation and sulfinylation. *J. Biol. Chem.*, **288**, 26480-26488.

25. Gupta, V. and Carroll, K.S. (2014) Sulfenic acid chemistry, detection and cellular lifetime. *Biochim. Biophys. Acta.*, **1840**, 847-875.